

FATIGUE ANALYSIS OF RIVETED CONNECTIONS IN STEEL BRIDGES

A DISSERTATION

*Submitted in partial fulfillment of the
requirements for the award of the degree*

of

MASTER OF TECHNOLOGY

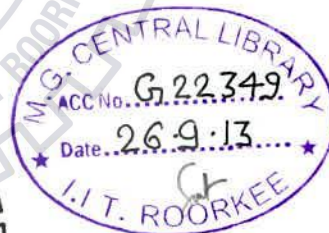
in

CIVIL ENGINEERING

(With Specialization in Structural Engineering)

By

SHAIKH MOHAMMED ADIL AKHIL SHAHIDA



DEPARTMENT OF CIVIL ENGINEERING
INDIAN INSTITUTE OF TECHNOLOGY ROORKEE
ROORKEE -247 667 (INDIA)

JUNE, 2013

CANDIDATE'S DECLARATION

I hereby certify that the work which is being presented in the dissertation entitled "**FATIGUE ANALYSIS OF RIVETED CONNECTIONS IN STEEL BRIDGES**" in partial fulfilment of the requirement for the award of the degree of Master of Technology in Civil Engineering with specialization in Structural Engineering, submitted in the Department of Civil Engineering, Indian Institute of Technology, Roorkee, is an authentic record of my own work carried out during the period from October 2012 to June 2013, under the supervision of **Dr. N.M. Bhandari**, Emeritus Fellow, Department of Civil Engineering, Indian Institute of Technology, Roorkee and **Dr. Pradeep Bhargava**, Professor, Department of Civil Engineering, Indian Institute of Technology, Roorkee.

The matter embodied in this dissertation work has not been submitted by me for the award of any other degree or diploma.

Place: Roorkee

Date: 13-06-2013

Akhil
13/06/13
Shaikh Mohammed Adil Akhil Shahida

CERTIFICATE

This is to certify that the above statement made by the candidate is true to the best of my knowledge.

N. Bhandari

Dr. N.M. BHANDARI

Emeritus Fellow

Department of Civil Engineering

Indian Institute of Technology, Roorkee

Roorkee-247667, India

T. Bhargava

Dr. PRADEEP BHARGAVA

Professor

Department of Civil Engineering

Indian Institute of Technology, Roorkee

Roorkee-247667, India

ACKNOWLEDGEMENT

I take this opportunity to affirm my earnest gratitude and indebtedness to my supervisors **Dr. N.M. Bhandari**, Emeritus Fellow, Department of Civil Engineering, Indian Institute of Technology, Roorkee, and **Dr. Pradeep Bhargava**, Professor, Department of Civil Engineering, Indian Institute of Technology, Roorkee, for their valuable suggestions, meticulous guidance perpetual inspiration and support in completion of this dissertation submitted in partial fulfilment for the award of the degree of Master of Technology with specialization in Structural Engineering.


I also thank all my batch-mates and juniors for their kindness and moral support during my study. Thanks for the friendship and memories.

I would like to thank the management of M/s. Spectrum Techno Consultants Pvt. Ltd. Mumbai, for having belief in my abilities and relieving me of my duties during the duration of this course apart from sponsoring my education at IIT Roorkee. Above all I would like to thank my mentor Mr. Umesh Rajeshirke, for motivating me to continue my studies.

Last but not the least it is beyond my literary capability to express my gratitude to my parents and my siblings in absence of whom I could never have reached this position. Their love, blessings, motivation and inspiration have provided me a high mental support.

Finally, I am grateful to the one above all of us, the omnipresent Almighty, for answering my prayers and giving me the strength to plod on.

Date: 13 June, 2013


13/06/13
Shaikh Mohammed Adil Akhil Shahida

Place: Roorkee

ABSTRACT

There are numerous bridges across India which were built about 100 years ago. A large proportion of these bridges are made of steel, relatively old, past their design life. They are subjected to much larger loads running on them than that had been considered in their design. Moreover, fatigue which is an important factor for failure of steel bridges was not popular during the design of these bridges. Fatigue is a problem where vehicular live load forms major part of total loading. In such a scenario, the assessment of residual fatigue life of steel bridges becomes an important issue.

There has been a lot of research in this field. But none of the methods suggested are fool proof and the fatigue life assessed using these methods has often been found to be unreliable. Most of the theories ask for assumptions to be made regarding certain things like material properties, joint rigidities, current health of the bridge etc. The assumed presence of fatigue cracks and the fear of brittle fracture are often unjustified. Hence a more sophisticated and reliable procedure needs to be developed for the assessment of residual fatigue life of steel bridges.

Stringer-to-cross-girder connections in riveted bridges have been found to be susceptible to fatigue damage. Due to multiple cycles of loading on the stringers, these connections are one of the most fatigue critical connections in steel bridges. It is a well-documented fact through experiments carried out on riveted connections that the clamping force in a rivet plays an important role in its fatigue behaviour.

An effort has been made to model the stringer-to-cross-girder connection using finite element method in ABAQUS by incorporating the detailed local geometry of the connection. The fatigue life of the connection is evaluated using the S-N curve and Palmgren-Miner linear damage hypothesis. The effect of clamping force of the rivet on the fatigue life of the connection is studied.

Keywords: Fatigue damage, Finite element method, Life assessment, Riveted connections, S-N method, Steel bridges.

TABLE OF CONTENTS

CANDIDATE'S DECLARATION	i
ACKNOWLEDGEMENT	ii
ABSTRACT	iii
TABLE OF CONTENTS	iv
LIST OF FIGURES	vii
LIST OF TABLES	xi
Chapter 1	
INTRODUCTION	1
1.1 NEED OF THE STUDY	2
1.2 PURPOSE OF THE STUDY	2
1.2.1 PREVIOUS STUDIES	3
1.3 SCOPE OF THE STUDY	3
1.4 ORGANIZATION OF THE DISSERTATION	4
Chapter 2	
FATIGUE ANALYSIS – THEORY	5
2.1 INTRODUCTION	5
2.2 FATIGUE LIFE ASSESSMENT PROCEDURE	6
2.2.1 SITE-VALIDATED NUMERICAL MODELLING	6
2.2.2 FATIGUE LOAD HISTORY	8
2.2.3 CYCLE COUNTING METHODS	9
2.2.4 STRESS RANGE AND NUMBER OF CYCLES	11
2.2.5 S-N CURVE	11
2.2.6 MINER'S RULE	12
Chapter 3	
BEHAVIOUR OF RIVETED STRINGER-TO-CROSS-GIRDER CONNECTIONS	14
3.1 RIVETED CONNECTIONS	14
3.1.1 CLAMPING FORCE	15
3.2 TENSION CONNECTIONS	16
3.3 SHEAR CONNECTIONS	17

3.4	FATIGUE CRITICAL LOCATIONS IN STRINGER-TO-CROSS-GIRDER CONNECTIONS	18
Chapter 4		
	MODELLING OF RIVETED CONNECTION IN ABAQUS-CAE	21
4.1	GENERAL	21
4.2	RIVETED DOUBLE LAP JOINT	21
4.2.1	MODELLING.....	22
4.2.2	BOUNDARY CONDITONS AND INTERACTION	23
4.2.3	APPLICATION OF CLAMPING FORCE.....	24
4.2.4	APPLICATION OF EXTERNAL LOAD	25
4.2.5	RESULTS	26
4.3	STRINGER-TO-CROSS-GIRDER CONNECTION.....	30
4.3.1	MODELLING.....	31
4.4	JOINT RIGIDITY.....	36
4.5	SUMMARY	38
Chapter 5		
	FATIGUE ANALYSIS OF A STRINGER-TO-CROSS-GIRDER CONNECTION	39
5.1	GENERAL INFORMATION	39
5.2	GLOBAL MODEL OF THE TRUSS BRIDGE	40
5.2.1	DEAD LOAD AND SUPER IMPOSED DEAD LOAD.....	41
5.2.2	LIVE LOAD	42
5.2.3	RESULTS OBTAINED FOR LIVE LOAD.....	43
5.3	ANALYISS OF LOCAL CONNECTION MODEL IN ABAQUS.....	47
5.3.1	APPLICATION OF RIVET CLAMPING FORCE.....	47
5.3.2	APPLICATION OF DEAD LOAD	47
5.3.3	APPLICATION OF LIVE LOAD	48
5.3.4	ANALYSIS.....	49
5.4	SUMMARY	51
Chapter 6		
	FATIGUE LIFE EVALUATION	52
6.1	GENERAL	52
6.2	POST-PROCESSING OF RESULTS	52

6.2.1	SHEAR STRESS HISTORY	52
6.2.2	RAIN FLOW COUNTING METHOD.....	53
6.2.3	STRESS RANGE HISTOGRAM.....	55
6.3	SHEAR STRESS HISTORY	56
6.3.1	STANDARD TRUCK LOADING	56
6.3.2	HEAVY TRUCK LOADING.....	57
6.3.3	35.2 TON TRUCK LOADING.....	58
6.3.4	44 TON TRUCK LOADING.....	59
6.4	STRESS RANGE HISTOGRAM	60
6.4.1	STANDARD TRUCK LOADING	60
6.4.2	HEAVY TRUCK LOADING.....	61
6.4.3	35.2 TON TRUCK LOADING.....	62
6.4.4	44 TON TRUCK LOADING.....	63
6.5	FATIGUE DAMAGE IN RIVET	65
6.5.1	DAMAGE IN RIVET FOR CLAMPING STRESS 150 MPa.....	66
6.5.2	DAMAGE IN RIVET FOR CLAMPING STRESS 100 MPa.....	68
6.5.3	DAMAGE IN RIVET FOR CLAMPING STRESS 150 MPa.....	70
6.5.4	DAMAGE CALCUALTION PER DAY.....	72
6.6	ESTIMATION OF FATIGUE LIFE.....	73
6.7	SUMMARY.....	74
Chapter 7		
CONCLUSIONS		75
7.1	SUMMARY	75
7.2	CONCLUSIONS.....	75
7.3	LiMITATIONS	76
7.4	SCOPE FOR FUTURE RESEARCH	76
REFERENCES		78

LIST OF FIGURES

Figure 2.1 – Fatigue failure of a bolt, with clear beach marks (Larsson, T. 2009).....	6
Figure 2.2 – General fatigue load history.....	8
Figure 2.3 – A typical cyclic stress history reduced to peaks and troughs.....	10
Figure 2.4 – Rain flow counting method.....	10
Figure 2.5 – Damage accumulation calculation (Kuehn et al., 2008).....	13
Figure 3.1- Hot-driven riveting process (Larsson, T. 2009).....	14
Figure 3.2 – Cross section of a hot-driven rivet. (Vermes et al., 2011).....	15
Figure 3.3 – Rivet clamping force distribution (Åkesson, B. 1994).....	16
Figure 3.4 – Deformation scenarios in tension connections depending upon stiffness of rivets and connecting angles (Larsson, T., 2009).....	17
Figure 3.5 – Fatigue critical locations in a Stringer-to-cross-girder connection.....	18
Figure 3.6 – Failure of rivet shank under fatigue (Åkesson, B., 1994).....	19
Figure 3.7 – (a) Complete loss of rivets due to failure of rivet shank. (b) Crack propagating in a connection angle (Haghani, et al., 2012).....	20
Figure 3.8 – Crack propagating from coped girder (Haghani, et al., 2012).....	20
Figure 4.1 – Dimensions of the riveted double lap joint.....	22
Figure 4.2 – Finite element model of the riveted double lap joint.....	22
Figure 4.3 – Highlighting the boundary conditions of the double lap joint.....	23
Figure 4.4 – Interaction surfaces for friction modelling.....	24
Figure 4.5 – Internal surface of rivet selected for application of bolt load in ABAQUS.....	24
Figure 4.6 – Application of 30 MPa axial stress as external load on the middle plate.....	25
Figure 4.7 – Axial stress in rivet for different clamping stress. (a)50 MPa, (b)100 MPa, (c)150 MPa, (d)200 MPa.....	26
Figure 4.8 – Deformed shape of the riveted double lap joint for externally applied 30 MPa axial stress in the middle plate.....	27
Figure 4.9 – Deformed shape of the rivet for externally applied 30 MPa axial stress in the middle plate.....	27
Figure 4.10 – Bearing Stress in the rivet for externally applied 30 MPa axial stress in the middle plate.....	28
Figure 4.11 – Longitudinal stress in the middle plate of the riveted double lap joint for externally applied 30 MPa axial stress in the middle plate.....	28

Figure 4.12 – Stress Concentration Factor vs Rivet clamping stress in the middle plate for externally applied 30 MPa axial stress applied in the middle plate.....	29
Figure 4.13 – Details of the connection.....	30
Figure 4.14 – Local model of the cross girder using solid elements for a length of 1000mm.....	31
Figure 4.15 – Local model of the stringer using solid elements for a length of 500mm.	31
Figure 4.16 – Complete model of the cross-girder comprising of Solid and Shell elements.....	32
Figure 4.17 – Complete model of the stringer comprising of Solid and Shell elements.....	32
Figure 4.18 – Location of Shell to Solid constraint in cross-girder	33
Figure 4.19 – (a) Finite element model of the rivet. (b) Finite element mesh and arrangement of connecting angles.....	33
Figure 4.20 – Assembly of the stringer-to-cross-girder connection showing only the solid element mesh.....	34
Figure 4.21 – The connection model in totality.....	35
Figure 4.22 – The finite element mesh of the entire assembly.....	35
Figure 4.23 – Locations of applied boundary conditions.....	35
Figure 4.24 – Assembly of the connection model for checking the joint rigidity.....	36
Figure 4.25 – Boundary conditions for assembly of the connection model for checking the joint rigidity	36
Figure 4.26 – Deflection vs Rivet clamping stress for joint rigidity check.....	37
Figure 5.1 – General details of the truss bridge.....	39
Figure 5.2 – SAP-2000 model of the truss bridge	40
Figure 5.3 – Deflection in critical nodes of the connection considered for analysis due to DL and SIDL.....	41
Figure 5.4 – Commercial vehicles plying in India [IRC: SP - 37-1991]	42
Figure 5.5 – Shear force diagram of the connection for a load step of vehicle load.....	43
Figure 5.6 – Shear force history at the joint for standard vehicle in left stringer.....	44
Figure 5.7 – Shear force history at the joint for standard vehicle in right stringer.....	44
Figure 5.8 – Shear force history at the joint for heavy vehicle in left stringer	45
Figure 5.9 – Shear force history at the joint for heavy vehicle in right stringer.....	45
Figure 5.10 – Shear force history at the joint for 35.2 ton vehicle in left stringer.....	45
Figure 5.11 – Shear force history at the joint for 35.2 ton vehicle in right stringer	46
Figure 5.12 – Shear force history at the joint for 44 ton vehicle in left stringer.....	46
Figure 5.13 – Shear force history at the joint for 44 ton vehicle in right stringer	46
Figure 5.14 – Patch showing the location of applied displacement due to DL and SIDL.....	48
Figure 5.15 – Patch showing location of applied shear force as patch load for live load.....	48

Figure 5.16 – Critical location for maximum shear stress in the rivet.....	49
Figure 5.17 – Cross section of rivet at the face of the stringer.....	50
Figure 5.18 – Elements selected for fatigue analysis in the cross-section of the rivet.....	51
Figure 6.1 – Shear stress history for 50 MPa clamping stress under Heavy truck loading.....	52
Figure 6.2 – Sorted shear stress history for 150 MPa clamping stress under Heavy truck loading.....	53
Figure 6.3 – Working diagram for rain flow counting.....	54
Figure 6.4 – Stress range histogram for 50 MPa clamping stress under Heavy truck loading.....	55
Figure 6.5 – Shear stress history for 150 MPa clamping stress under standard truck loading.....	56
Figure 6.6 – Shear stress history for 100 MPa clamping stress under standard truck loading.....	56
Figure 6.7 – Shear stress history for 50 MPa clamping stress under standard truck loading.....	57
Figure 6.8 – Shear stress history for 150 MPa clamping stress under heavy truck loading.....	57
Figure 6.9 – Shear stress history for 100 MPa clamping stress under heavy truck loading.....	57
Figure 6.10 – Shear stress history for 50 MPa clamping stress under heavy truck loading.....	58
Figure 6.11 – Shear stress history for 150 MPa clamping stress under 35.2 ton truck loading....	58
Figure 6.12 – Shear stress history for 100 MPa clamping stress under 35.2 ton truck loading....	58
Figure 6.13 – Shear stress history for 150 MPa clamping stress under 35.2 ton truck loading....	59
Figure 6.14 – Shear stress history for 150 MPa clamping stress under 44 ton truck loading.....	59
Figure 6.15 – Shear stress history for 100 MPa clamping stress under 44 ton truck loading.....	59
Figure 6.16 – Shear stress history for 50 MPa clamping stress under 44 ton truck loading.....	60
Figure 6.17 – Stress range histogram for 150 MPa clamping stress under standard truck loading.....	60
Figure 6.18 – Stress range histogram for 100 MPa clamping stress under standard truck loading.....	61
Figure 6.19 – Stress range histogram for 50 MPa clamping stress under standard truck loading.....	61
Figure 6.20 – Stress range histogram for 150 MPa clamping stress under heavy truck loading ..	61
Figure 6.21 – Stress range histogram for 100 MPa clamping stress under heavy truck loading ..	62
Figure 6.22 – Stress range histogram for 50 MPa clamping stress under heavy truck loading	62
Figure 6.23 – Stress range histogram for 150 MPa clamping stress under 35.2 ton truck loading.....	62
Figure 6.24 – Stress range histogram for 100 MPa clamping stress under 35.2 ton truck loading.....	63
Figure 6.25 – Stress range histogram for 50 MPa clamping stress under 35.2 ton truck loading.....	63

Figure 6.26 – Stress range histogram for 150 MPa clamping stress under 44 ton truck loading 63

Figure 6.27 – Stress range histogram for 100 MPa clamping stress under 44 ton truck loading 64

Figure 6.28 – Stress range histogram for 150 MPa clamping stress under 44 ton truck loading 64

Figure 6.29 – Wöhler’s curve or S-N Curve 65



LIST OF TABLES

Table 4.1 – Clamping Stress and Bolt force in ABAQUS	25
Table 4.2 – Values of deflection corresponding to different clamping stress	37
Table 5.1 – Type of vehicles	43
Table 5.2 – Clamping stress and Bolt load in ABAQUS.....	47
Table 6.1 – Stress range and corresponding number of cycles for 50 MPa clamping stress under Heavy truck loading.....	55
Table 6.2 – Damage – 150 MPa - Single passage of two standard trucks	66
Table 6.3 – Damage – 150 MPa – Single passage of two heavy trucks.....	66
Table 6.4 – Damage – 150 MPa – Single passage of two 35.2 ton trucks.....	67
Table 6.5 – Damage – 150 MPa – Single passage of two 44 ton trucks.....	67
Table 6.6 – Damage - 100 MPa – Single passage of two standard trucks	68
Table 6.7 – Damage – 100 MPa – Single passage of two heavy trucks.....	68
Table 6.8 – Damage - 100 MPa – Single passage of two 35.2 ton trucks	69
Table 6.9 – Damage – 100 MPa – Single passage of two 44 ton trucks.....	69
Table 6.10 – Damage – 50 MPa – Single passage of two standard trucks.....	70
Table 6.11 – Damage - 50 MPa – Single passage of two heavy trucks	70
Table 6.12 – Damage – 50 MPa – Single passage of two 35.2 ton trucks.....	71
Table 6.13 – Damage – 50 MPa – Single passage of two 44 ton trucks.....	71
Table 6.14 – Total damage per day for 150MPa rivet clamping stress.....	72
Table 6.15 – Total damage per day for 100MPa rivet clamping stress.....	72
Table 6.16 – Total damage per day for 50MPa rivet clamping stress.....	73
Table 6.17 – Fatigue life in years for different clamping stress	74

Chapter 1

INTRODUCTION

Numerous bridges in service today are nearing the end of their design life having been built in the early 20th century. Although there has been a major overhaul in traffic which used to ply over hundred years ago and the present day traffic both in terms of vehicular axle loads and frequency of the vehicles, many of those bridges are still in service today. It may perhaps be surprising that even after such drastic changes in the traffic these bridges seem to function well under the current scenario. This feat can be credited to the fact that these bridges were designed for overcapacity due to the volatile changes in the traffic during the time of their design. Also due to the lack of confidence on the material used during that time, a higher factor of safety was adopted in the design. All these factors have contributed in extending the design life of the bridges substantially.

Materials used in the construction of bridges have seen a drastic change over the turn of the last century. By the end of the 18th century cast iron, then wrought steel and finally steel has increasingly been used as a construction material. Steel products like rolled members and cold-formed elements became available with the advancement of industrial processes. For the construction of structures such as bridges, buildings, industrial plants, etc. structural steel has been extensively used as a construction material. At the beginning of the 19th century, civil engineering saw a mammoth development and engineering design rules became more scientific. The use of new materials and new construction methodologies led to certain setbacks with several dramatic collapses. These setbacks however led to further research and development of new theories. The setbacks suffered, also led to advancements in better understanding of the structural behaviour.

Bridges are among the structures most often damaged. Fatigue is a major contributor in the failure of structures. Of all the recorded causes of damage, fatigue ranks third in terms of frequency for general structures. But in case of bridges, it ranks first. Extensive studies in the field of fatigue has led to the conclusion that, fatigue cracks have been induced by the evolution of secondary stresses along with overload, but also because the assumed detail category used in design was too high and/or the workmanship was too poor.

In the field of fatigue assessment the word “failure” is widely used, but it often has a different meaning. The growth of fatigue crack depends upon the redundancy of the cracked element.

The crack will grow exponentially in a small non-redundant component, beginning gradually and progressively accelerating. However if the structure is large and redundant, there will be redistribution of load away from the crack element and hence there will be a stable period of crack growth. Theoretically, when the fracture of the remaining net section occurs, it marks the end of fatigue life.

1.1 NEED OF THE STUDY

It is a well-documented fact that the bridges constructed during the early 20th century were designed with a large factor of safety due to lack of rational design methods during the time. This over capacity in the design has therefore acted in advantage of these bridges which have been able to sustain the increased axle loads over the last century. A large number of old bridges are still in service in all of India are reaching the end of their design life. Due to constant increase in traffic density and axle loads, it has become necessary to assess the remaining life of these bridges. It is impossible to replace all bridges at the same time due to the large number of these bridges. There is a need to devise a step by step procedure to replace these bridges one after the other. To do this we must first identify the bridges with worst condition and replace them first. Also, to enhance the service life and performance of old bridges, enhancement of the existing assessment methods has to be made. To do this the procedure of an assessment must be known to be able to recognize where improvements can be made (Larsson, T. 2009).

This scenario leads to a scope for further research in this area. There is a need to enhance the existing methods of assessment. The critical areas in a bridge with respect to health of a bridge must be identified. This can be done by studying closely the reasons behind major failure of bridges and identifying the ways to avoid such failures.

Fatigue is the most common cause of failure in steel structures and the most critical mode of failure for steel bridges in particular. When conducting an assessment of a bridge, it is of great importance to understand the process of how fatigue develops in the material and as well as in the structure.

1.2 PURPOSE OF THE STUDY

Most of the research related to fatigue life of riveted bridges has been concerning the fatigue life assessment of the individual member. The fatigue life estimates have been carried out using the Wohler's curve or S-N curve and Palmgren-Miner's rule. Apart from this, fracture mechanics approach has been used to assess the fatigue life of critical locations in riveted and welded bridges by studying the crack propagation pattern and time required for the crack to

propagate. Also, the fatigue life assessment of riveted connections has been carried out using experimental methods.

Stringer-to-cross-girder connections have been found to one of the most critical connections in a steel bridge. This is due to the fact that, a stringer experiences more number of cycle repetitions than the main girder or truss girder for a single passing of a vehicle because the influence lengths of the two are different. Experimental methods have their limitations. The actual field scenarios and the actual material properties cannot be replicated in a lab unless the actual bridge part is taken out of the bridge and tested in the lab. Finite element method provides numerous possibilities to perform such tasks by precisely modeling the bridge in a finite element software package like ABAQUS. Numerous researchers have performed the fatigue analysis of riveted connections using finite element method.

1.2.1 PREVIOUS STUDIES

- *Al-Emrani and Kliger (2003)* have performed experimental investigation on the rigidity of stringer-to-floor-beam connections and analyzed the same connection using finite element method. Fatigue damage susceptibility due to appreciable restraint in the connection was studied.
- *Imam et al., (2007)* have analyzed a stringer-to-floor-beam connection of a plate girder bridge using ABAQUS. Having modeled the connection in true sense by modeling the rivets and connection angles, the bridge was analyzed for different rivet defect scenarios like loss of rivet head, loss of clamping force in rivet, complete loss of rivet, presence of gap between rivet and rivet hole, partial loss of rivet head due to corrosion etc. Based on the analysis, several damage critical points in the rivets, connecting angles and girders were identified as hot-spots for cracks to originate.
- *de Jesus et al., (2010)* have analyzed a similar stringer-to-floor-beam connection and using ANSYS. Fatigue and fracture assessments were made. Different crack propagation scenarios were investigated.

1.3 SCOPE OF THE STUDY

The scope of the study is limited to obtaining the fatigue life of the most critical rivet in a stringer-to-cross-girder connection of a truss bridge. A brief methodology is enlisted below.

- Execute the global analysis of the complete bridge in SAP-2000.
- Analyze the bridge for four different vehicle types plying on Indian roads available in SP-37 of IRC.

- Perform the stress analysis of the connection analyzing the finite element local connection model in ABAQUS.
- Carry out the fatigue life assessment by estimating the damage using the Wohler's curve and Palmgren-Miner's hypothesis.
- Understand the behavior of the connection due to loss in clamping force of the rivet and to compare the fatigue life of the connection for different clamping forces.

1.4 ORGANIZATION OF THE DISSERTATION

Chapter 2 “Fatigue analysis - theory”

This chapter briefly discusses about the available literature on fatigue and fatigue life assessment procedure.

Chapter 3 “Behaviour of riveted stringer-to-cross-girder connections”

This chapter briefly discusses about the riveting procedure, clamping force, tension connections, shear connections and fatigue critical locations in stringer-to-cross-girder riveted connections.

Chapter 4 “Modelling of riveted connections in ABAQUS-CAE”

This chapter describes the methodology involved in preparing the finite element model of a riveted connection in ABAQUS. Further, the modelling of stringer-to-cross-girder connection and its validation is also discussed.

Chapter-5 “Fatigue analysis of a stringer-to-cross-girder connection”

In this chapter the global analysis of the truss bridge and the local analysis of the connection are discussed in detail.

Chapter-6 “Fatigue life evaluation”

The fatigue life evaluation of the connection by S-N method is discussed in detail in the chapter.

Chapter-6 “Conclusions”

Summarize the conclusion drawn from the results presented in chapter 5 and 6. It also gives recommendation for further studies in the area of fatigue in riveted steel connections.

Chapter 2

FATIGUE ANALYSIS – THEORY

2.1 INTRODUCTION

First coined by Braithwaite in 1854, the word ‘fatigue’ originated from the Latin expression ‘fatigare’ which means ‘to tire’. *Fatigue* is the process of initiation and propagation of microscopic cracks into macro cracks by the repeated application of stresses. An old phenomenon, fatigue has puzzled researchers for over 200 years attracting attention since the use of metal in structures. Wöhler (1819-1914) was one of the first to investigate the fatigue phenomenon by conducting systematic investigations on train axles and studying their failure under repeated loads lower than the static design load. Tests from fatigue investigations were plotted in diagrams with the stress range on the vertical axis and the number of cycles on the horizontal axis. The diagram was log scaled to get a better overview of the results. This enabled in detecting a linear result of the components fatigue life. Known as Wöhler diagrams or S-N diagrams, where S stands for the stress range and N for the number of cycles the diagrams developed to predict fatigue life of details and structures are still used today.

Fatigue failures occur in details or whole structures due to repeated loading, the load levels leading to a fatigue failure are lower than the static resistance. The failure is due primarily to the repeated stress from a maximum to a minimum. The most important factor concerning fatigue is the stress range $\Delta\sigma$, but the exact form of the stress range has a marginal influence. Generally fatigue only develops through tension stresses; hence compressive loading will not contribute to fatigue. This is only valid if the material is free from residual stresses, which seldom is the case due to processes such as rolling and welding. This makes it possible for compressive loading to contribute to fatigue. The damage and/or failure of materials under cyclic loads in engineering applications is called *fatigue damage*.

The process of fatigue failure can be divided into three stages - Crack initiation, Crack Propagation and Fracture. The number of cycles for the each stage can differ considerably from hundreds to millions of cycles depending on the stress range, stress initiation factors, material properties etc.

Crack Initiation: Cracks initiate through plastic deformations due to tension in grains situated in the steel structure. This occurs when the stresses in a crystal reach its yield point and the crystal begins to deform plastic. Plastic deformations in the crystals often have its

origin at a notch or stress raisers such as dislocations, blisters, and inclusions of impurities etc.

Crack Propagation: The second stage in the fatigue process, crack propagation, occurs due to a continued cyclic loading, making cracks form in to one or more main cracks. A plastic zone forms in front of the crack with the size of a few grains. The growth of cracks is not as dependent on the internal structure of the material in this stage and the direction of the cracks is normal to the far field tensile axis. A phenomenon associated with the second stage is the formation of beach marks. In Figure 2.1, the crack propagation can be seen to move from the bottom to the top of the bolt leaving marks due to the growth of the crack.

Fracture: The last stage in the fatigue process is rapid crack growth leading to failure when the remaining area of a section can no longer withstand the load.

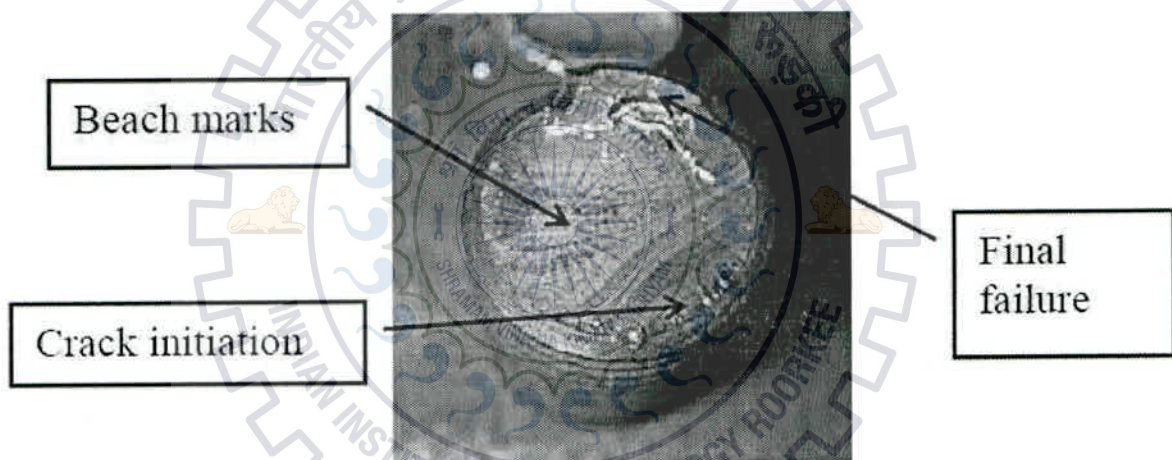


Figure 2.1 – Fatigue failure of a bolt, with clear beach marks (Larsson, T. 2009)

2.2 FATIGUE LIFE ASSESSMENT PROCEDURE

2.2.1 SITE-VALIDATED NUMERICAL MODELLING

In order to assess the strength, stability and remaining fatigue life of the bridge, a numerical model representing the present behaviour and condition of the bridge has to be developed. Once the numerical model is validated, it can be used to analyse the bridge for load combinations involving different train types (Chaminda et al., 2007). Following are the steps for developing and validating the numerical model.

- a. **Preliminary Investigation:** The linear and elastic behaviour of the bridge should be verified through continuity of strain histories. The neutral axis of flexural members shall

be located, moment resistance at supports of the girders should be detected and the behaviour should be qualitatively evaluated. A comprehensive site measurement shall be used even if the structural drawings are available (Banerji and Chikermane, 2010). This shall be done to make sure that there has not been any deviation during the construction.

- b. **Testing of bridge materials:** Laboratory tests shall be carried out to determine the mechanical properties and chemical composition of the materials that were used for construction of the bridge. The properties of material thus obtained shall be assigned to the software developed model.
- c. **Consider other factors:** Other factors such as the condition of the bridge and/or substructure, bearings, traffic volume, and other information available in the inspection report should be taken into consideration.
- d. **Development of representative model:** The numerical model of the bridge can be created on various software packages available like ABAQUS, ANSYS, SAP2000, STAAD PRO etc. The actual geometry of the structure viz. span length, girder spacing, skew angle, transverse members and deck shall be modelled appropriately. Gauge locations on model identical to those applied in the field shall be identified.
In case of a truss bridge, joint fixities shall be introduced in the form of rotational springs instead of pin joints to ensure proper behaviour of the joint. For an ideal model, the roller is considered as being perfectly smooth. However, in reality, there is some degree of fixity. This can be modelled using translational spring elements (Banerji and Chikermane, 2010).
- e. **Simulate load test on computer model:** A design train identical to the vehicle on site shall be modelled. Analysis shall be performed and strains at gauge location for different loading conditions shall be computed.
- f. **Compare site measured and software generated strain values:** Various global and local values at each gauge location shall be obtained from site and shall be compared with the values obtained by the software simulation.
- g. **Evaluate modelling parameters:** Improve model based on data comparisons. Engineering judgment and experience is required to determine the variables to be modified. A combination of direct evaluation techniques and parameter optimization can be used to obtain a realistic model.
- h. **Model Evaluation:** In some cases it may not be desirable to rely on secondary stiffening effects as their effectiveness may be questionable at higher load levels. It is beneficial, though, to quantify their effects on the structural response so that a representative

computer model can be obtained. The stiffening effects that are deemed unreliable can be eliminated from the model.

- i. **Perform analysis:** By applying loads as per IRS/IRC loading to the calibrated model an analysis true to the present state of the bridge can be carried out.

2.2.2 FATIGUE LOAD HISTORY

Fatigue load history or load spectrum in the form of stresses or forces shall be obtained from the refined numerical model for different vehicle configurations the structural detail including secondary effects that are relevant. Fatigue load spectrum is a vital requirement for fatigue analysis. Load, stress or load spectrum is engineering definition of the fatigue environment that an element experiences throughout its design life and is defined by the load/stress amplitude versus the number of cycles.

To develop fatigue spectrum, it is important to define all loading actions the element will be subjected to and the number of times that each action will take place. The fatigue spectrum for each action may be a function of numerous variables like vehicle composition, velocity, direction of motion, number of loaded lanes etc. After recognising the actions, variation of load or stress versus time should be obtained.

The load history occurring in bridge members is variable-amplitude loading history, which cannot be characterized by an analytical function. In a variable-amplitude loading history, the probability of identical sequence and magnitude of stress ranges repeating during a particular time interval is minimal.

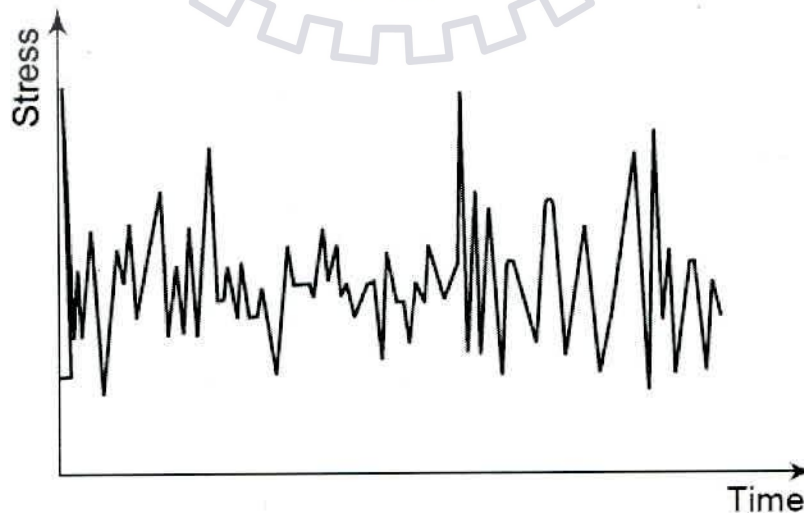


Figure 2.2 – General fatigue load history

2.2.3 CYCLE COUNTING METHODS

The loading time history plotted for each action consists of complex stress cycles. It is necessary to derive stress ranges and number of cycles in order to plot the stress histogram or the fatigue spectrum.

The load histories are irregular and complex. These irregular load histories need to be converted into regular simple load cycles. To do this, different counting methods are used. The basic principle of all counting methods is to count a cycle with the range from the highest peak to the lowest valley. The cycles are counted in a way that maximum range is counted. In case of fatigue, it is assumed that the intermediate fluctuations are of less importance than the overall differences between high and low points. To perform this task, many counting methods are available. The most reasonable and practical method must be selected from amongst the most widely used counting methods. The different kinds of counting methods available in the literature are enlisted below.

- a. Rain flow counting method,
- b. Range pair counting method,
- c. Modified range pair counting method,
- d. Peak count method,
- e. Mean crossing peak counting method,
- f. Level crossing count method,
- g. Fatigue meter count method,
- h. Range count method,
- i. Range mean count method,
- j. Modified range count method,
- k. Race track or ordered overall range method

The most extensively used counting methods are rain flow counting method, reservoir counting method and the race track counting method.

In the present study, rain flow counting method has been adopted. The methodology of using rain flow counting method is as follows.

- i. The variable-amplitude load time history which is very complex shall be reduced to a sequence of peaks and troughs by selecting the maximum points on either side and eliminating the smaller intermediate values.

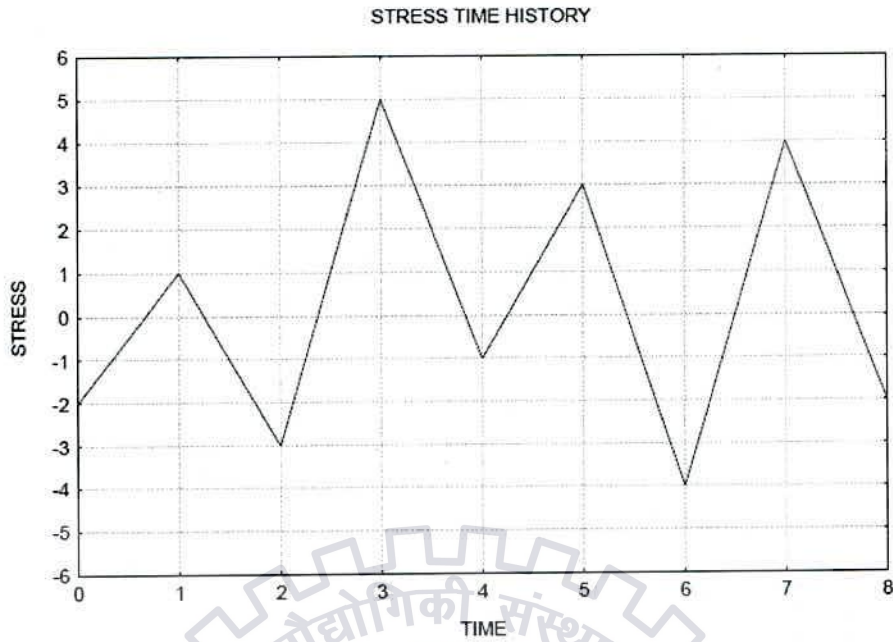


Figure 2.3 – A typical cyclic stress history reduced to peaks and troughs

- ii. The horizontal time history shall be rotated clockwise by 90° .

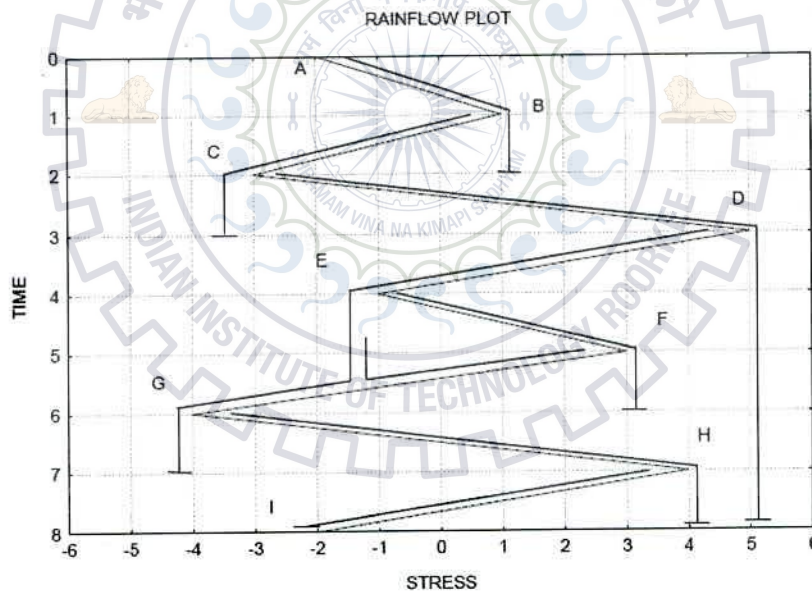


Figure 2.4 – Rain flow counting method

- iii. Imagine the time history graph to be Japanese pagoda roof and allow the rain to flow down from the top.
- iv. Count the number of half cycles.
- v. Terminate the flow of the rain when,
- The rain reaches the end of time history.
 - The rain encounters a trough of greater magnitude.
 - The rain encounters a previous flow.

- vi. The above steps shall be carried out for both the compressive and tensile troughs.
- vii. The stress difference between the start and end of a rain flow is the stress range and is assigned a half cycle.
- viii. The half cycles of similar magnitude shall then be combined together.

2.2.4 STRESS RANGE AND NUMBER OF CYCLES

The stress range and no. of cycles are obtained from the counting method discussed in the previous section. The passage of a vehicle over a bridge produces a single major stress cycle. One cycle is the smallest segment of stress versus time variation which is repeated periodically. Under variable amplitude loading the definition of one cycle is not clear, therefore reversal of stresses is considered. In constant amplitude loading, one cycle contains two reversals. The difference between maximum stress (σ_{Max}) and the minimum stress (σ_{Min}) corresponding to dead load, is called the stress range ($\Delta\sigma$). The stress range obviously varies with the size of the vehicle, but the minimum stress corresponding to dead load (σ_{Min}) remains essentially constant throughout the life of the bridge (Oka, et al., 1989).

In practice, bridges are always subjected to variable amplitude loading with a compact load spectrum. For the purpose of analysis, it is convenient to represent a complex load spectrum with an equivalent number of simple load cycles. This is particularly helpful for bridge applications since each vehicle passage produces one complex cycle and this can be represented by equivalent number of simple cycles (Oka, et al., 1989).

For most of the metals, it is accepted that the stress which can be withstood for repeated loading does not drop greatly below that which can be resisted for two million cycles. Moreover in design practice two million cycles is considered a suitable maximum life for railway bridges and as a result, it has become conventional to limit fatigue determination to two million cycles. Although lower stress level may not cause any fatigue damage yet when loads cause stresses higher than the fatigue limit, the lower stress become damaging too.

2.2.5 S-N CURVE

The relationship between constant amplitude stress range ($\Delta\sigma$) applied to the specimen and number of cycles up to its failure (N) is called S-N Curve. It is the most common way to describe the fatigue testing data. Generally it is plotted on log-log scale with number of cycles in millions on abscissa and stress range in N/mm^2 on ordinates. The slopping line represents the finite fatigue life of the material. Mathematically S-N curves are defined in log-log form by the following equations:

$$\text{Log } N = \text{Log } a - M \cdot \text{Log } \Delta\sigma \dots \dots \dots \text{Equation 2-a}$$

Where,

Log a is the intercept on x-axis

M is the reciprocal of the slope of the finite life portion of the S-N curve

In normal form N is represented by the following equation

$$N = \frac{a}{(\Delta\sigma)^m} \dots \dots \dots \text{Equation 2-b}$$

2.2.6 MINER'S RULE

In case of bridges, damage accumulation is a continuous process due to the application of varying stress-amplitude. Under service loading, different stress ranges and their corresponding frequencies combine together to cause the fatigue damage

The calculation of residual fatigue life normally takes the form of a damage accumulation calculation. The most commonly used method is the linear Palmgren-Miner damage rule which can be stated that "The damage at a certain stress range is proportional to the number of cycles". The fatigue endurance for a section is given by the maximum number of cycles N for a particular stress range $\Delta\sigma_i$. The effect the number of cycles at a certain stress range has on a detail is compared to the allowable number of cycles and the fatigue life is reached when the accumulated damage equals one. The values of N_i are determined by Wöhler curves for the corresponding value of $\Delta\sigma_i$.

$$\sum_{i=1}^n \frac{n_i}{N_i} = \frac{n_1}{N_1} + \frac{n_2}{N_2} + \dots + \frac{n_n}{N_n} = 1 \dots \dots \dots \text{Equation 2-c}$$

$$D = \sum \frac{n_i}{N_i} \leq 1 \dots \dots \dots \text{Equation 2-d}$$

Where,

n_i = number of cycles occurring at stress range , $\Delta\sigma_i$ of a stress history

N_i = number of cycles corresponding to particular fatigue strength at stress range $\Delta\sigma_i$

Once the fatigue damage is estimated, the residual fatigue life of the bridge elements can be assessed by subtracting the accrued fatigue damage produced by the traffic for the period since preparation of S-N curve.

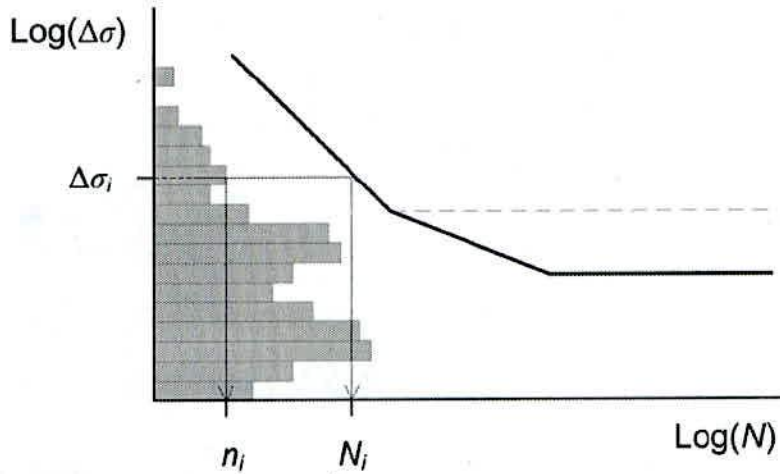


Figure 2.5 – Damage accumulation calculation (Kuehn et al., 2008)

The residual fatigue life can be computed from the following equation

$$\text{Residual fatigue life (in days)} = \frac{D_f - D_a}{D_p} \dots \dots \dots \text{Equation 2-e}$$

Where,

D_f is the fatigue damage sum at failure

D_a is the fatigue damage produced by past traffic

D_p is the fatigue damage produced by traffic during 24 hours

In Palmgren-Miner Hypothesis D_f is taken as unity. D_a would be zero if the S-N curves are generated for undamaged component.

Chapter 3

BEHAVIOUR OF RIVETED STRINGER-TO-CROSS-GIRDER CONNECTIONS

3.1 RIVETED CONNECTIONS

Riveting today has become obsolete due to the popularity of bolted and welded connections, however the method of riveting was used widely before the 1950's to assemble all kind of metal structures and especially civil structures. These days riveting is only used in the aviation sector. Riveting is a unique and ingenious method of connecting steel plates and members together permanently (Åkesson, B. 1994).

The step by step procedure of riveting process is discussed in the following points,

- i. Heating the rivet head to a high temperature of about 1000°C .
- ii. Creating the rivet hole by drilling, punching, sub-drilling and reaming, sub-punching and reaming (Larsson, T. 2009). The diameter of the rivet hole should be at least 1.5 millimetres larger than the nominal diameter of the rivet.
- iii. Hot glowing rivet is inserted into the rivet hole.
- iv. The second head of the rivet is formed by the riveting machine which tends to increase the diameter of the rivet shank and thus fill the gap between the face of the rivet hole and that of the rivet.
- v. When the rivet cools, it contracts in both the longitudinal and radial direction. This contraction thereby helping in joining the plated together.



Figure 3.1- Hot-driven riveting process (Larsson, T. 2009)

Cross section of a hot driven rivet is shown in figure 3.2. The shop head is on the left and the field head is on the right side. It can be seen that there is a large variation in both the heads due to which the load transfer mechanism on both sides will be different.



Figure 3.2 – Cross section of a hot-driven rivet. (Vermes et al., 2011)

3.1.1 CLAMPING FORCE

The contraction of the plate in the longitudinal direction produces tensile force in the rivet and applies a compressive force on the outer plates. This compressive force is known as clamping force. The clamping force of a rivet is not reliable as it is difficult to control during the riveting process. Previous studies have shown that increase in the grip length of the rivets increases the clamping force (Åkesson, B. 1994). This is due to the fact that with increase in length of the rivet, during cooling the tendency to contract is greater than that of a short rivet. But this contraction is restricted by the plates and the residual force generated due to restricted contraction is transferred as a compressive force on the plates. The compressive stress generated in plates is hence known as clamping stress. The dispersion angle of the clamping force applied by the rivet head on the plate is assumed to be 30–45° from the outermost part of the rivet head to the mid-plane of the plates (Åkesson, B. 1994). The variation of clamping force along the thickness of the plates is shown in the figure 3.3.

The clamping force is directly dependent on the driving temperature. A low driving temperature will lead to a low clamping force. Also, the surface treatment and surface finish is of great importance to obtain good clamping force (Åkesson, B. 1994).

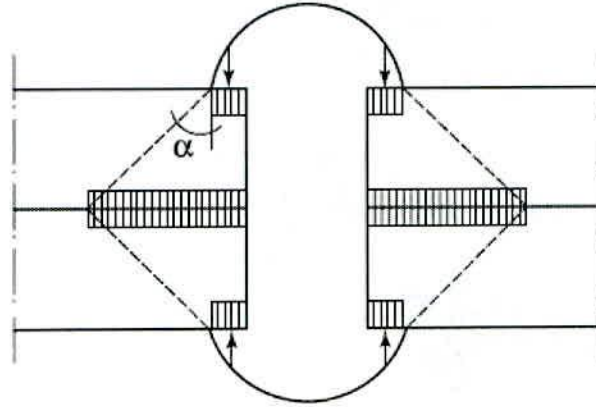


Figure 3.3 – Rivet clamping force distribution (Åkesson, B. 1994)

Clamping force in a group of rivets in the same connection may vary depending on various reasons. Åkesson, B. (1994) carried out certain experiments to find out the clamping stress in the rivets extracted from old bridges which were in service for more than 50 years. Among the nine rivets tested, the maximum clamping stress was found to 189 MPa and minimum was 110 MPa. The average value was 151 MPa. This shows that, the actual clamping stress in a rivet usually lays between 100 MPa and 200 MPa. The average clamping stress in a rivet can be considered to be 150 MPa. Over a period of time, there can be a loss in the rivet clamping force. The causes of this loss can be corrosion, faulty workmanship, etc. A plastic deformation of a rivet also can lead to a release or in a worse case a total loss of clamping force, which drastically lowers the fatigue endurance (Imam et al., 2006).

3.2 TENSION CONNECTIONS

The clamping force in the rivet and the stiffness of the connecting angle influences behaviour of riveted connections exposed to tension. According to Larsson, T., (2009) there are three different scenarios for load transfer in riveted connections subjected to tension as shown in figure 3.4. The riveted connection is exposed to an external load of $2F$.

Scenario 1: In this scenario, the connecting angles are considered to be rigid and their stiffness is much more higher than the rivets. The equally divided external load is transferred equally to the two rivets. When the tensile force in each rivet F equals the clamping force of the rivets, the angles separates from the back wall.

Scenario 2: If the stiffness of the connection angles is less than the rivets, the outstanding legs of the connections angles bend and deform due to the loading of the external force. In this case the angle separates from the back wall. The largest separation occurs in the middle

of the connection. In this case, minimum deformation occurs in the rivet as angle deforms flexing in the direction of external load.

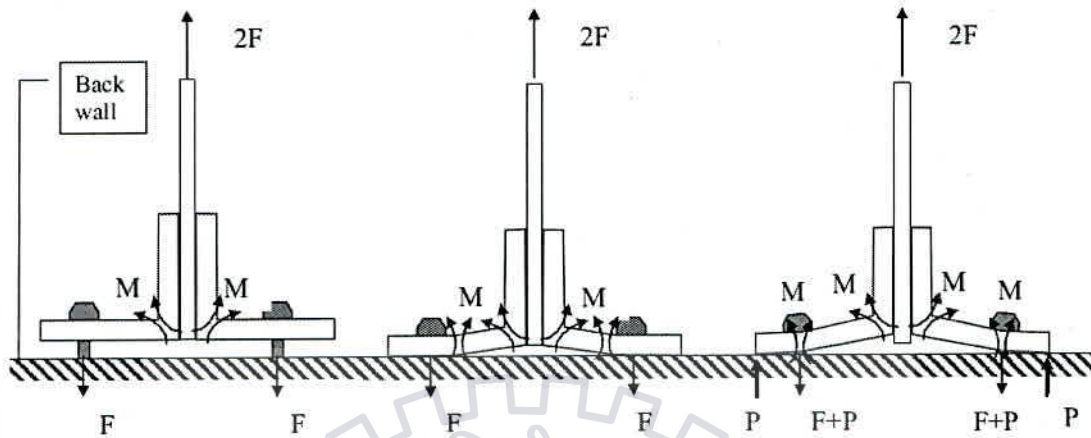


Figure 3.4 – Deformation scenarios in tension connections depending upon stiffness of rivets and connecting angles (Larsson, T., 2009)

Scenario 3: In this case too, the stiffness of the connection angles is less than the rivets. In this scenario, the angles separate from the back wall as a combination of deformation of the angles and the rivets. Additional axial and bending stresses originates in the rivet due to this prying action, the increase of force in the rivet is directly related to the bending and axial stiffness of the rivet and the angles (Al-Emrani and Kligler, 2003).

The most common causes of deformations in riveted bridges are scenario 2 and 3 causing fatigue cracking in angles and also can cause plastic deformations of the rivets.

3.3 SHEAR CONNECTIONS

In case of shear connections, the shear force is transferred through a mix of friction between the connecting faces and shearing of rivets. The frictional coefficient between the faces depends upon the clamping force in the rivets. The clamping force in a rivet may vary but still be enough to transfer some shear by friction. Initially the forces are transferred by friction at the ends of the joints, but as the load increases the friction zone extends towards the centre of the connection until the friction resistance is exceeded (Larsson, T., 2009). Bearing stress is produced when the frictional resistance is exceeded and the joint slips. With increase in load, the end rivets and the holes deform until all rivets are in bearing. The fatigue life of riveted connections is highly affected by the bearing ratio (Al-Emrani and Kligler, 2003). Due to increase in bearing ratio, the fatigue strength of riveted connections decreases because of the increase of stress concentration at the edge of the rivet hole. To avoid the slip in connection, the frictional resistance is important which is achieved by adequate clamping

force. As mentioned earlier the amount of clamping force in rivets differ and therefore the common engineering practice when assessing riveted shear connections is to disregard the effect of friction, and only treat them as a pure shear connection. (Al-Emrani and Klinger, 2003).

3.4 FATIGUE CRITICAL LOCATIONS IN STRINGER-TO-CROSS-GIRDER CONNECTIONS

For the same passage of train, different locations in a truss bridge may experience totally different kind of fatigue stresses. The stress range at the two locations may be same but the number of cycles of a particular stress range may be different at the two locations. The influence length of a truss member is equal to the span of the truss bridge. However, in comparison to this, the influence length of a stringer which is simply supported between cross girders, is equal to the c/c distance between the cross girders which is in fact the span of the stringer. Due to this, a stringer will be subjected to a substantially high number of stress cycles for the same train as compared to that of a truss member. The number of stress cycles for the truss member will be one whereas for the stringer, it can be the same as that of the number of axles in the vehicle crossing over the bridge (Åkesson, B., 1994).

The stringer-to-cross-girder connection is one of the most difficult non-moment resistant joint to design for failure. The connection is bound to have certain flexural stiffness in lieu of making the connection more shear resistant. Hence the connection will resist some longitudinal bending moment additionally. Due to this, it has been a major practice to connect only the stringer web to web of the cross girder with the help of connecting angles.

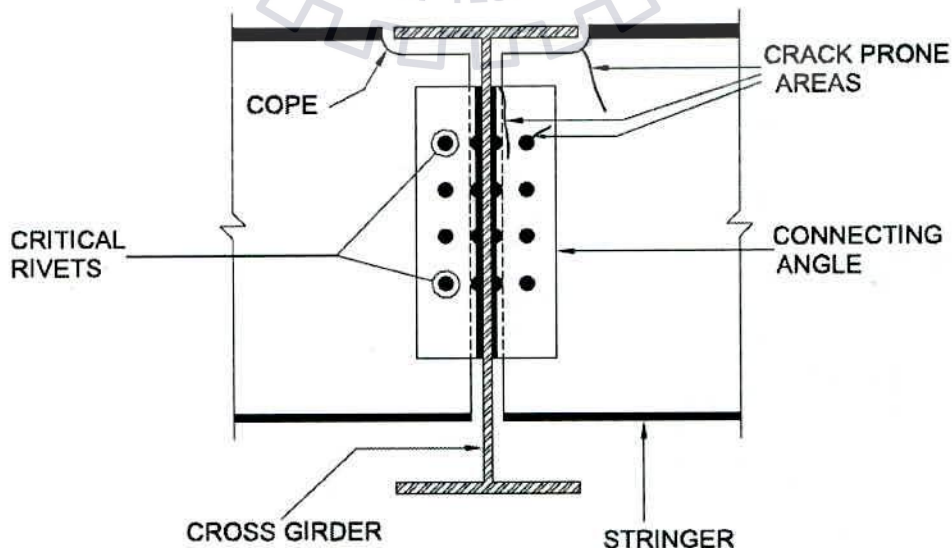


Figure 3.5 – Fatigue critical locations in a Stringer-to-cross-girder connection

The common mode of failure of a stringer-to-cross-girder connection is the shear failure of rivets, cracking of connection angle at the angle fillet, cracking of stringers at the cope, cracks originating from rivet holes, etc. The fatigue critical locations listed above are shown in figure 3.5.

Failure of rivets is one of the most critical aspects of the stringer-to-cross-girder connections. Mostly, it is one rivet at the extreme corner that fails first. But it will lead to overloading of the other rivets present in the connection, thereby exceeding their design capacity. After being subjected to sufficient number of repetitive cyclic loading, the rivet shank will fail in shear and the rivet head will snap off the connection. Figure 3.6 and figure 3.7(a) shows a rivet which failed at the shank and the rivet head has come apart.



Figure 3.6 – Failure of rivet shank under fatigue (Åkesson, B., 1994)

The other critical failure pattern in a stringer-to-cross-girder connection is the failure of connection angles. Imam et al., (2007) have shown that the angle fillet and rivet holes are the most critical locations for origination of fatigue cracks in case of connecting angles. Figure 3.7(b) shows a vertical crack running along the angle fillet. Imam et al., (2007) have observed that with the increase in the clamping stress of rivet, the angle fillet becomes more susceptible to fatigue damage and if the clamping stress is less, the rivet and rivet holes are more prone to fatigue damage.

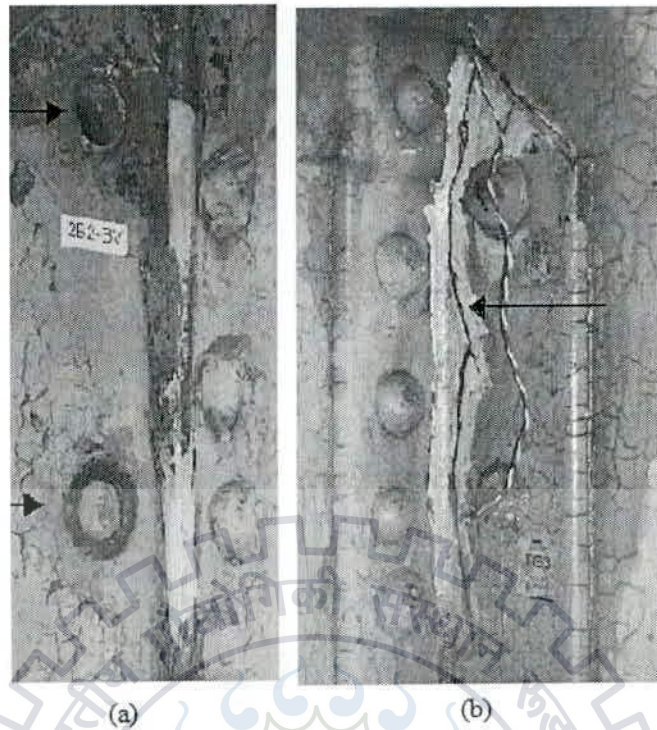


Figure 3.7 – (a) Complete loss of rivets due to failure of rivet shank. (b) Crack propagating in a connection angle (Haghani, et al., 2012)

Failure of the stringer beam itself is the third scenario in the fatigue failure of stringer-to-cross-girder connections. The cope of a stringer is a location of high stress concentration. The fatigue crack tends to grow from this location. Figure 3.8 shows the crack propagation from such location. To avoid such a scenario, curved cope shall be used instead of right angled ones. However, even in curved copes, crack is seen to develop and propagate in radial direction.

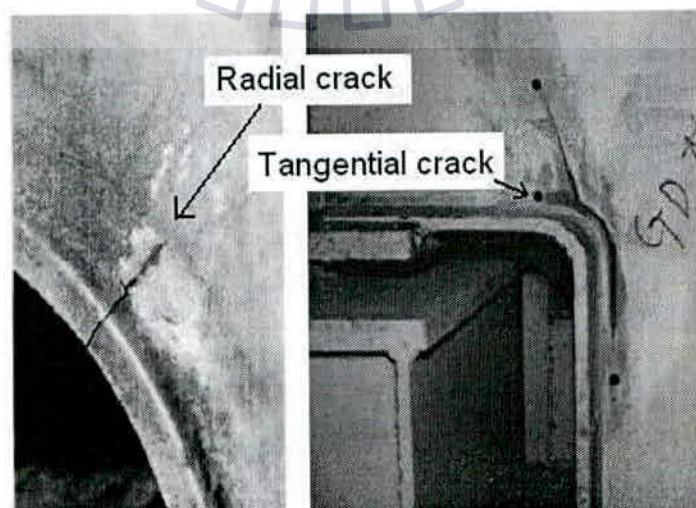


Figure 3.8 – Crack propagating from coped girder (Haghani, et al., 2012)

Chapter 4

MODELLING OF RIVETED CONNECTION IN ABAQUS-CAE

4.1 GENERAL

Before advancing into modelling a riveted connection in its actual form as close as to the real connection in ABAQUS-CAE, we should understand the nuances involved in such modelling. It is important to understand the method of incorporating the clamping force of rivet and frictional contact between different components like connection angle-cross girder, connection angle-stringer, connection angle-rivet, etc.

To tackle this situation, previous researchers Imam et al., (2007) and de Jesus et al., (2010) have used a simple double lap joint as a benchmark study. In the present study, an effort has been made to model the same double lap joint and compare the results available in the previously stated literature to validate the methodology adopted.

It was also required to ensure that the finite element model of the connection prepared in ABAQUS-CAE behaves as expected. Therefore a benchmark study on effect of clamping stress of rivet on deflection of the connection was carried out. Both the benchmark studies stated above are discussed in detail in the following sections.

4.2 RIVETED DOUBLE LAP JOINT

A finite element model of a riveted double lap joint having a single rivet and three plates is discussed in this section. The dimensions of the lap joint have been taken to be same as that considered by Imam et al., (2007) and de Jesus et al., (2010). The details of the lap joint are shown in figure 4.1. The thickness of the top and bottom plate is 9.5mm each and that of the middle plate is 11.1 mm. The diameter of the rivet is 25.4 mm. The width of the cap was considered to be 1.6 times the diameter of the rivet and the depth of the cap was considered to be 0.7 times the diameter of the rivet. Therefore, the width of cap was taken as 40.64 mm and the depth of the cap was taken as 17.78 mm.

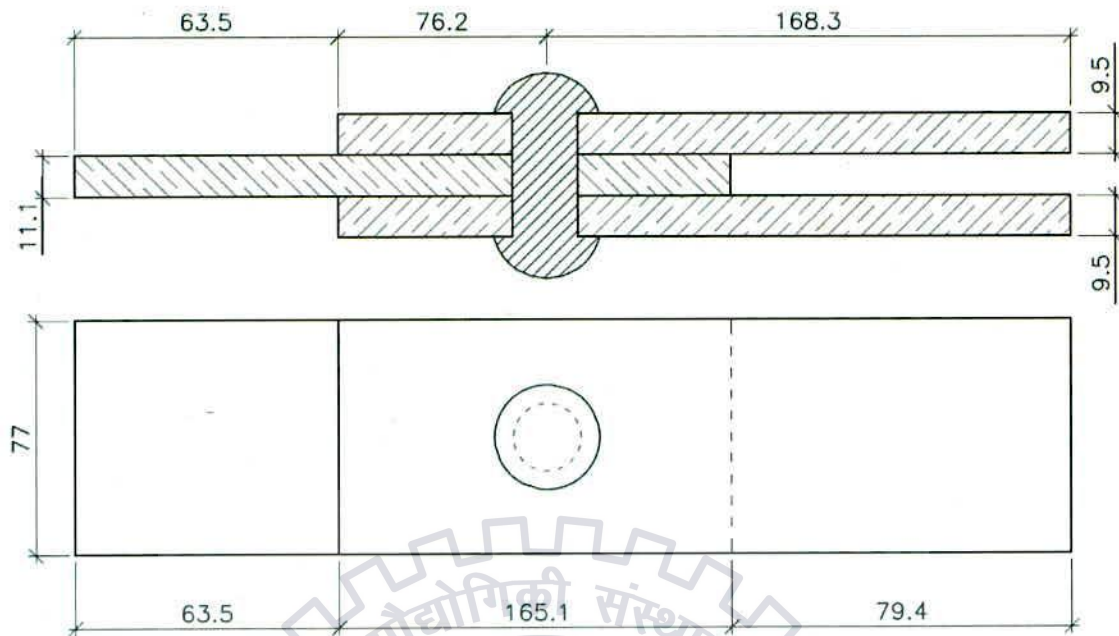


Figure 4.1 – Dimensions of the riveted double lap joint

4.2.1 **MODELLING**

The assembly of the riveted lap joint model is shown in the figure 4.2. The meshing of rivet and plates was carried out using the “SWEEP” command in ABAQUS. The finite element mesh consists of 21382 nodes and 17088 elements. C3D8 brick element was used for all the parts. Linear elastic behaviour is considered for the finite element analysis. Young’s Modulus (E) for steel was defined as 2×10^5 MPa and Poisson’s ratio (ν) of 0.3 was considered.

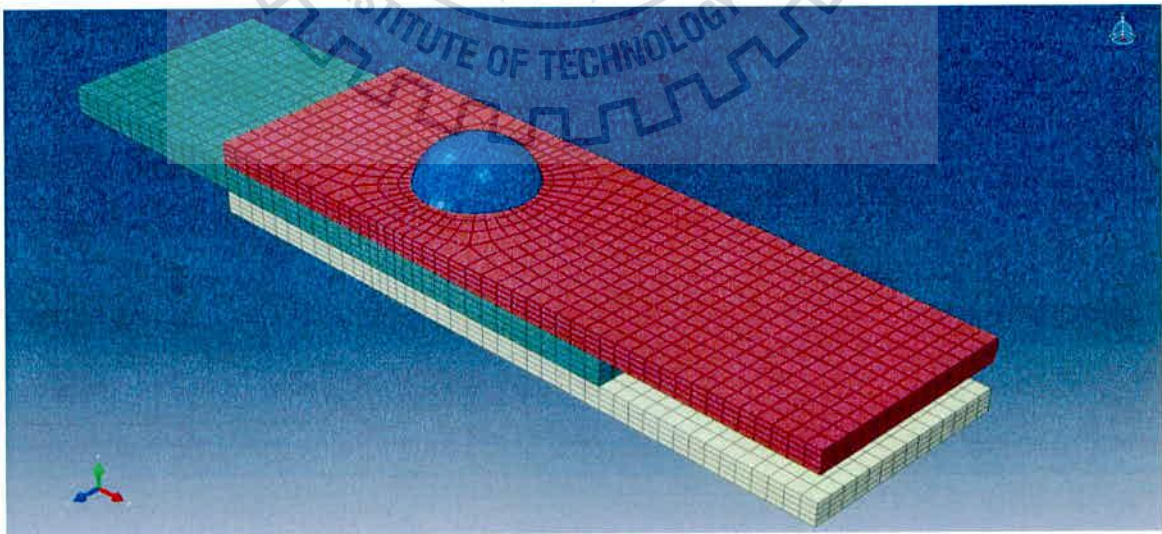


Figure 4.2 – Finite element model of the riveted double lap joint

4.2.2 BOUNDARY CONDITIONS AND INTERACTION

The top and bottom plates are restrained against translation in the longitudinal direction. All the three plates are restrained against translation in the transverse direction. The surfaces which were assigned the boundary conditions are shown in figure 4.3. The surfaces highlighted in green are restrained in longitudinal direction and the surfaces highlighted in red are restrained in the transverse direction.

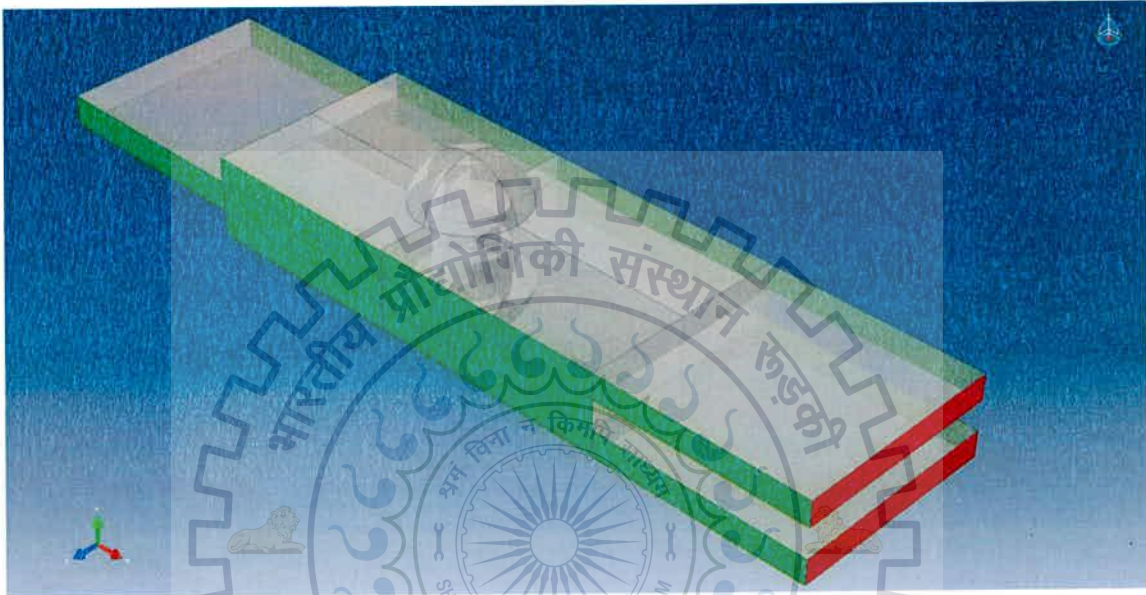


Figure 4.3 – Highlighting the boundary conditions of the double lap joint

To model the frictional contact between the plates, the contact properties available in ABAQUS was used, which is based on the Coulomb friction model. Using the “SURFACE TO SURFACE” contact property, the “PENALTY” friction formulation was adopted under the “TANGENTIAL BEHAVIOUR” command. The friction coefficient between the plates was considered to be 0.3. Under “NORMAL BEHAVIOUR” command, “PRESSURE-OVERCLOSURE” was selected as “HARD CONTACT” and provision was made to allow separation after contact.

Once the contact properties are defined, they are assigned to the model using the interaction properties command. The interaction property command demands to define the master and slave surfaces for interaction. In case of the interaction between rivet and plates, rivet surfaces was considered to be master and the plate surface was considered to be slave. In case of interaction between the plates, the surfaces of the inner plate were considered to be master and the surfaces of the outer plates were considered to be slave. The surfaces which were assigned interaction properties are shown in figure 4.4. The surfaces highlighted in green

indicate the surfaces pertaining to frictional contact between the rivet and the outer plates. The surfaces highlighted in blue indicated the surfaces pertaining to frictional contact between the middle plate and outer plates.

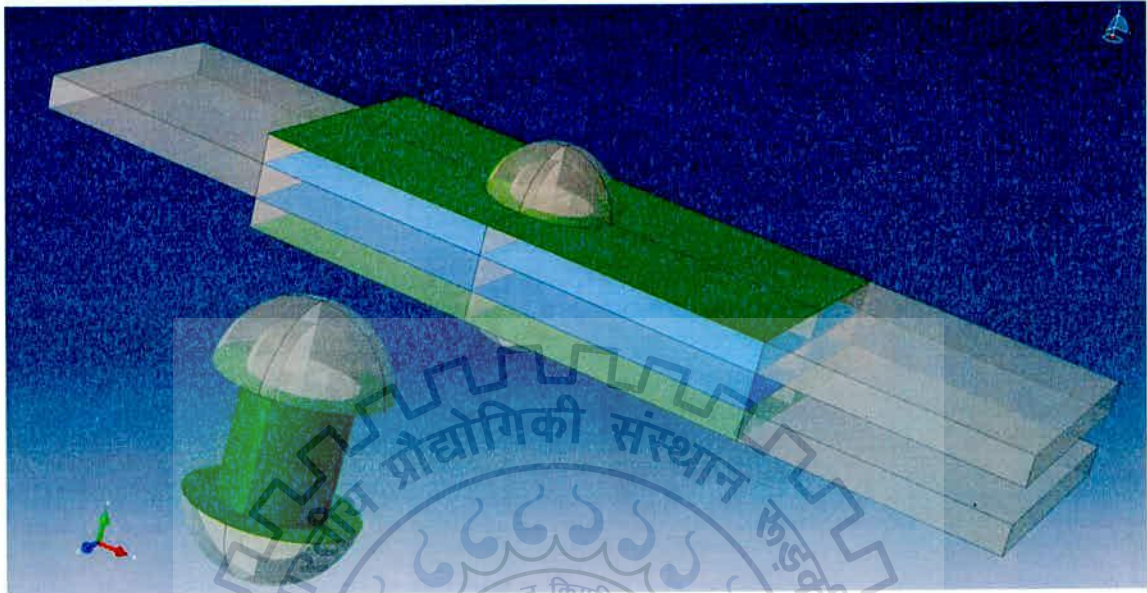


Figure 4.4 – Interaction surfaces for friction modelling

4.2.3 APPLICATION OF CLAMPING FORCE

The clamping stress of the rivet was varied to get the response of the lap joint to variation in clamping force of the rivet. The clamping force of the rivet was assigned using the “BOLT LOAD” command available in ABAQUS. For assigning this load, we have to select a surface at the centre of the rivet shank as shown in figure 4.5.

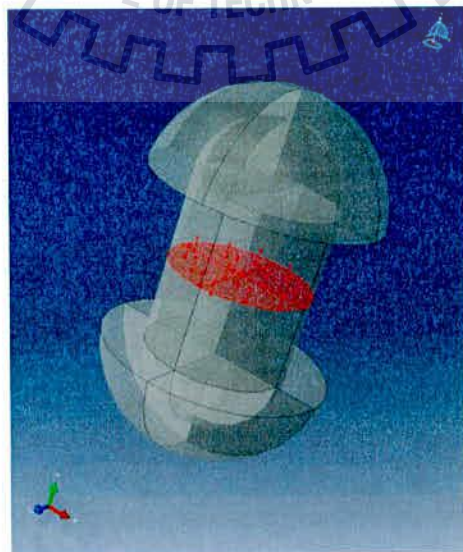


Figure 4.5 – Internal surface of rivet selected for application of bolt load in ABAQUS

The load to be applied is obtained by multiplying the clamping stress required with the area of rivet cap in contact with the outer plate. The values of bolt force applied in ABAQUS for different clamping stresses and their corresponding area of contact are tabulated in table 4.1 below.

Table 4.1 – Clamping Stress and Bolt force in ABAQUS

Clamping Stress [MPa]	Contact Area [mm ²]	Bolt Force [N]
0	790	0
1	790	790
5	790	3952
25	790	19762
50	790	23523
75	790	59285
100	790	79046
150	790	118570
200	790	158093

4.2.4 APPLICATION OF EXTERNAL LOAD

The external load in the form of uniform surface pressure $P = 30$ MPa was applied on the middle plate in longitudinal direction, opposite to that the restraints in the outer plates. The load applied on the plate is shown in the figure 4.6.

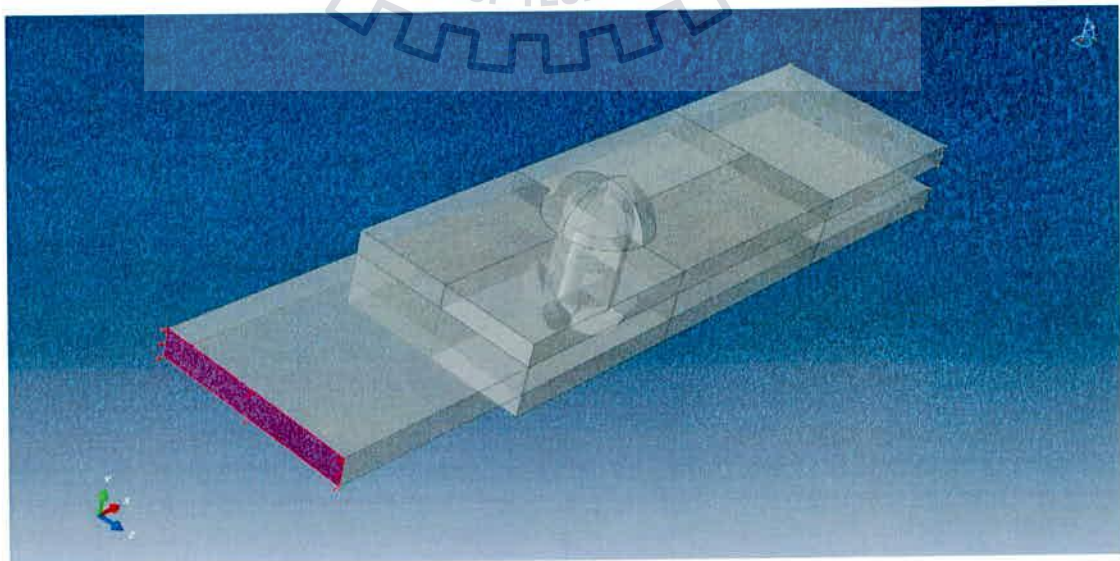


Figure 4.6 – Application of 30 MPa axial stress as external load on the middle plate

4.2.5 RESULTS

Multiple models having clamping stress of 0MPa, 1 MPa, 25 MPa, 50 MPa, 75 MPa, 150 MPa and 200 MPa were analysed and the results were extracted. The variation of axial stress in the rivet due to clamping force is shown in figure 4.7.

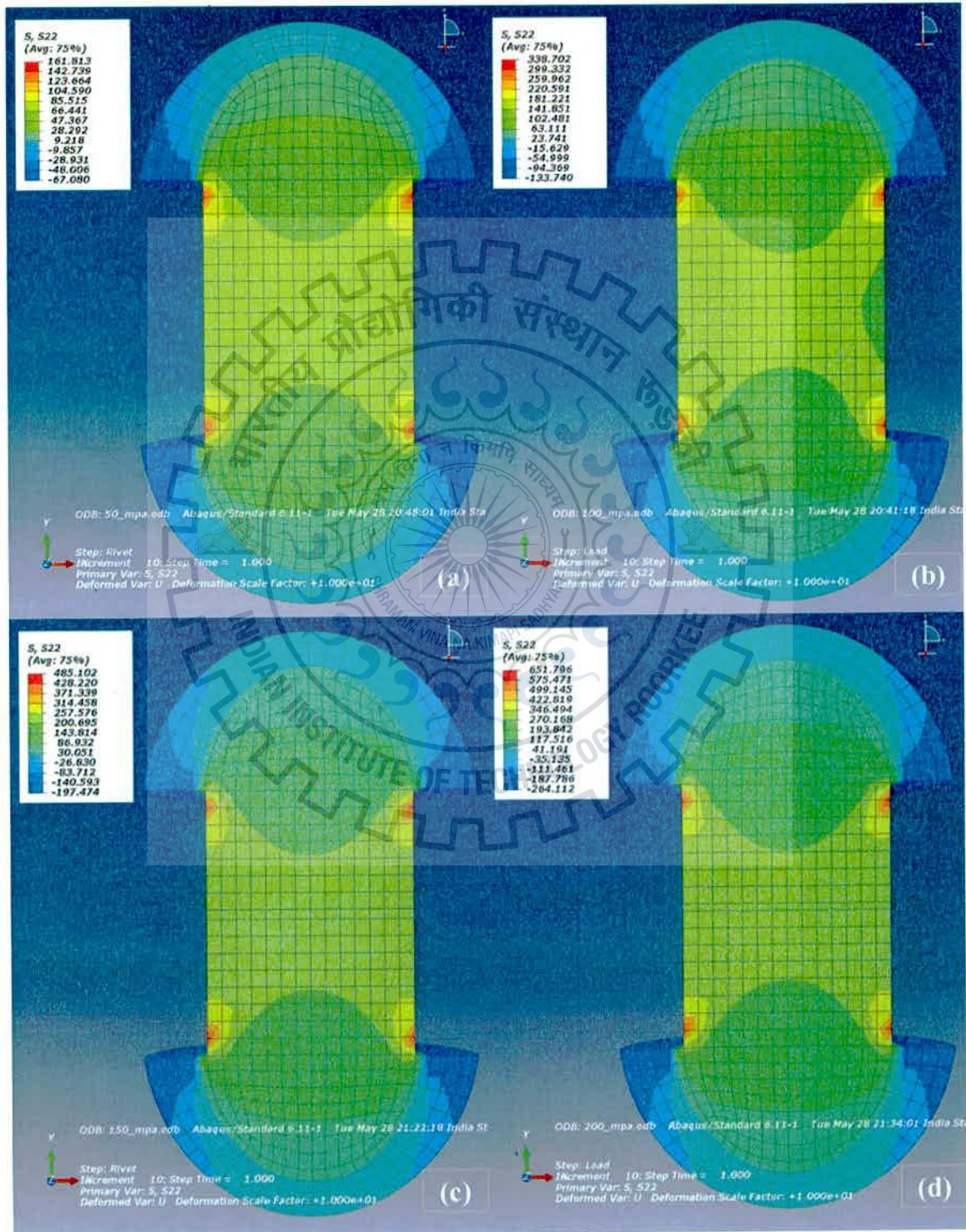


Figure 4.7 – Axial stress in rivet for different clamping stress. (a)50 MPa, (b)100 MPa, (c)150 MPa, (d)200 MPa

The deformed shape of the lap joint for 1 MPa rivet clamping stress and 30 MPa longitudinal stress is shown in the figure 4.8. The deformed shape of the rivet is shown in figure 4.9.

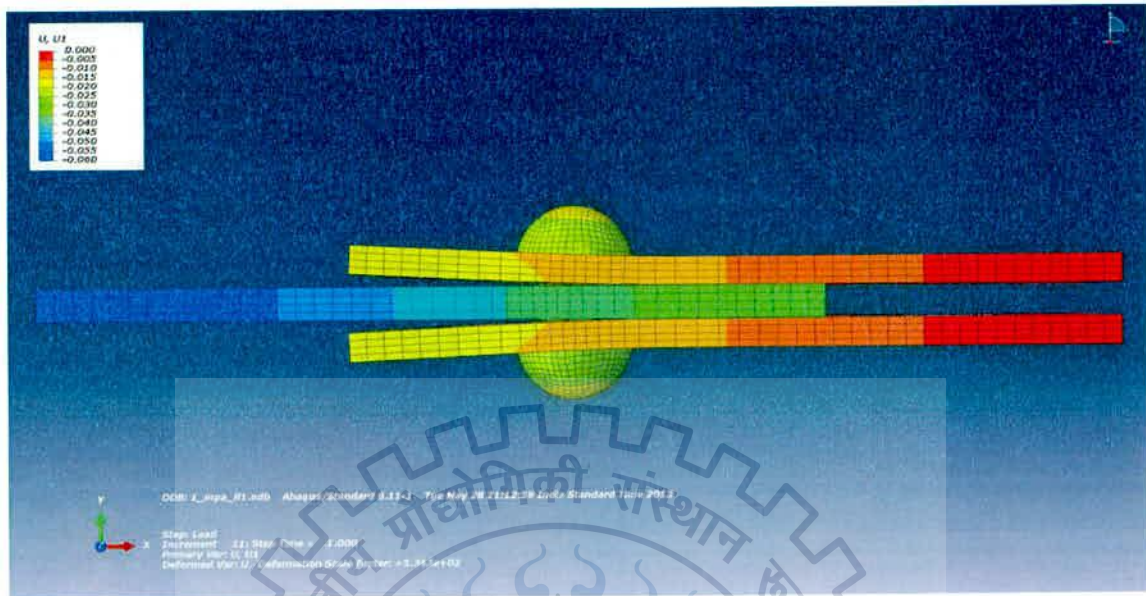


Figure 4.8 – Deformed shape of the riveted double lap joint for externally applied 30 MPa axial stress in the middle plate

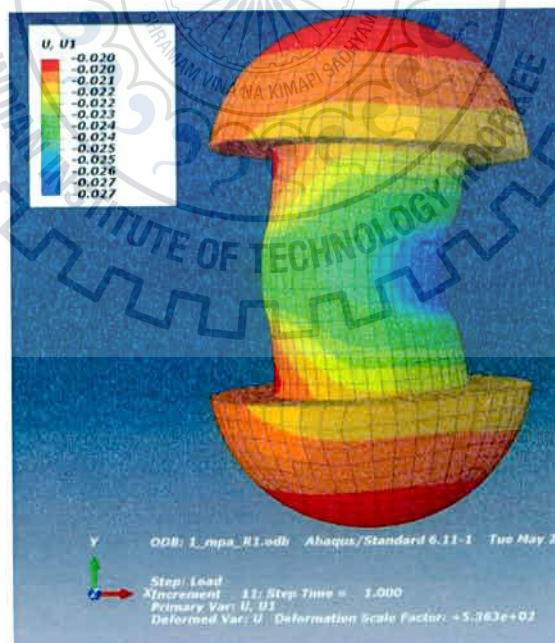


Figure 4.9 – Deformed shape of the rivet for externally applied 30 MPa axial stress in the middle plate

The bearing stress in the rivet is shown in the figure 4.10.

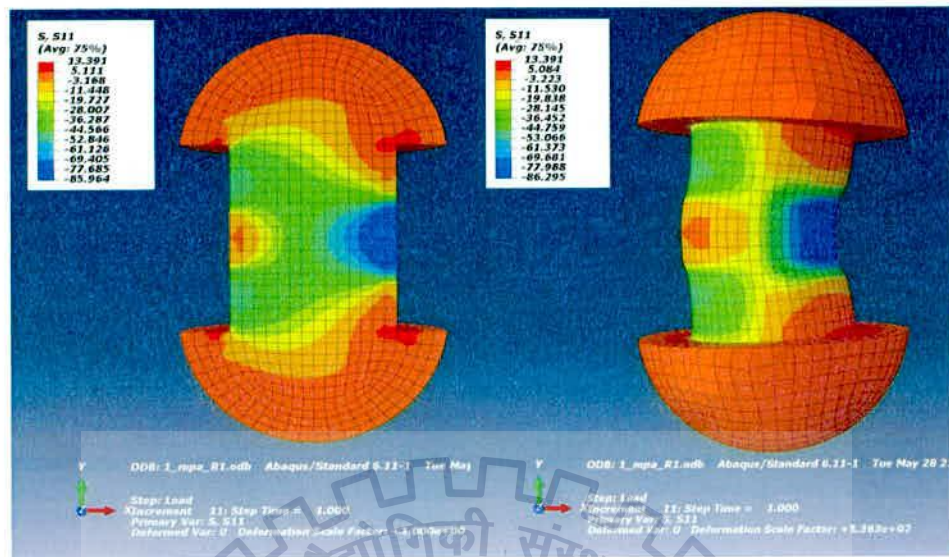


Figure 4.10 – Bearing Stress in the rivet for externally applied 30 MPa axial stress in the middle plate

The longitudinal stress in the middle plate is shown in the figure 4.11.

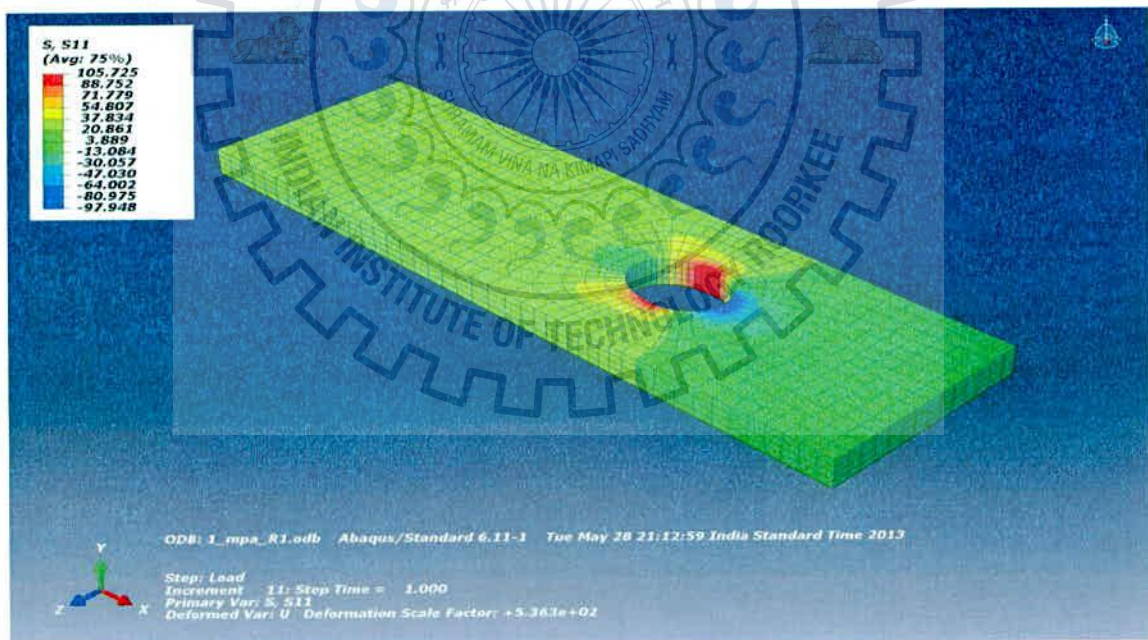


Figure 4.11 – Longitudinal stress in the middle plate of the riveted double lap joint for externally applied 30 MPa axial stress in the middle plate

The results obtained for the lap joint are presented in the form of Stress Concentration Factor (SCF). “Stress Concentration Factor is defined as the ration between the maximum stress at the surface of the rivet hole, in the loading direction, and the uniform net stress, evaluated in

the plate cross section containing the rivet axis and is normal to the loading” (Rodrigues *et al.*, 2011). As per the above definition, the SCF is given by the following expression.

$$SCF = \frac{\sigma_{max}}{\sigma_n} \dots \dots \dots \text{Equation 4-a}$$

Where,

σ_{max} = maximum stress at the surface of the rivet hole,

σ_n = uniform net stress,

The values of SCF were computed for different clamping stress and the results obtained were compared with the results of de Jesus *et al.*, (2010).

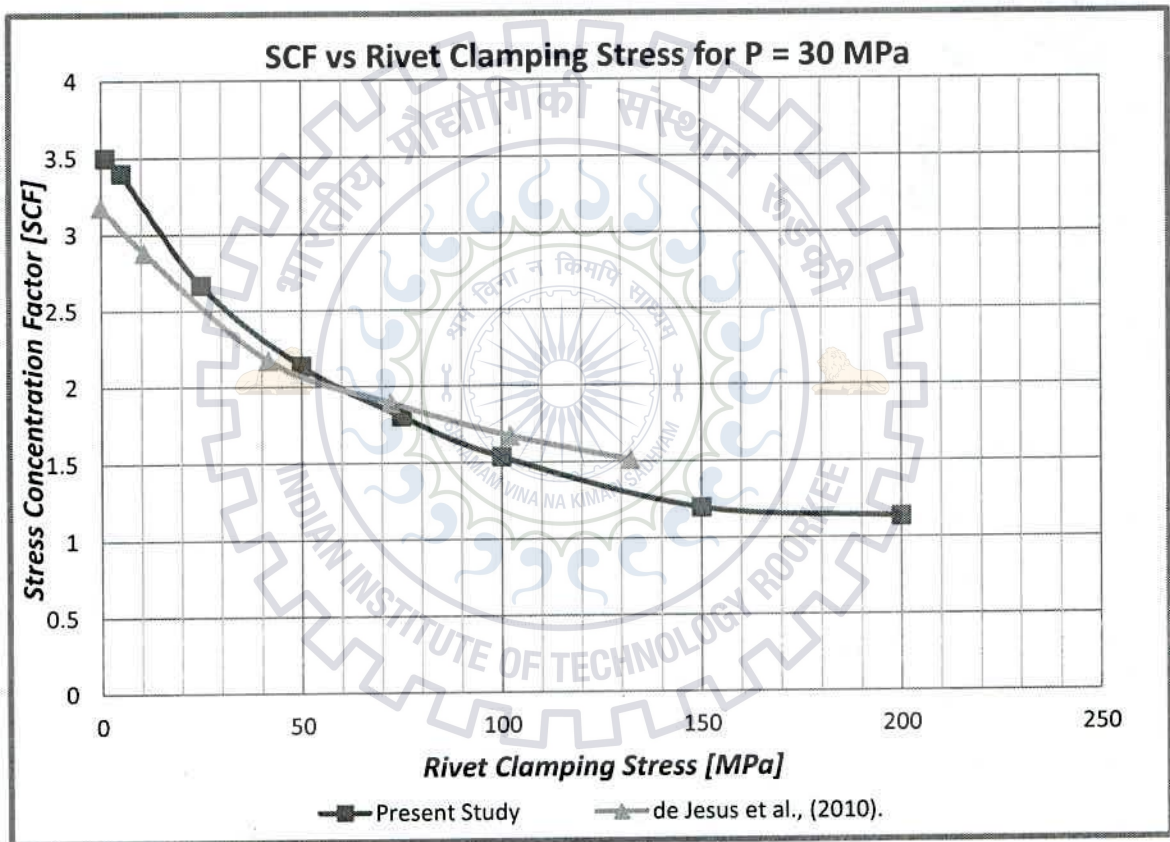


Figure 4.12 – Stress Concentration Factor vs Rivet clamping stress in the middle plate for externally applied 30 MPa axial stress applied in the middle plate.

4.3 STRINGER-TO-CROSS-GIRDER CONNECTION

Using the modelling techniques discussed above for a riveted lap joint, a local bridge connection model is developed. The connection is a stringer-to-cross-girder connection, which is a part of a truss bridge having a span of 60m. The details of the truss bridge will be discussed in the next chapter. . The total width of the bridge is 5.4m. The bridge has three stringers running longitudinally with c/c distance of 2m. The cross girders are spaced at 5m c/c. Therefore the length of each stringer is 5m and that of the cross girder is 5.4m. The stringer is connected to the cross girder with the help of two connection angles ISA 75 x 75 x 10. The stringer is of ISMB 500 and the cross girder is of ISWB 600. The connection between stringer and cross girder is predominantly a shear connection. The rivets here are susceptible to fail under shear. The nominal diameter of the rivet is 22 mm. The outer diameter of the cap is 35.2mm and the depth of the rivet cap is 15.4 mm.

A similar analysis of a riveted stringer-to-cross-girder connection was performed by Imam et al., (2007). Similar approach is applied here. A single stringer-to-cross-girder connection was considered for analysis. The central stringer was considered to be the most critical among the three stringers. Hence it was considered for analysis. The full length of the stringer was considered for the analysis and was modelled. The cross girder was modelled up to the adjacent stringer. The details of the connection are shown in the figure 4.13.

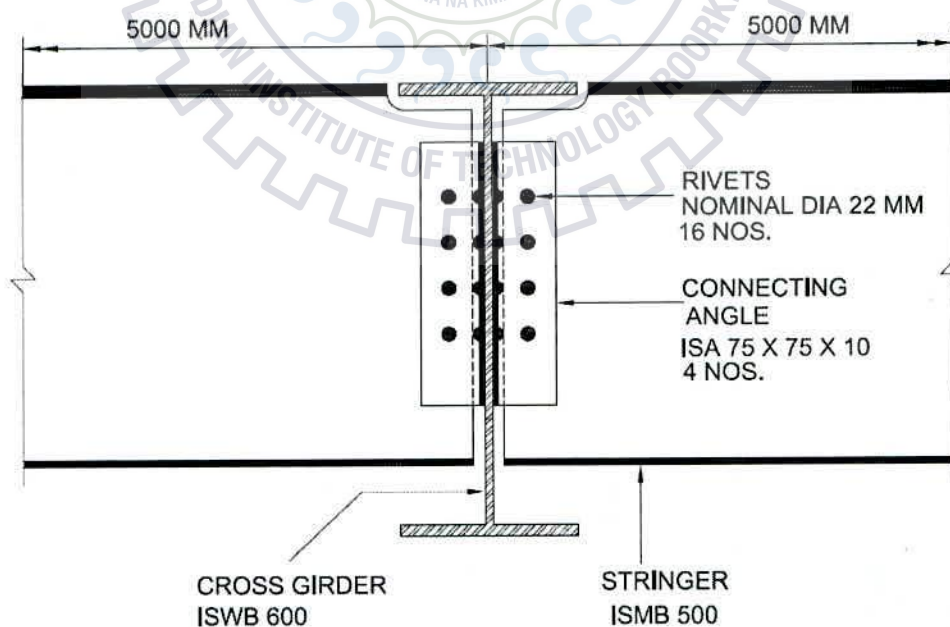


Figure 4.13 – Details of the connection

4.3.1 MODELLING

Linear elastic behaviour is considered for the finite element analysis. Young's Modulus (E) for steel was defined as 2×10^5 MPa and Poisson's ratio (ν) of 0.3 was considered. The rivets and connection angles were modelled using 8- node (C3D8) solid elements. A part of the stringer and cross girder, 500 mm on either side of the connection is modelled using the same 8-node solid elements.

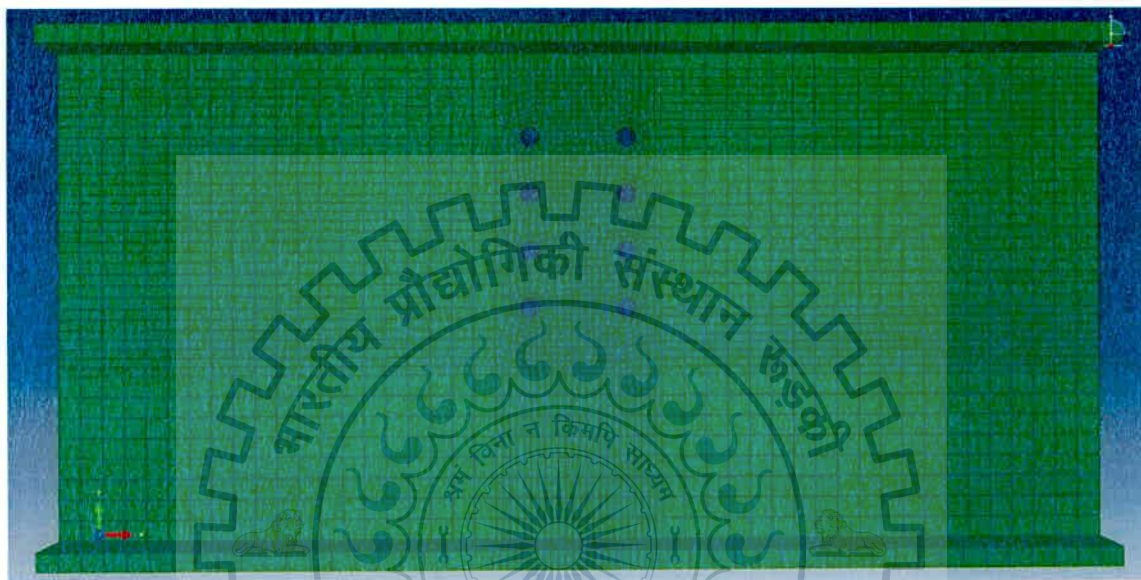


Figure 4.14 – Local model of the cross girder using solid elements for a length of 1000mm

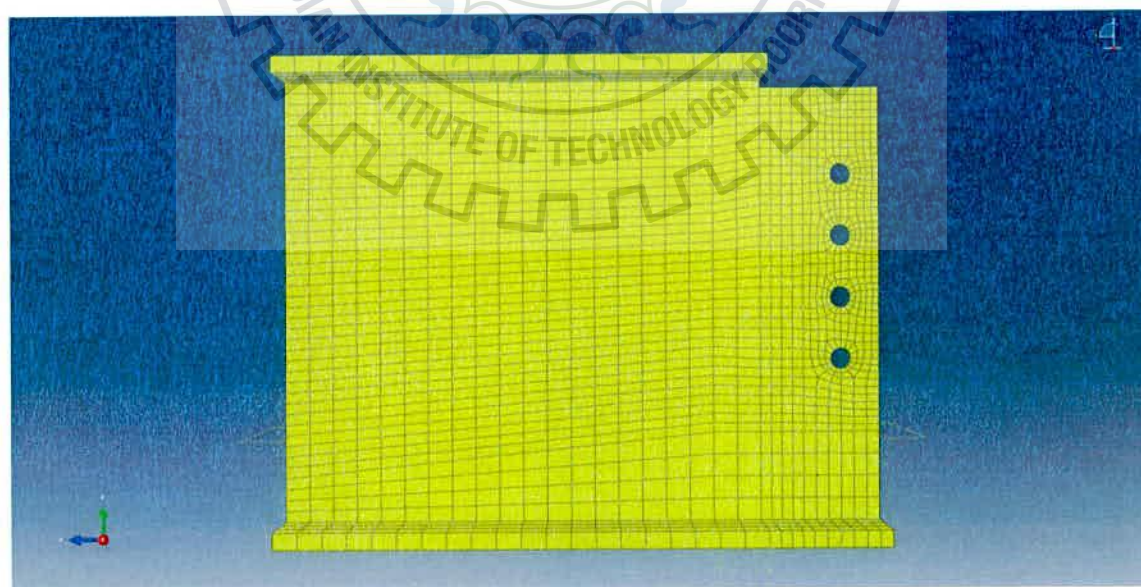


Figure 4.15 – Local model of the stringer using solid elements for a length of 500mm.

The rest of the stringer and cross girder is modelled using 4-node (S4) shell element. The “SHELL TO SOLID” constraint command available in ABAQUS was used to model

interface between the shell and brick elements. The FE model of the cross girder is shown in the figure 4.16. The portion in green is the zone of having 8-node solid elements and the portion of the beam in orange has been modelled using 4-node shell element. Figure 4.18 shows the shell to solid interface. The interface zone is highlighted in red. Figure 4.17 shows the FE model of the stringer. The portion in yellow is modelled using 8-node solid element and the portion in blue is modelled using 4-node shell element.

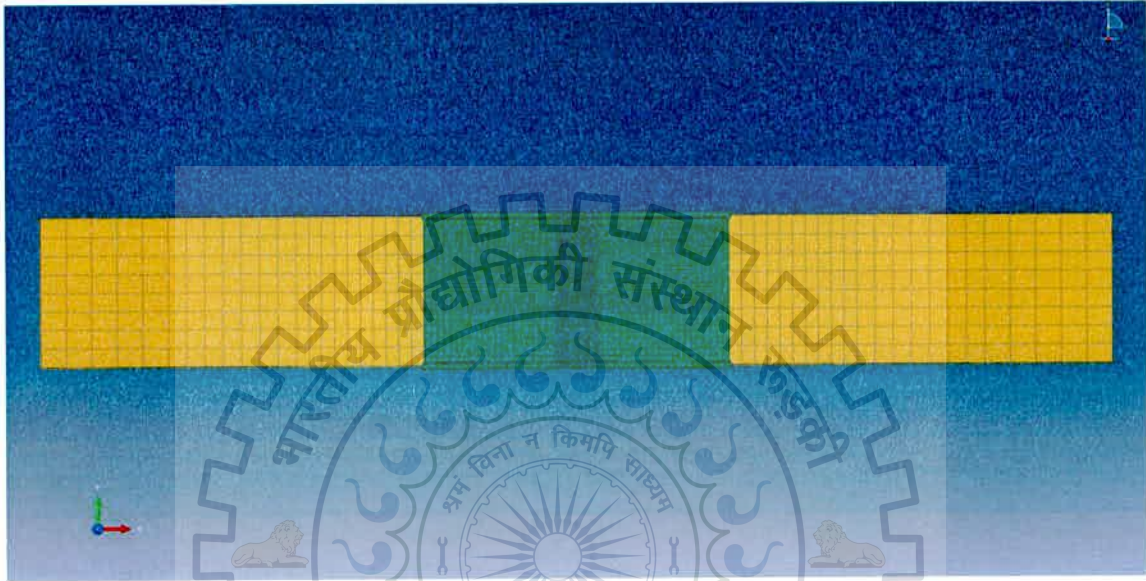


Figure 4.16 – Complete model of the cross-girder comprising of Solid and Shell elements

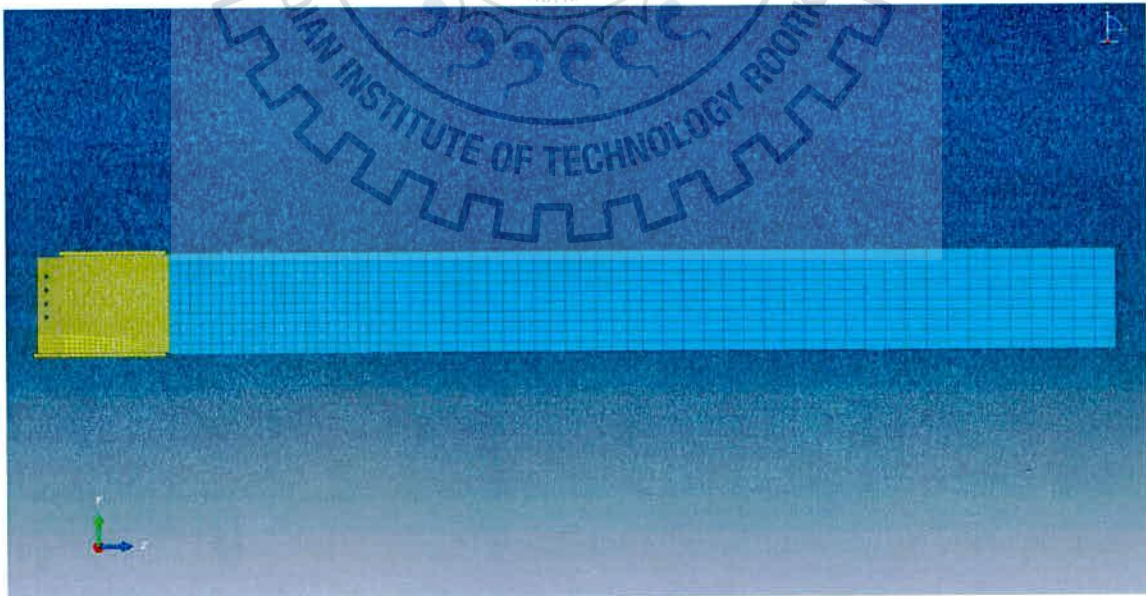


Figure 4.17 - Complete model of the stringer comprising of Solid and Shell elements

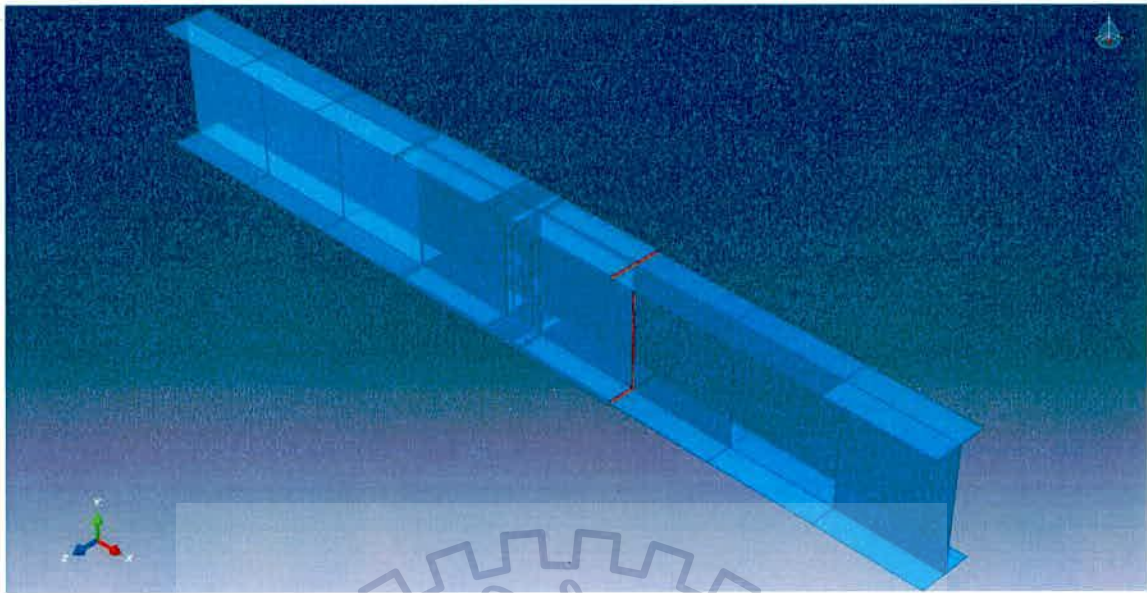


Figure 4.18 – Location of Shell to Solid constraint in cross-girder

The FE model of the connection angle is shown in figure 4.19(b). The connection angle has been modelled using 8-node brick elements. Similarly the rivets have been modelled using 8-node solid elements. The FE model of the rivet is shown in the figure 4.19(a).

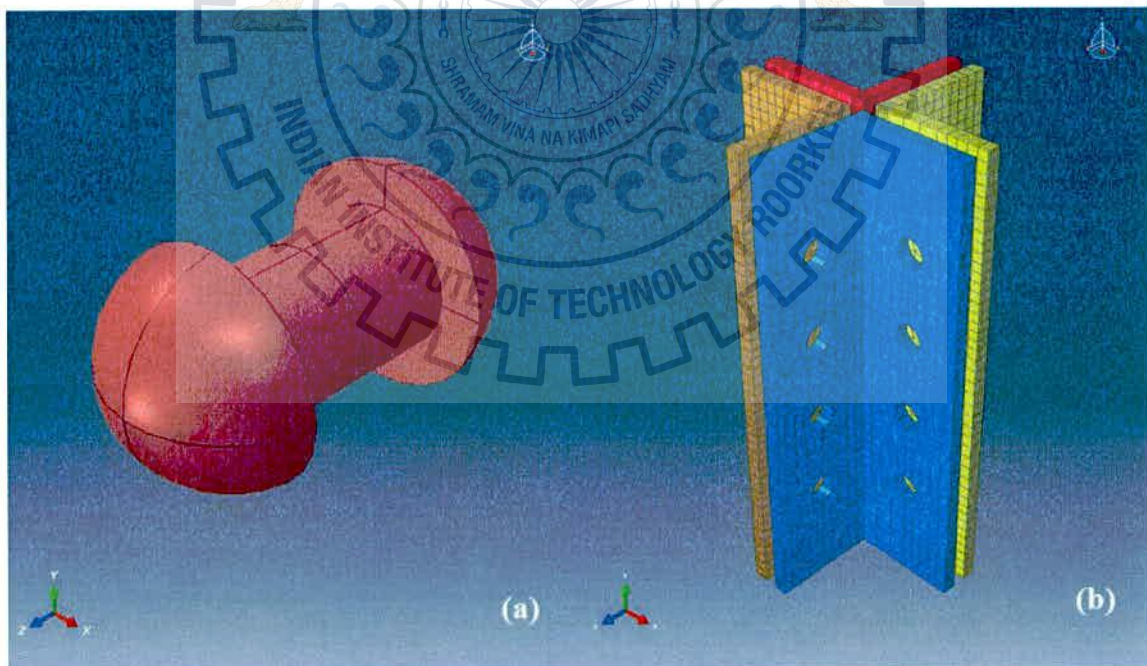


Figure 4.19 – (a) Finite element model of the rivet.
(b) Finite element mesh and arrangement of connecting angles

The assembly of complete connection for a length of 500mm on either side of the connection is shown in the figure 4.20. The local connection model in this zone is modelled using 8-node solid elements as discussed earlier.

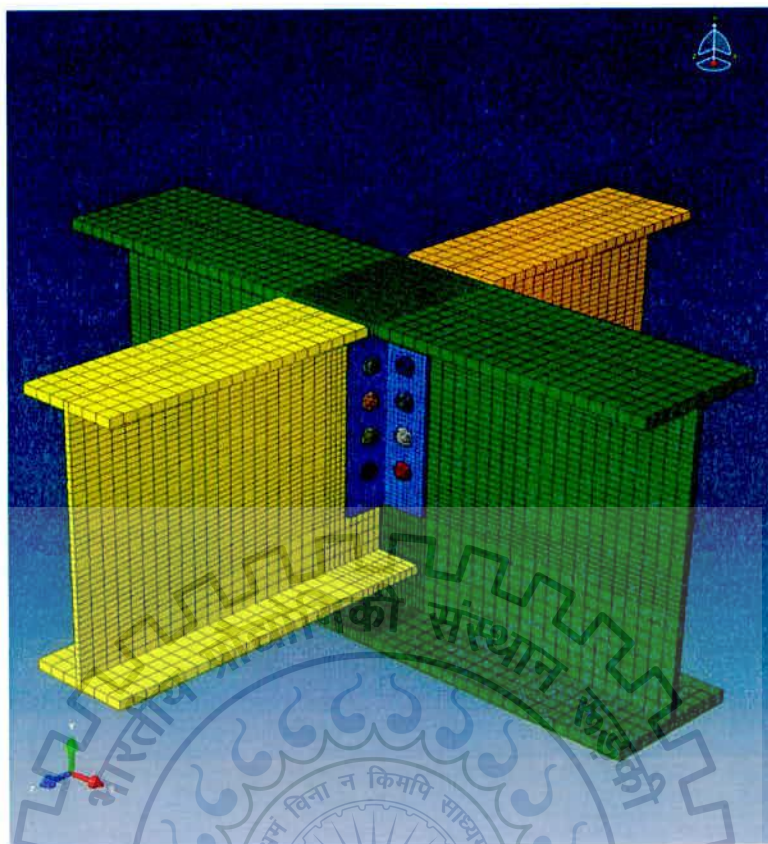


Figure 4.20 – Assembly of the stringer-to-cross-girder connection showing only the solid element mesh

The entire local analysis model of the connection comprising of the full length of stringers and the cross girder is shown in the figure 4.21. The zone outside the local connection shown in figure 4.21 coloured orange and blue has been modelled using 4-node shell elements.

The finite element mesh of the complete model is shown in the figure 4.22. A combination of “SWEEP” and “STANDARD” meshing technique was used to mesh the components according to the geometry to obtain a consistent mesh. The finite element mesh comprises of 117983 solid elements 9(C3D8), 2864 shell elements (S4) and 149210 nodes.

The boundary conditions applied to the model are restraint against translation in the three global directions at the extreme edges of the stringers and cross girder. The edges pertaining to the applied boundary conditions highlighted in red in the figure 4.23.

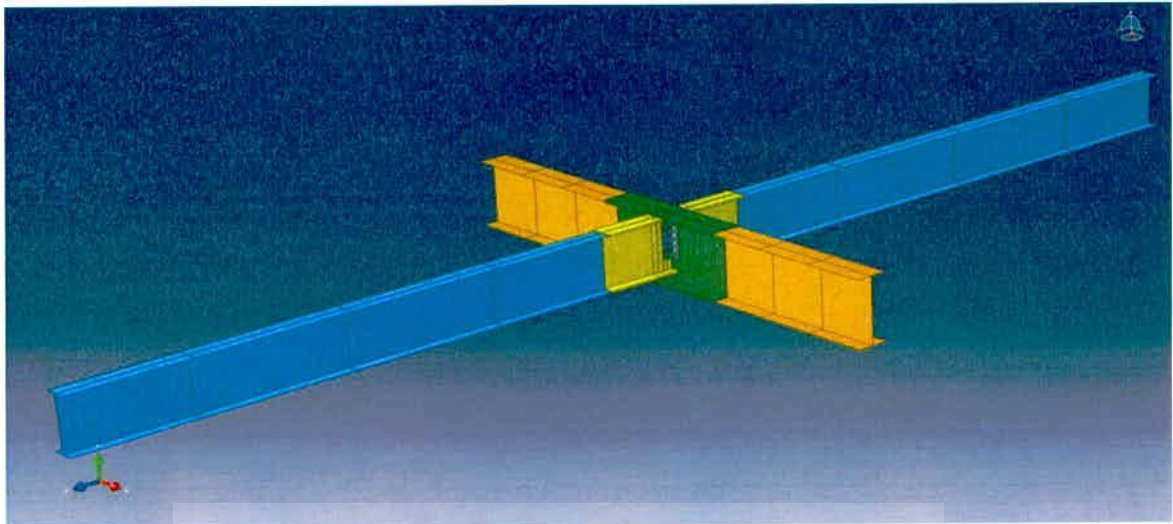


Figure 4.21 – The connection model in totality



Figure 4.22 – The finite element mesh of the entire assembly

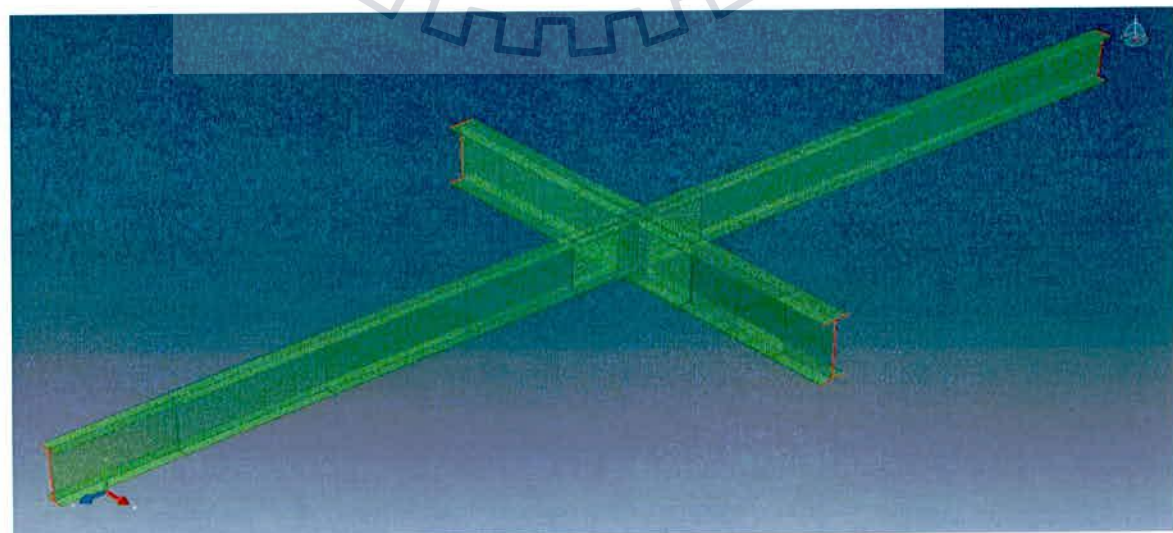


Figure 4.23 – Locations of applied boundary conditions

4.4 JOINT RIGIDITY

Once the modelling of the connection in ABAQUS is complete, it is necessary to check the rigidity of the joint and the behaviour of the connection under different clamping stresses. The connection model discussed in the previous section was modified to perform this check. Imam et al., (2007) have performed a similar analysis where one stringer was modelled as a cantilever and the rest of the members were considered to be rigidly fixed at the extreme ends away from the connection.

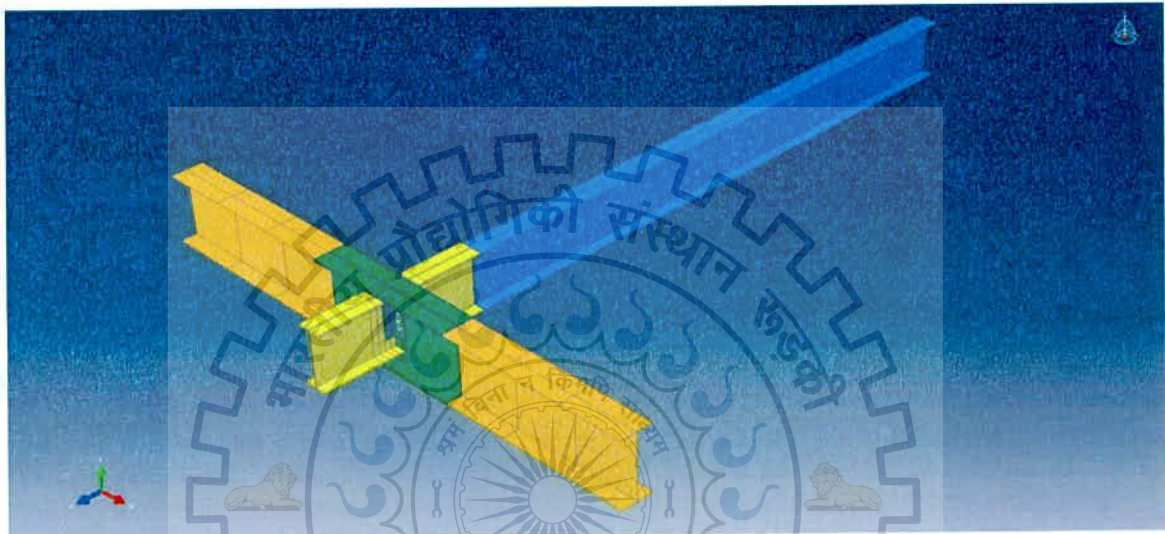


Figure 4.24 – Assembly of the connection model for checking the joint rigidity

Same approach was employed in the present study. The shell element portion of the left stringer was removed and the left stringer was made to behave as a free cantilever with a span of 500 mm. The assembly of the connection model is shown in figure 4.24.

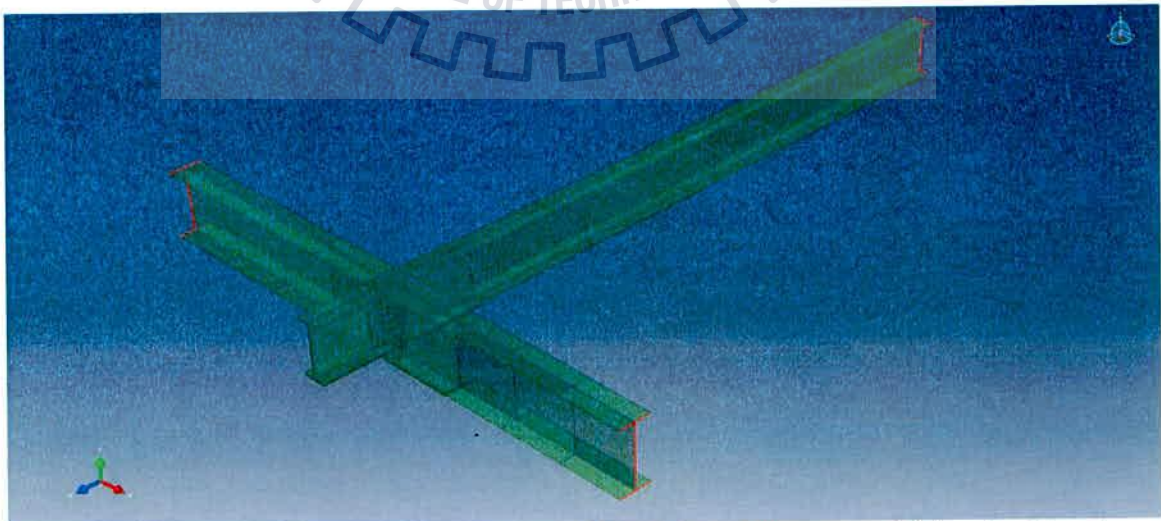


Figure 4.25 – Boundary conditions for assembly of the connection model for checking the joint rigidity

A vertical point load of 1 ton acting in the direction of gravity was applied at free end of the cantilever. The boundary condition at the far end of the stringers and cross girders is same as that of the complete connection model discussed in the previous section. The edges highlighted in red in figure 4.25 are the ones where the boundary condition is applied.

The clamping stress in all the rivets was varied and the maximum deflection at the connection was obtained for each case of rivet clamping stress. The values of deflection for different clamping stress are shown in the table 4.2.

Table 4.2 – Values of deflection corresponding to different clamping stress

Clamping Stress [MPa]	Deflection [mm]
25	3.928
50	3.85
75	3.8
100	3.771
150	3.728
200	3.708

The variation in deflection with respect to rivet clamping stress is shown in the figure 4.26. The results show that the value of deflection decreases with increase in the rivet clamping stress. This is seen as a positive result and is comparable to the results obtained in previous studies by Imam et al., (2007) and de Jesus et al., (2010). The exact values of the deflection cannot be compared with the previous study since the dimensions are different.

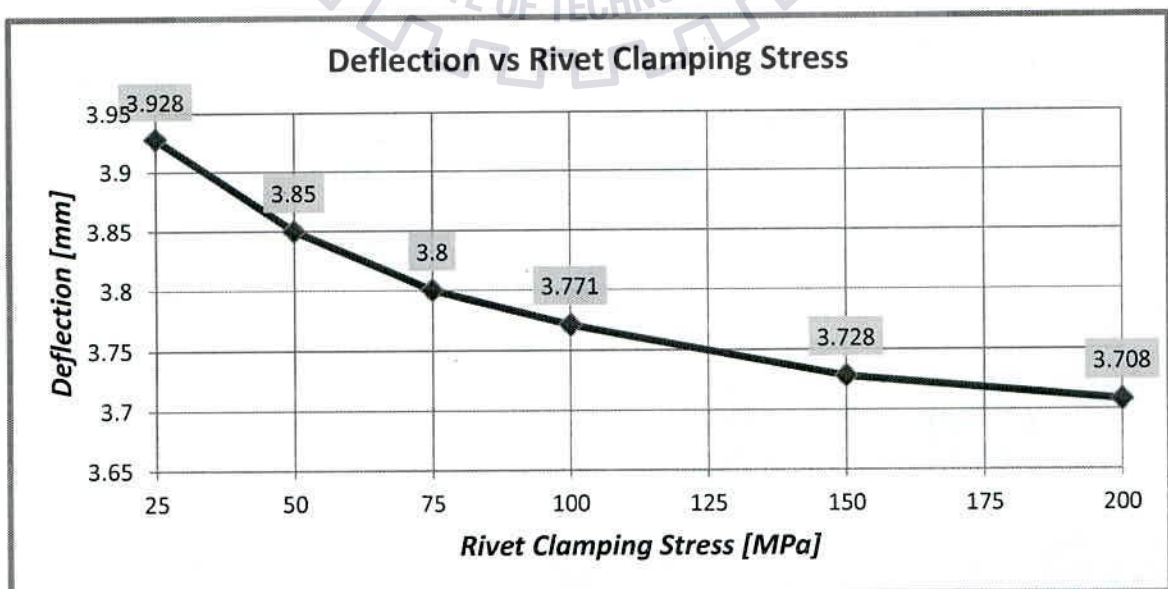


Figure 4.26 – Deflection vs Rivet clamping stress for joint rigidity check

4.5 SUMMARY

- The analysis of double lap joint carried out in ABAQUS gave sufficient confidence to model the stringer-to-cross-girder connection along with the detailed local geometry of the connection.
- The deflection check carried out for checking the joint rigidity confirmed the robustness of the connection model.
- Based upon the above conclusions a full scale fatigue test can be carried out on the Stinger-Cross girder connection model in ABAQUS.
- Fatigue analysis can be carried out by obtaining the load history at the connection due to live load by modelling the entire global model of the truss bridge in any typical analysis software like SAP2000, STAAD-PRO, etc.



Chapter 5

FATIGUE ANALYSIS OF A STRINGER-TO-CROSS-GIRDER CONNECTION

5.1 GENERAL INFORMATION

The single lane roadway bridge considered for analysis is a single lane truss bridge located in Ranikhet in Uttarakhand. The bridge is composed of two equal trusses. The structural system of each truss is shown in the figure 5.1. Although it is a relatively new bridge, it was considered for analysis since the structural drawings were easily available. The purpose of this thesis being to develop a methodology for assessment of residual fatigue life of old riveted steel bridges, the methodology proposed in this thesis can be applied to any bridge with similar configuration henceforth.

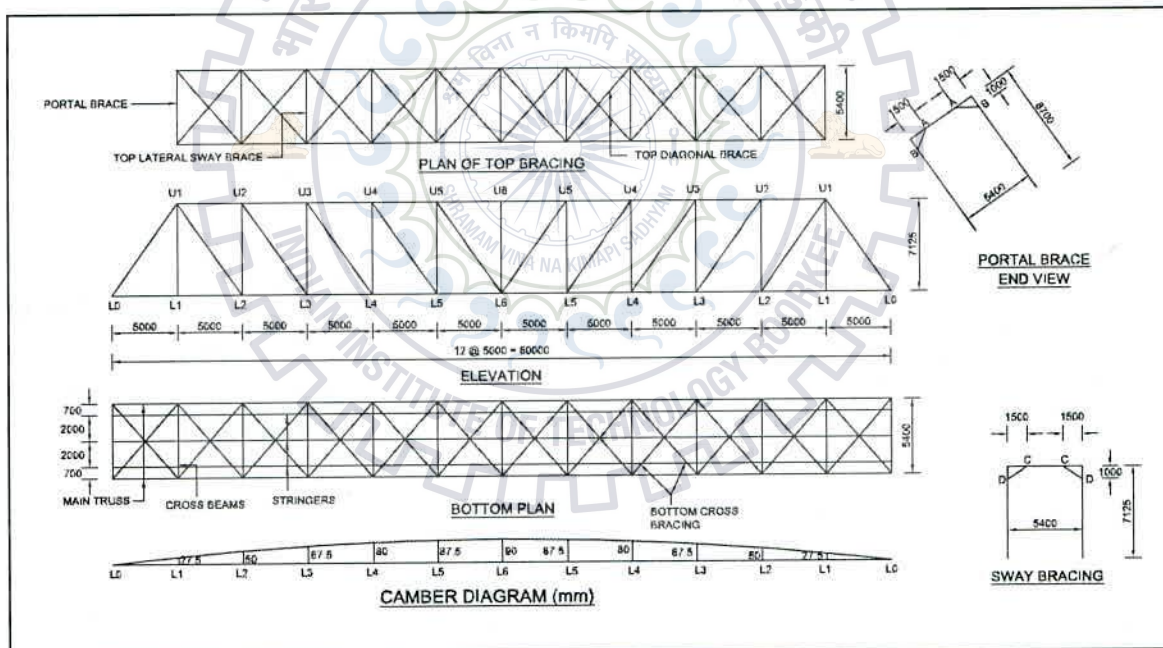


Figure 5.1- General details of the truss bridge

The same riveted truss bridge was previously analysed by Ghule, V.V (2012) and the fatigue life of the main truss members was assessed. It was concluded that the fatigue life of the bridge is governed by the most critical member in the truss which turned out to be a inclined tie member U_4-L_5 . The fatigue life of the inclined tie member was found to be 237 years and hence it was concluded to be the fatigue life of the bridge itself which was way beyond the expected service life of the bridge which is 100 years.

However, past studies have shown that the stringer-to-cross-girder connection is one of the most critical locations in a riveted bridge with respect to fatigue. The stringer is exposed to more repetition of loads as compared to the whole bridge. So, there is more probability of cyclic loading acting on the stringer and hence, similar cyclic loading will be acting on the stringer-to-cross-girder connection as well. Therefore there is a necessity to understand the response of a stringer-to-cross-girder connection under repeated cyclic loading.

To analyse such a connection with exact details of the connection viz., rivets, connection angles and girders, a comprehensive software package having such capabilities was required. Hence ABAQUS-CAE 6.11, finite element software was selected to perform the analysis. Before modelling the connection in ABAQUS it was necessary to obtain the load history on the connection due to vehicle load. Hence the global analysis of the riveted truss bridge was carried out in SAP-2000 and the load history on the connection was obtained. The load history was then applied on the local model of the connection, modelled in ABAQUS.

5.2 GLOBAL MODEL OF THE TRUSS BRIDGE

The global model of the truss bridge was modelled in SAP-2000. The truss members, stringers, cross girders and bracings were modelled as frame elements. The slab was modelled using 200 mm thick thin shell area elements. Since the structural drawings were available, the actual member properties were assigned to each element.

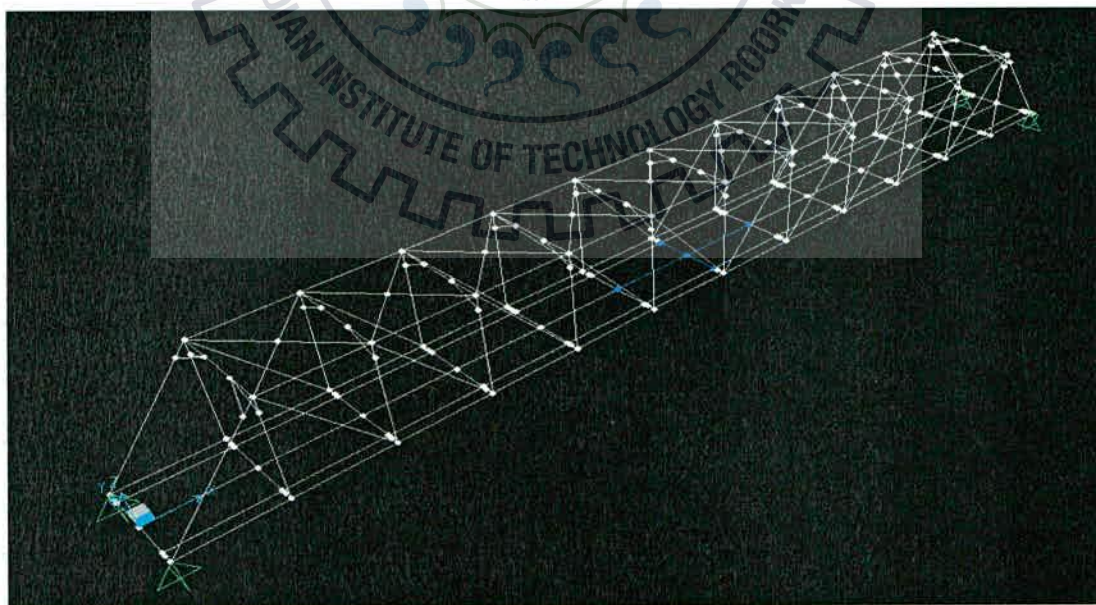


Figure 5.2 – SAP-2000 model of the truss bridge

(The critical stringer-to-cross-girder connection considered for analysis is highlighted in blue)

The end moments of the truss elements were released to achieve the pin jointed behaviour in the truss members. The cross girders were considered to be simply supported between the two trusses. The stringers were assumed to be simply supported between the cross girders. The slab was meshed to the stringers and cross girders with a mesh size of 1m x 1m. Meshing of the slab was required to ensure proper load transfer to the stringers and cross girders.

5.2.1 DEAD LOAD AND SUPER IMPOSED DEAD LOAD

Dead Load (DL) of the structure was assigned using self-weight multiplier command available in SAP-2000. The Super Imposed Dead Load (SIDL) was assigned using the loading features available in the software. The loads of wearing coat, crash barrier and services were applied under SIDL case. The load of wearing coat was assigned as a surface pressure on the slab and the load due to services and crash barrier was assigned as concentrated load on the external nodes of the slab.

It was observed that out of the three stringers running longitudinally along the bridge, the central stringer is most critical. The stringer-to-cross-girder connection in the mid-span of the bridge was considered for the analysis. The values of the deflection in the due to DL and SIDL are shown in the figure 5.3. These displacement values will be applied in the local connection model prepared in ABAQUS to obtain the displaced shape of the connection due to DL and SIDL.

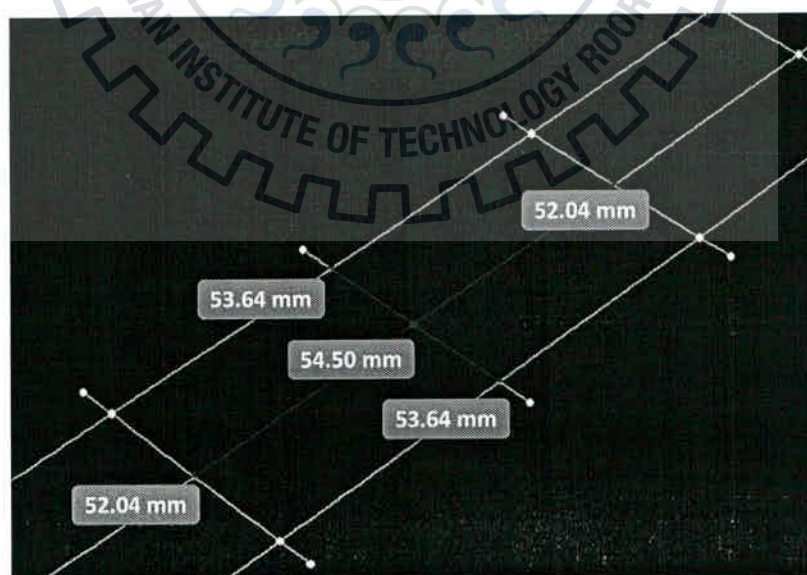


Figure 5.3 – Deflection in critical nodes of the connection considered for analysis due to DL and SIDL

5.2.2 LIVE LOAD

Live load on the bridge is the major contributor towards fatigue. The vehicular load moving in and out of the bridge causes cyclic stresses in the bridge members. Therefore, for fatigue analysis it is very important to have the exact vehicle types, axle loads, axle distances and frequency of the vehicles. The live load specified in IRC: 6-2000 like Class A, Class 70R etc. are hypothetical loads and will not be running on roads or bridges. The details of axle loads of the trucks plying on Indian roads are available in SP-37:1991 of IRC. Four different types of trucks have been defined in the code. The axle load of each vehicle is shown in the figure 5.4.

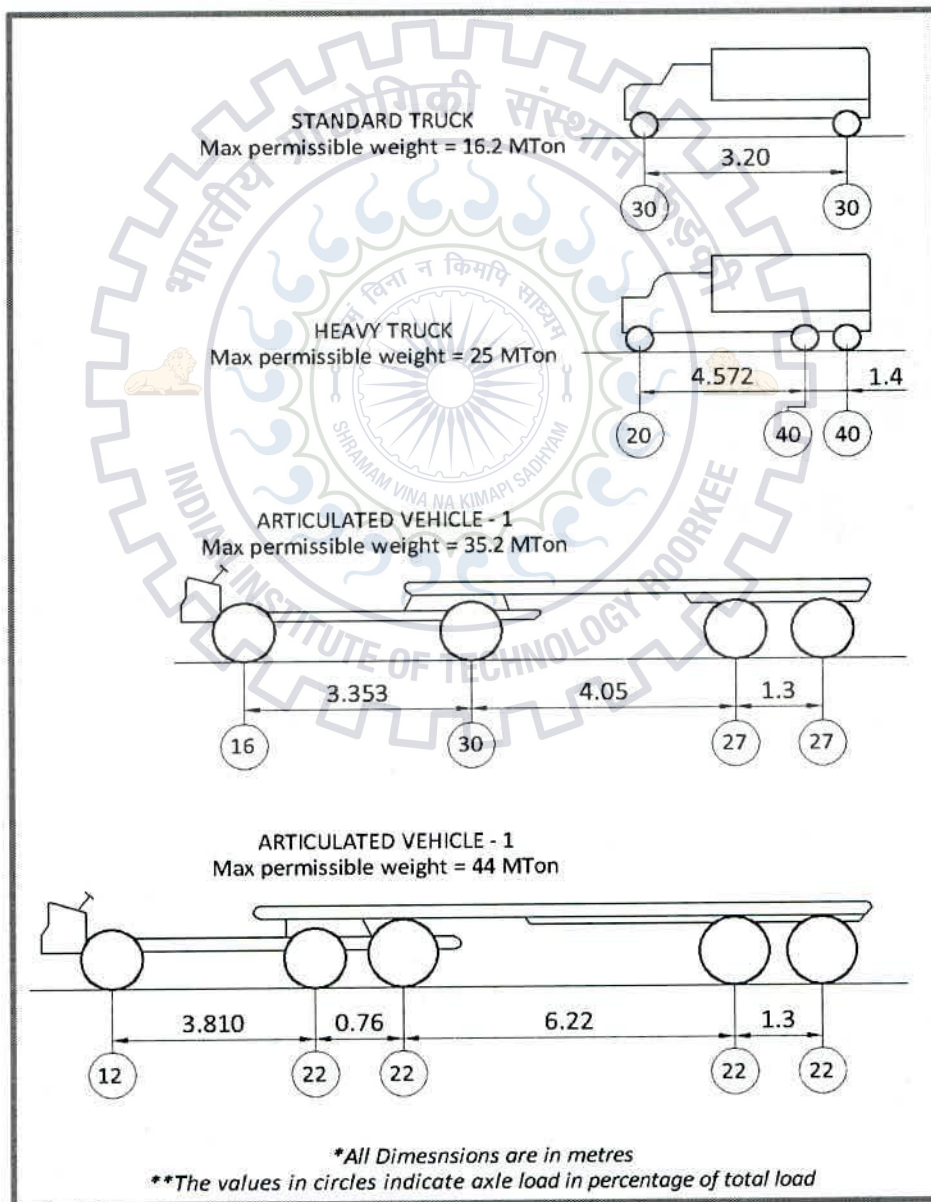


Figure 5.4 – Commercial vehicles plying in India [IRC: SP - 37-1991]

The average number of vehicles of each type assumed to ply over the bridge in a single day has been listed in the table 5.1.

Table 5.1 – Type of vehicles

Sr. No.	Type of vehicle	No. of repetitions per day
1	Standard Truck	200
2	Heavy Truck	150
3	35.2 Ton Truck	100
4	44 Ton Truck	50

The vehicular load is applied as a combination of two trucks of the same configuration, moving back to back with a distance of 18m between the two vehicles. This was done to ensure maximum response. The width of the axle was considered to be 1.8m c/c. The live load was applied using the multi-step static command available in SAP-2000. A total of 80 load steps were generated for each vehicle type. An impact factor of 1.12 was considered for the analysis. For worst condition, the eccentricity of live load with respect to the central stringer was considered to be zero. This means that both the wheels in an axle of the vehicle are equidistant from the stringer.

5.2.3 RESULTS OBTAINED FOR LIVE LOAD

The values of the shear force at the critical connection are extracted from the analysis of global model to be applied as force in the local model of the connection in ABAQUS-CAE. The shear force values of the stringers on either side of the cross girder is obtained.

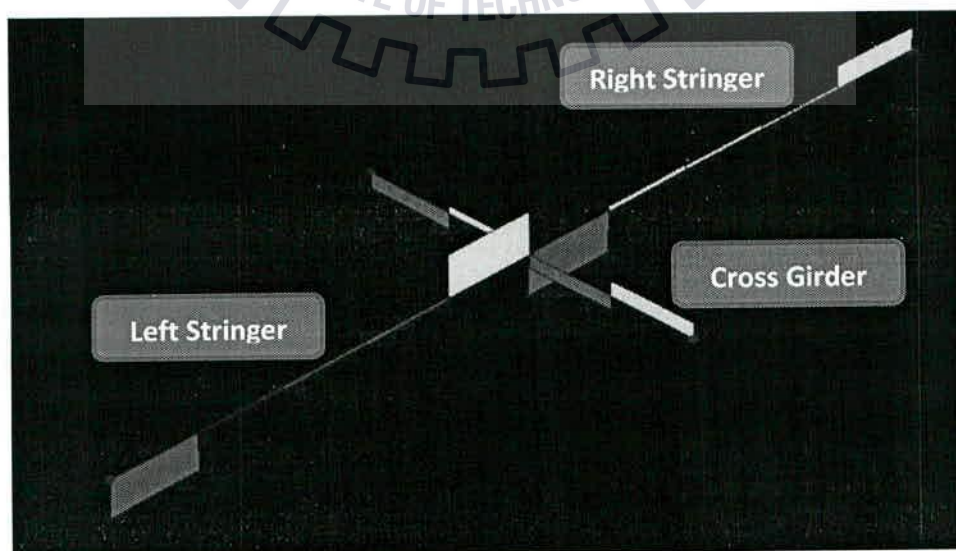


Figure 5.5 – Shear force diagram of the connection for a load step of vehicle load

Out of the 80 load steps generated for each vehicle type, the load steps relevant for the critical connection were sorted. The shear force history extracted from the analysis for each vehicle type is shown in the following charts.

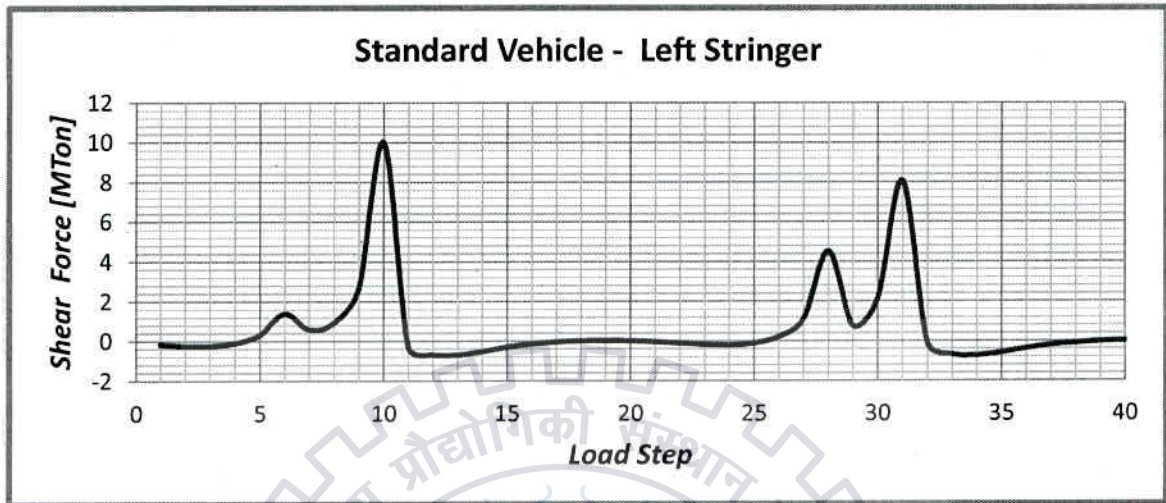


Figure 5.6 – Shear force history at the joint for standard vehicle in left stringer

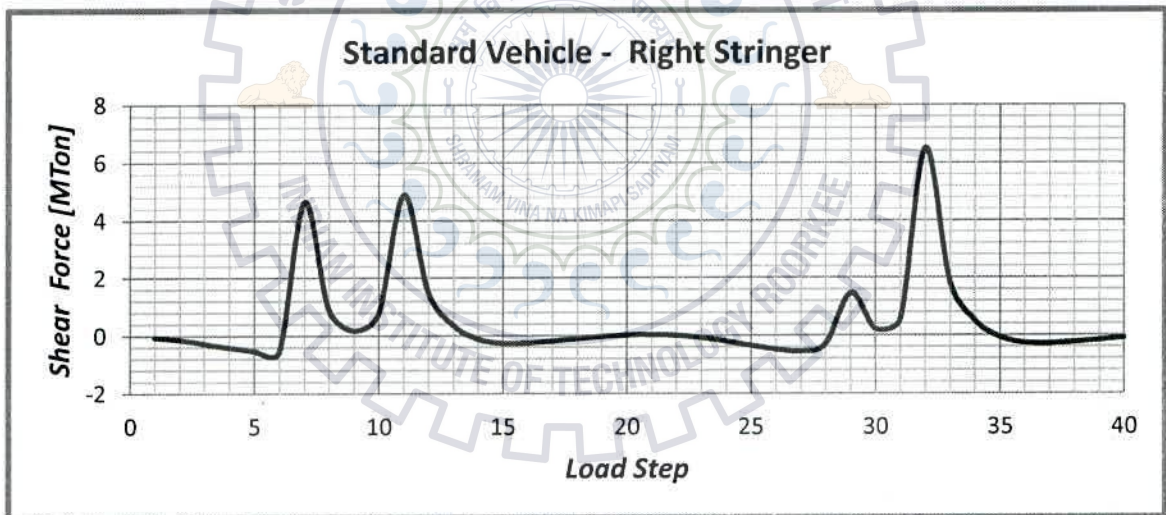


Figure 5.7 - Shear force history at the joint for standard vehicle in right stringer

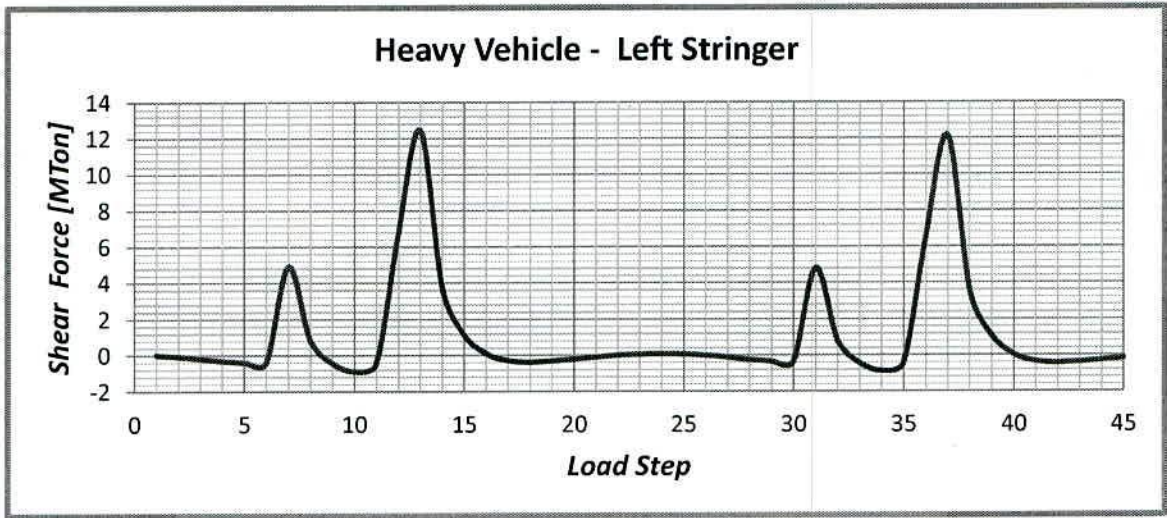


Figure 5.8 - Shear force history at the joint for heavy vehicle in left stringer

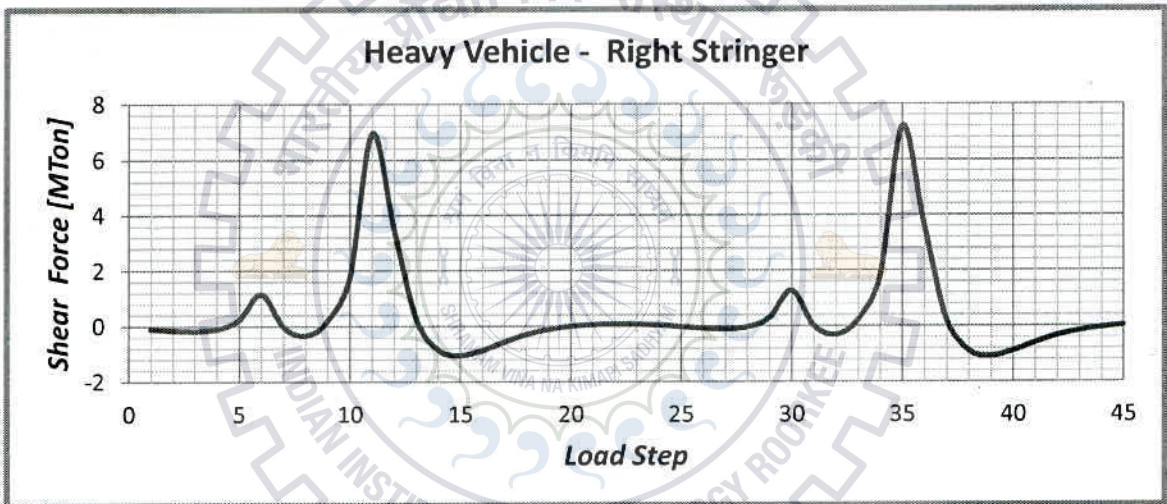


Figure 5.9 - Shear force history at the joint for heavy vehicle in right stringer

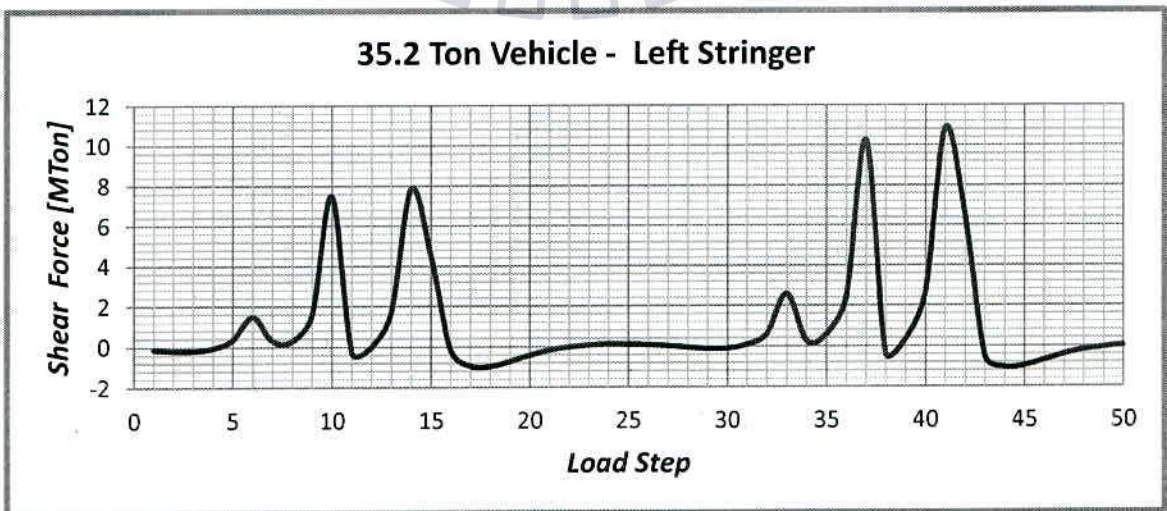


Figure 5.10 - Shear force history at the joint for 35.2 ton vehicle in left stringer

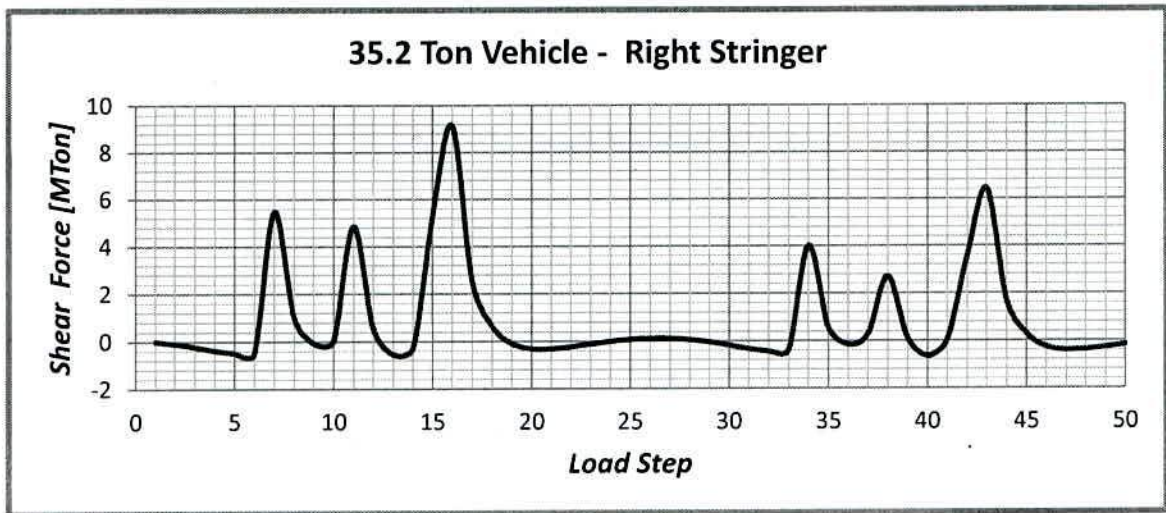


Figure 5.11 - Shear force history at the joint for 35.2 ton vehicle in right stringer

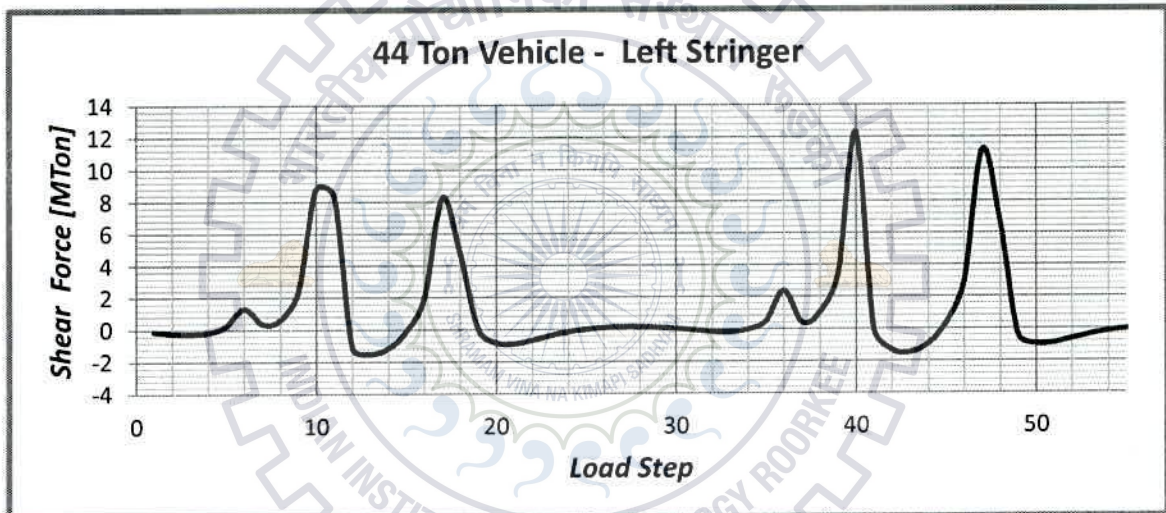


Figure 5.12 - Shear force history at the joint for 44 ton vehicle in left stringer

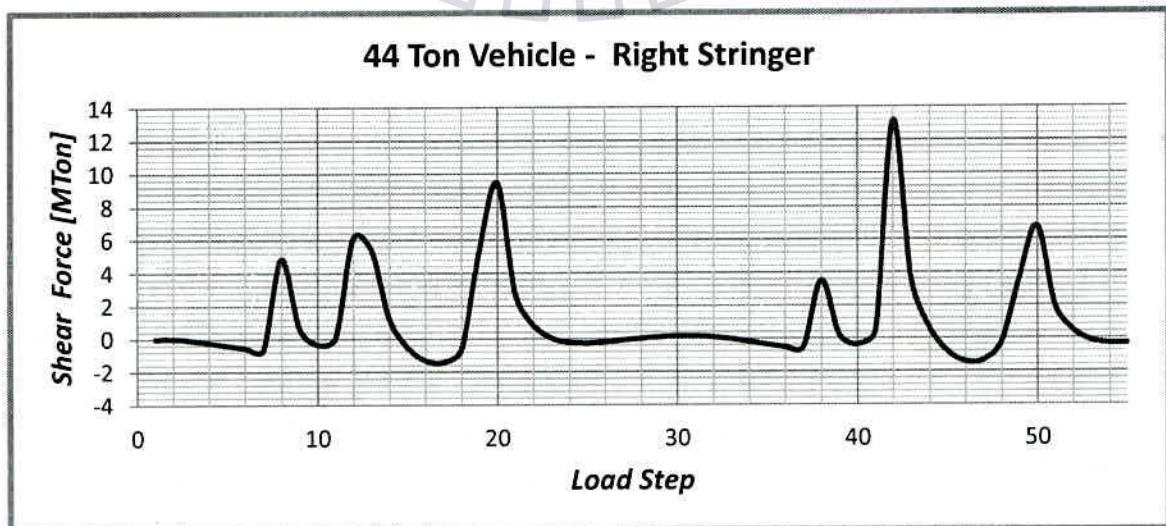


Figure 5.13 - Shear force history at the joint for 44 ton vehicle in right stringer

5.3 ANALYISS OF LOCAL CONNECTION MODEL IN ABAQUS

The modelling of the local stringer-to-cross-girder connection in ABAQUS was discussed extensively in chapter 4. A total of three load steps were created for the analysis. The first step was created for the application of rivet clamping force. The second step for the application of displacement due to dead load and super imposed dead load. The third load step for the application of fatigue load history generated due to the vehicular live load.

5.3.1 APPLICATION OF RIVET CLAMPING FORCE

The scope of the thesis was to study the behaviour of a stringer-to-cross-girder connection due to different clamping force of the rivet and to obtain the fatigue life of the connection in these scenarios. The method of application of clamping force in ABAQUS is discussed in detail in section 4.2.3. For this study, it was decided that the analysis will be carried out for three different clamping stresses - 150 MPa, 100 MPa and 50 MPa. The bolt load required as an input in ABAQUS to develop the required clamping force in the rivet is tabulated in table 5.2 below.

Table 5.2 – Clamping stress and Bolt load in ABAQUS

Clamping Stress [MPa]	Contact Area [mm ²]	Bolt Force [N]
50	593	29650
100	593	59301
150	593	88951

5.3.2 APPLICATION OF DEAD LOAD

The deflection due to dead load and super imposed dead load at the connection is applied as displacement at the connection location in ABAQUS. The value of deflection shown in figure 5.3 is the absolute deflection. However while modelling in ABAQUS, the extreme ends of the cross girder and the stringers were considered to be hinged. Hence relative displacement at the joint was calculated to be input in the analysis. The displacement at the far end of the connection, i.e. at the previous cross girder was 52.04 mm. The displacement at the connection was found to be 54.50 mm. Therefore the relative displacement turned out to be 2.46 mm. This displacement was input as a boundary condition in the dead load step in ABAQUS. The displacement was applied on a patch at the connection location. The patch is highlighted in orange in the figure 5.14.

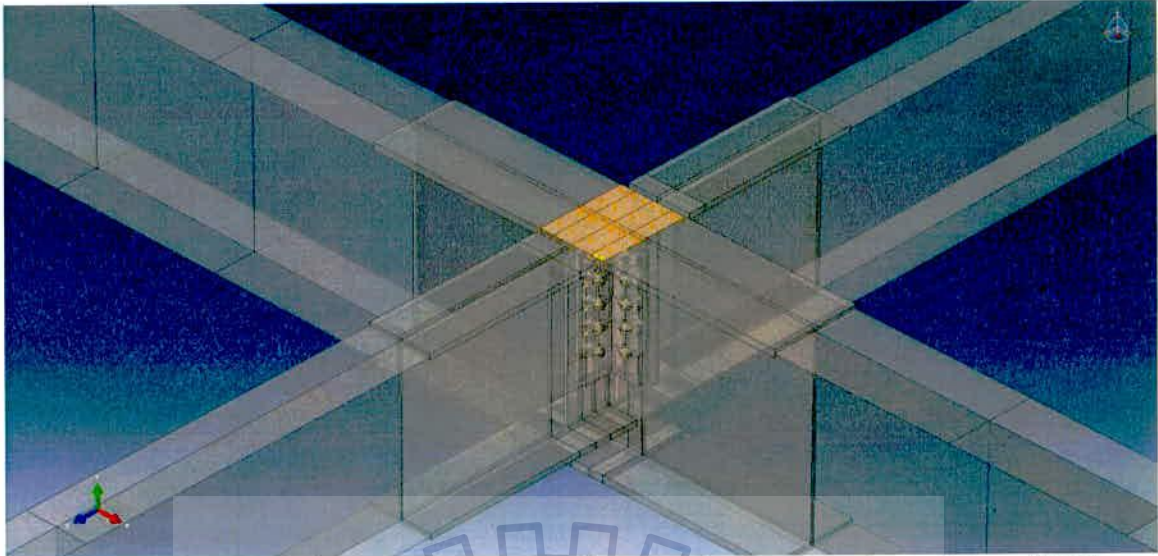


Figure 5.14 – Patch showing the location of applied displacement due to DL and SIDL

5.3.3 APPLICATION OF LIVE LOAD

For live load, the loading history obtained for the SAP-2000 analysis was in the form of shear force in the left and right stringer. The connection between stringer and cross girder being a shear connection, the live load is transferred to the cross girder from the stringer by shear action. If the stringer is considered to be simply supported between the cross girders, the shear force is nothing but the reaction applied by the stringer on the cross girder. Therefore a patch of 180mm x 50mm was created at the end of each stringer. The shear force history obtained from the SAP-2000 analysis was then converted into patch load and applied on the stringers.

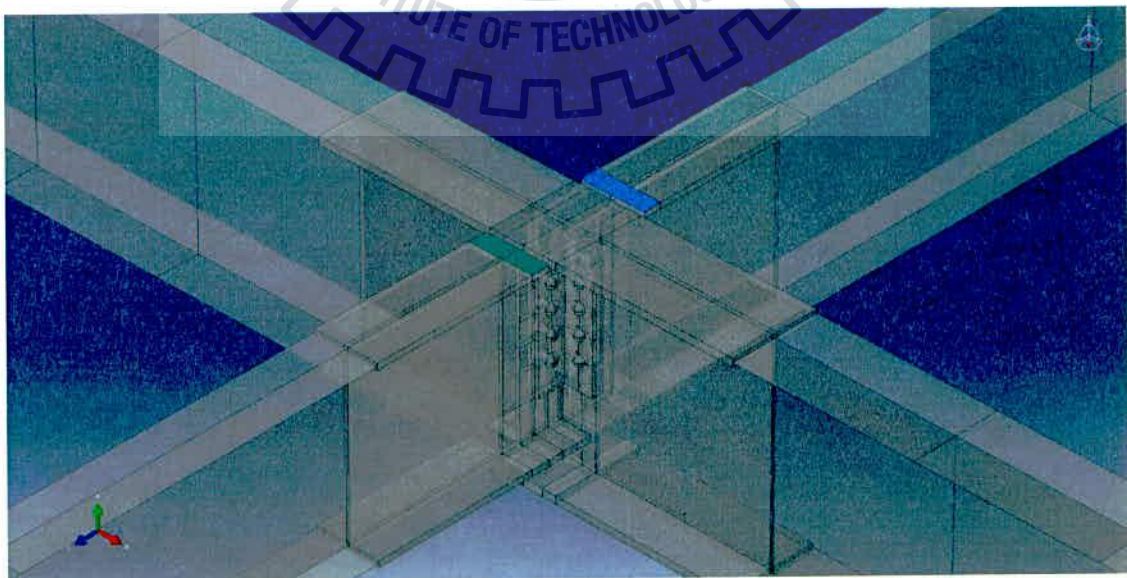


Figure 5.15 – Patch showing location of applied shear force as patch load for live load

The vehicular live load history was applied using the 'AMPLITUDE' command available in ABAQUS. The load history was input as tabular amplitude having the same variation as that obtained from SAP-2000 analysis. The patch load to be applied was given a magnitude of 1 MPa in the gravity direction and the amplitude previously defined was assigned to this patch load. The patches on the stringers are shown in figure 5.14. The green patch pertains to left stringer and the blue patch pertains to the right stringer.

5.3.4 ANALYSIS

Since there were four different vehicle classes and three different clamping stresses, a total of twelve different models were created and analysed. The top most rivet on the left stringer was seen to be the most critical rivet in the connection. On detailed study of the rivet in question, it was observed that maximum shear stress in the rivet occurred at the interaction face between the connection angle and the stringer. The critical section of the rivet and the elements considered for post-processing are highlighted in the figure 5.16.

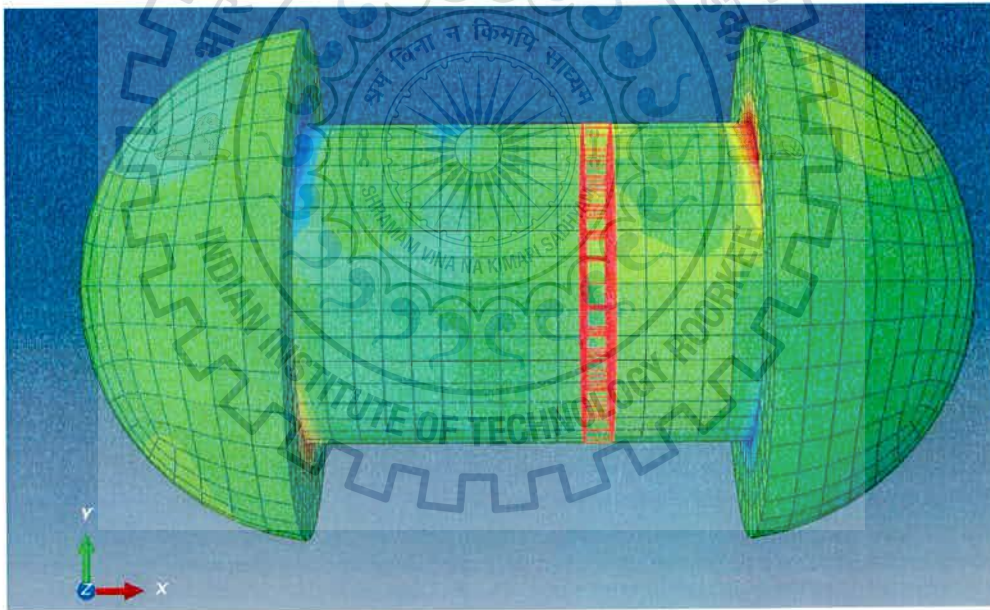


Figure 5.16 – Critical location for maximum shear stress in the rivet

Figure 5.17 shows the side view of the rivet cross-section at the face of the stringer. A part of the stringer is also shown in the figure. It can be observed that the stress concentration in the top rivet is relatively larger than the second rivet. Thus verifying our assumption that the top most rivet is the most critical rivet.

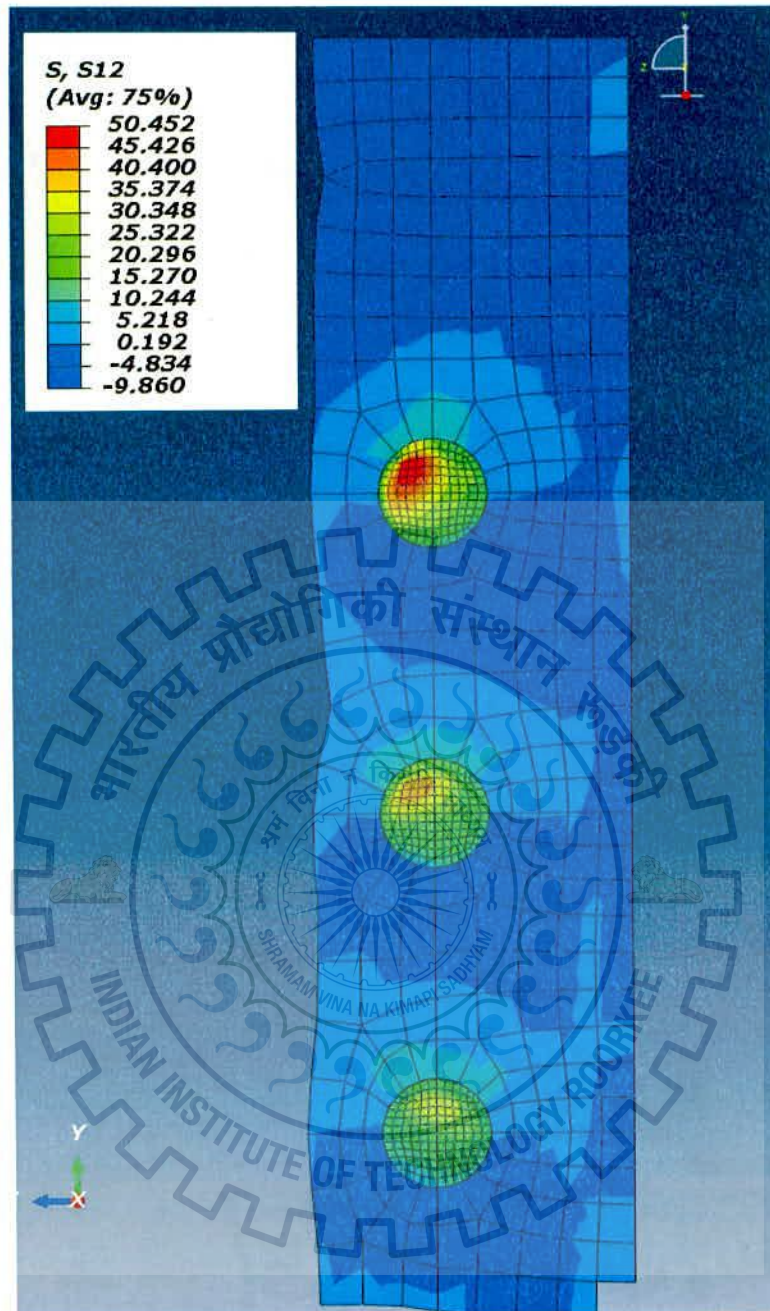


Figure 5.17 – Cross section of rivet at the face of the stringer

Maximum variation in the shear stress due to vehicular live load was observed in the first quadrant of the rivet cross-section. It is proven through previous studies that among the three stages of fatigue failure, the crack initiation phase is the most time consuming phase. Crack propagation and fracture can be sudden. An opinion was made that the stress fluctuation in the first quadrant will lead to crack initiation. Hence it was decided to perform the fatigue analysis of the elements in the first quadrant and estimate the life of the rivet based on this analysis. The elements selected for fatigue analysis are highlighted in the figure 5.18. The

stress history obtained for each element was then averaged out and the final stress history for the first quadrant was obtained.

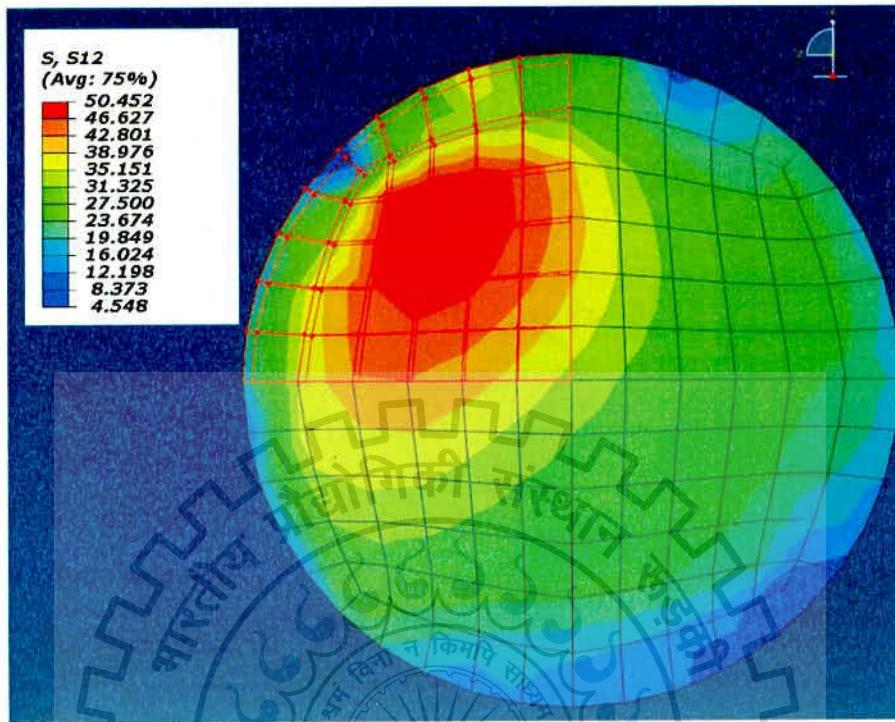


Figure 5.18 – Elements selected for fatigue analysis in the cross-section of the rivet

5.4 SUMMARY

- The global analysis of the truss bridge was carried out in SAP-2000 and the loading history for different vehicle types was obtained.
- The obtained load history was applied in the local connection model in ABAQUS.
- The analysis was carried out for three different clamping force in the rivet and the shear stress history in the critical rivet was obtained.
- The shear stress history of the rivet will further be used to assess the fatigue life of the critical rivet and hence the fatigue life of the connection.

Chapter 6

FATIGUE LIFE EVALUATION

6.1 GENERAL

The shear stress history at the critical section of the rivet discussed in the previous chapter was obtained for different vehicle classes under different clamping forces. The stress history obtained was of variable-amplitude type as expected under fatigue loading of bridges. It was necessary to process the obtained results and derive the stress range histograms as well as the number of cycles for each stress range. Rain flow counting method was employed to obtain the stress range histogram and number of cycles. The methodology of rain flow counting, generation of stress range histograms and evaluation of fatigue life of the rivet is discussed in this chapter.

6.2 POST-PROCESSING OF RESULTS

The methodology of post-processing will be discussed for 50 MPa clamping stress under heavy truck loading.

6.2.1 SHEAR STRESS HISTORY

The shear stress history obtained for the critical section in the rivet for 50 MPa clamping stress and heavy truck loading is shown in the figure 6.1.

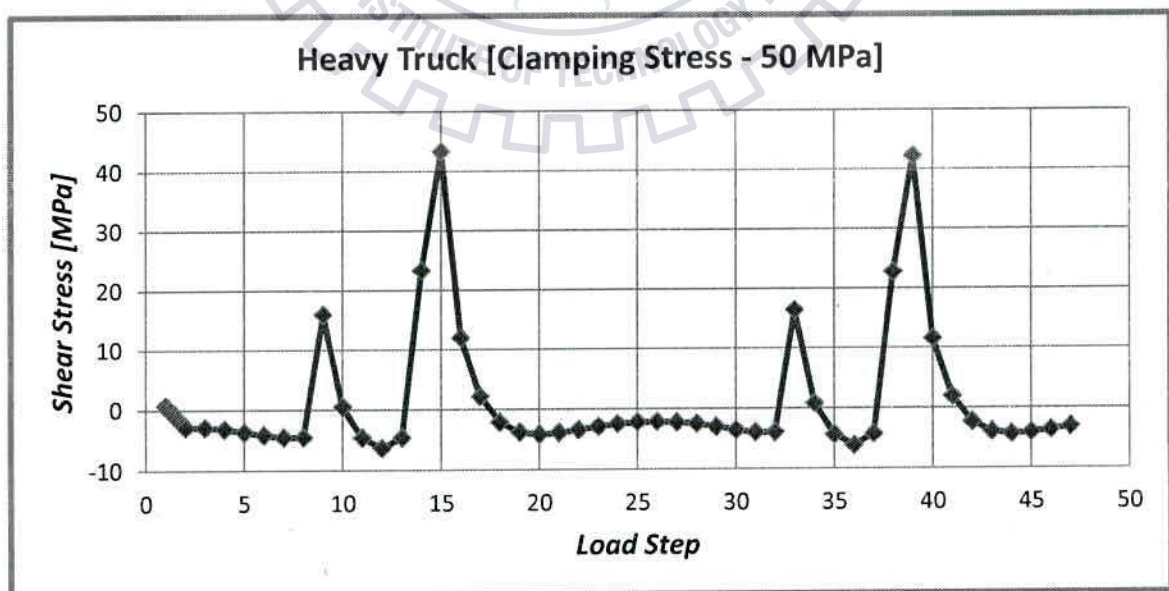


Figure 6.1 – Shear stress history for 50 MPa clamping stress under Heavy truck loading

6.2.2 RAIN FLOW COUNTING METHOD

Stress range and number of cycles are obtained from a complex stress history with the help of counting methods. Rain flow counting method is employed in the present work. Stress range is a function of maximum and minimum peaks in a stress history plot. The intermediate values are of no importance here. The stress history obtained was sorted to get the maximum and minimum peaks. The intermediate points were neglected. The sorted stress history diagram for the above plot is shown in the figure 6.2.

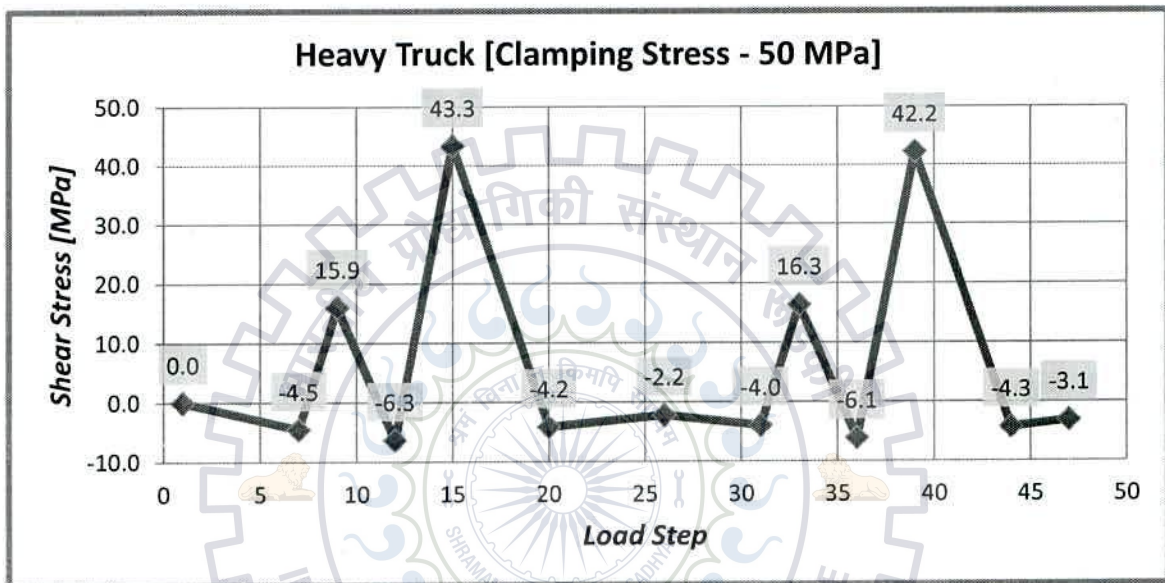


Figure 6.2 – Sorted shear stress history for 150 MPa clamping stress under Heavy truck loading

The sorted stress history is rotated clockwise by 90° and the diagram is treated as roof of a Japanese pagoda. It is then assumed that rain falls from the top most point and flows downwards as per the slope. The stress range and number of cycles is then calculated as per the rules discussed in chapter 2. The working sequence for rain flow counting method of the current case is shown in figure 6.3. The step by step procedure of finding the stress range and number of cycles is as follows.

- a. Start with point A, proceed towards B. Stop at B since the value of stress at C is greater than A.
Stress range = $0 - (-4.5) = -4.5$ MPa and Number of cycles = 0.5
- b. Continuing on the negative side, start from C and proceed towards D. D has the maximum value on the negative side. The flow will terminate here.
Stress range = $43.3 - (-6.1) = -49.4$ MPa and Number of cycles = 0.5

- c. Start from E and proceed towards F. Now, J is greater than F. Therefore the flow will continue till F and then terminate.

Stress range = $15.9 - (-6.3) = -22$ MPa and Number of cycles = 0.5

- d. Likewise the rest of the stress ranges on the negative side will be found out.

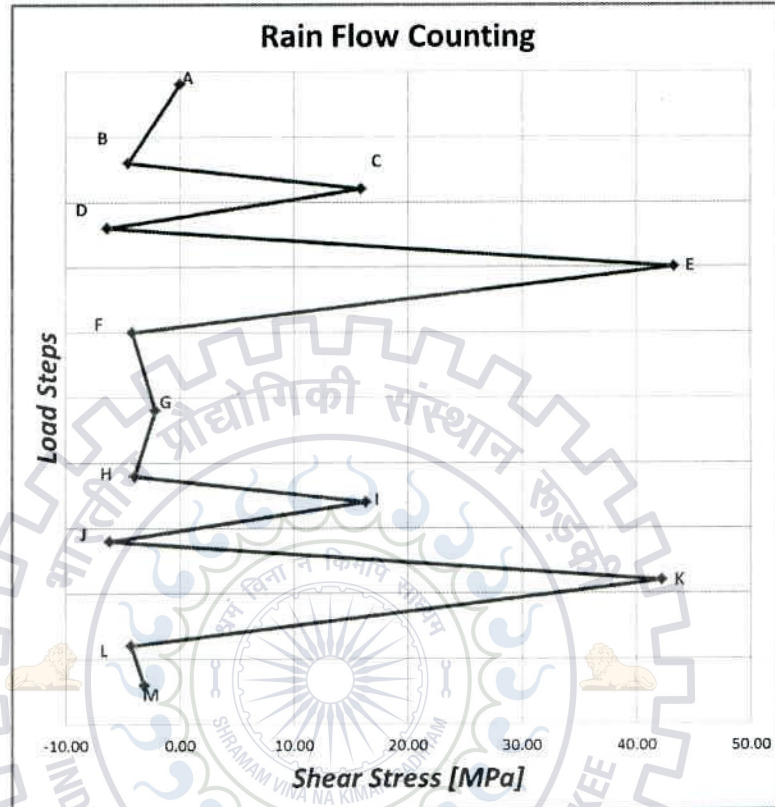


Figure 6.3 – Working diagram for rain flow counting

- e. On the positive side, begin with Band move toward C. Now, the value of stress at D is greater than B. Hence the flow will terminate at C.

Stress range = $-4.5 - (15.9) = -20.4$ MPa and Number of cycles = 0.5

- f. Start from D and proceed towards E. E has the maximum value on the positive side. The flow will terminate here.

Stress range = $-6.3 - (43.3) = -49.6$ MPa and Number of cycles = 0.5

- g. Start from F and move towards G. F is greater than H. Therefore continue towards I. Now, the flow will encounter a new flow originating from J. Since J is greater than F, the flow will terminate at I

Stress range = $-4.2 - (16.3) = -20.5$ MPa and Number of cycles = 0.5

- h. Similarly, the stress range and number of cycles for other flows can be calculated.

6.2.3 STRESS RANGE HISTOGRAM

Stress histogram is plotted from the stress ranges and corresponding number of cycles obtained by rain flow counting method, which are tabulated in table 6.1.

Table 6.1 – Stress range and corresponding number of cycles for 50 MPa clamping stress under Heavy truck loading

Stress Range	Cycle per vehicle n
1	0.5
2	1.0
5	0.5
21	1.5
22	0.5
47	0.5
48	0.5
49	0.5
50	0.5

The number of cycles obtained thus far is for the passing of only one vehicle. The number of cycles crossing the bridge per day is obtained from the traffic data and the total number of cycles per day is obtained. These findings are then used to evaluate the fatigue life of the connection using S-N curve and Miner's rule. The stress range histogram for one crossing of two heavy trucks back to back for 50 MPa clamping stress is shown in the figure 6.4.

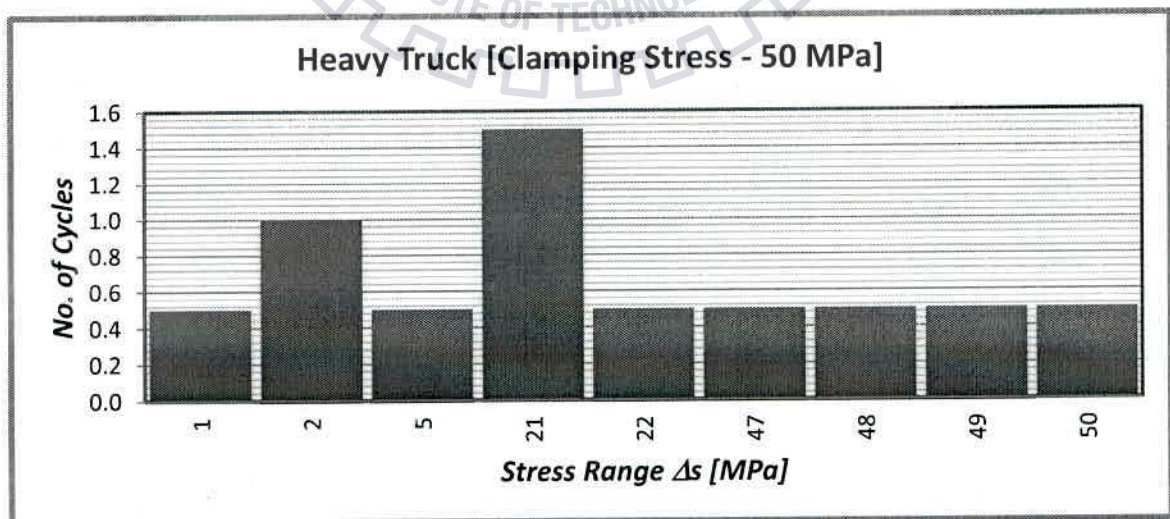


Figure 6.4 – Stress range histogram for 50 MPa clamping stress under Heavy truck loading

6.3 SHEAR STRESS HISTORY

The sorted average shear stress history in the rivet is shown for each type of vehicle with respect the three different clamping stresses in the following charts. These shear stress histories will further be used to obtain the stress range histogram followed by the evaluation of accumulated damage leading to estimation of fatigue life.

6.3.1 STANDARD TRUCK LOADING

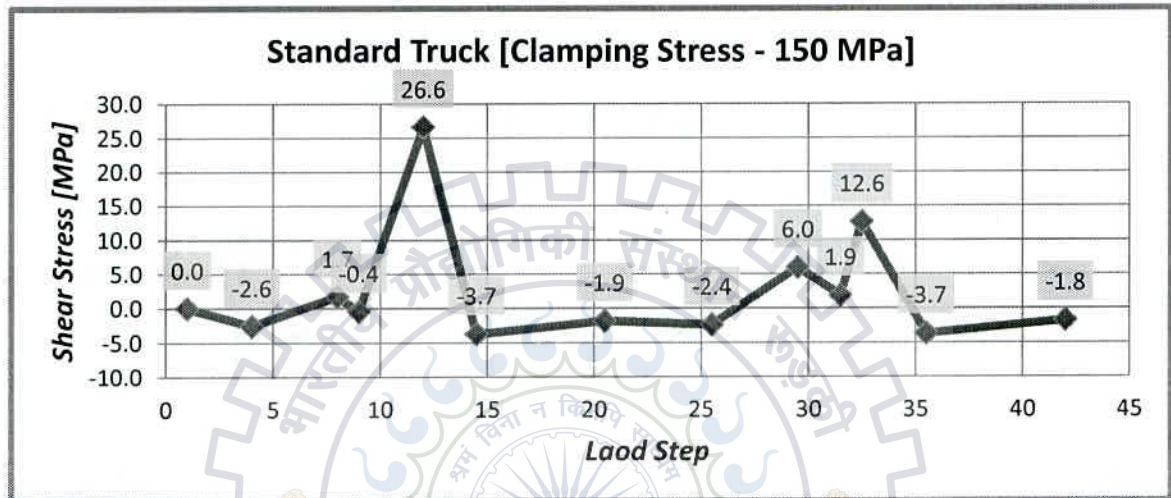


Figure 6.5 - Shear stress history for 150 MPa clamping stress under standard truck loading

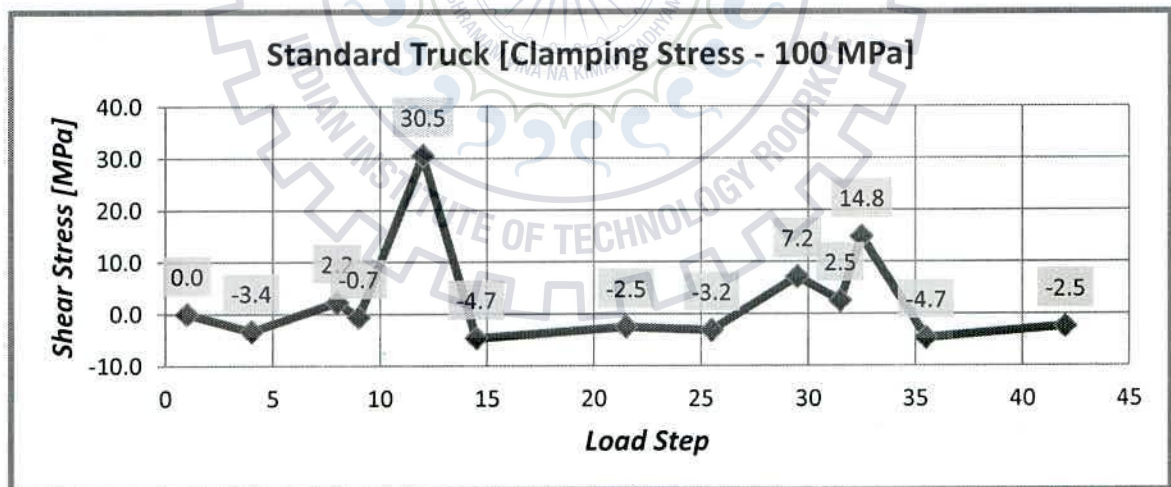


Figure 6.6 - Shear stress history for 100 MPa clamping stress under standard truck loading

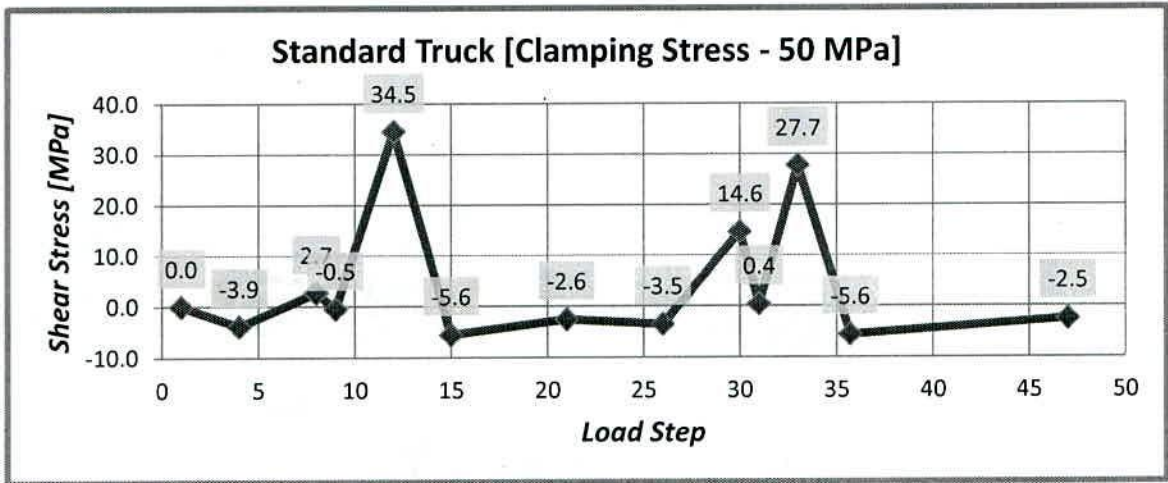


Figure 6.7 - Shear stress history for 50 MPa clamping stress under standard truck loading

6.3.2 **HEAVY TRUCK LOADING**

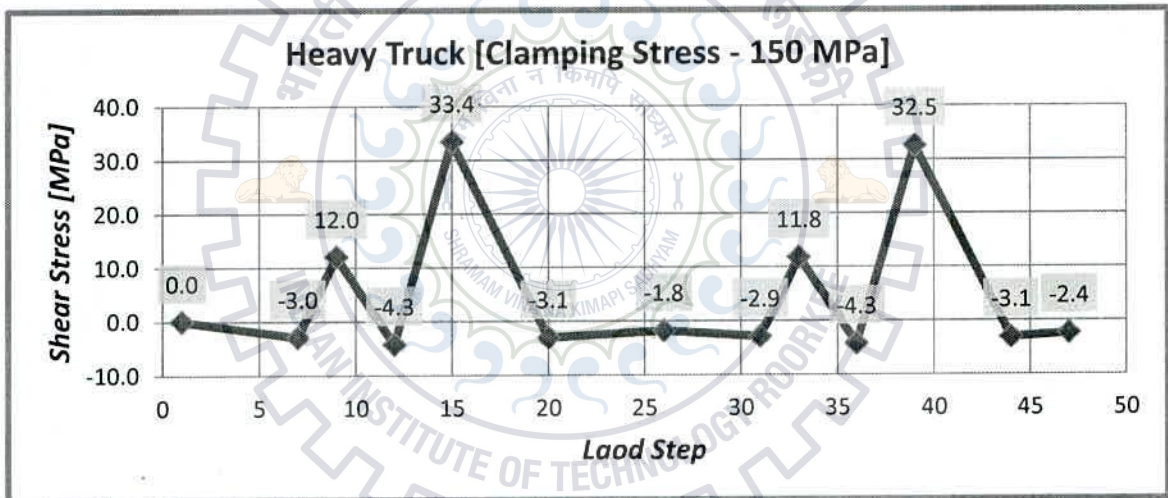


Figure 6.8 - Shear stress history for 150 MPa clamping stress under heavy truck loading

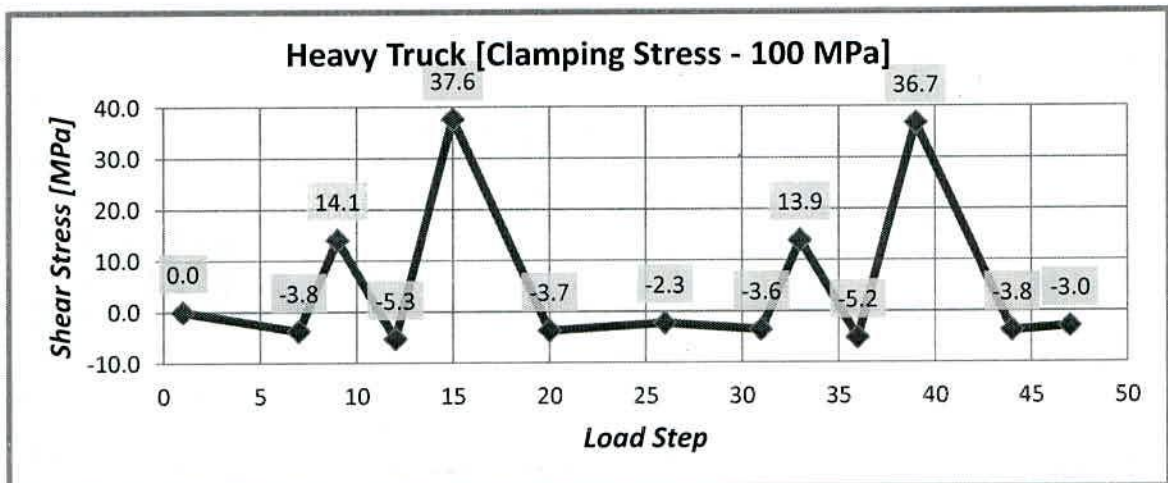


Figure 6.9 - Shear stress history for 100 MPa clamping stress under heavy truck loading

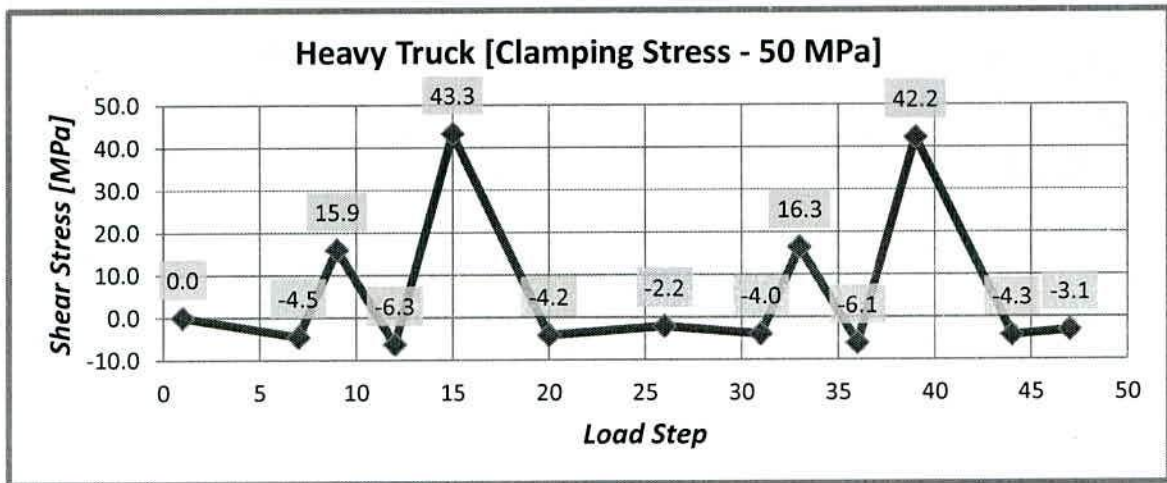


Figure 6.10 - Shear stress history for 50 MPa clamping stress under heavy truck loading

6.3.3 35.2 TON TRUCK LOADING

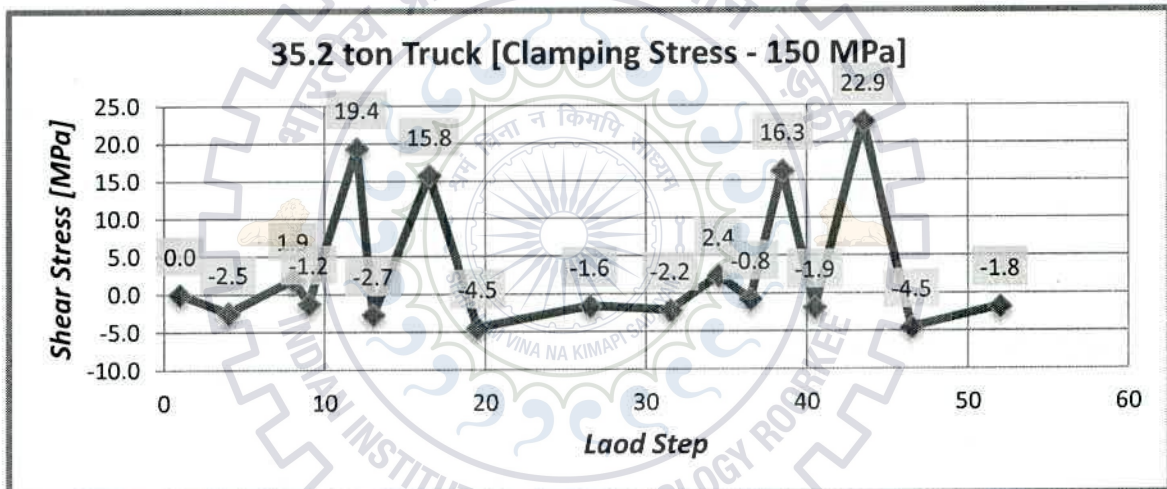


Figure 6.11 - Shear stress history for 150 MPa clamping stress under 35.2 ton truck loading

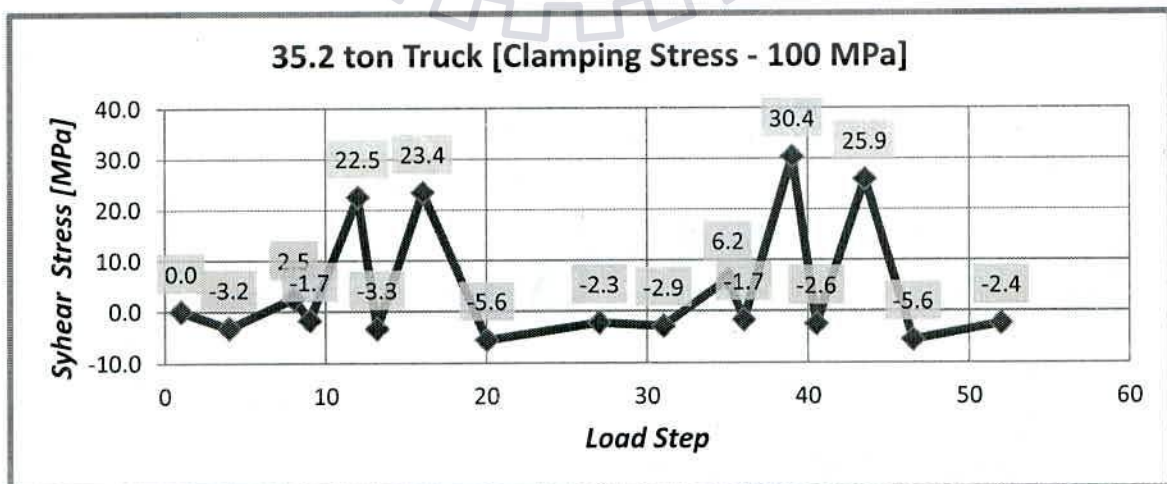


Figure 6.12 - Shear stress history for 100 MPa clamping stress under 35.2 ton truck loading

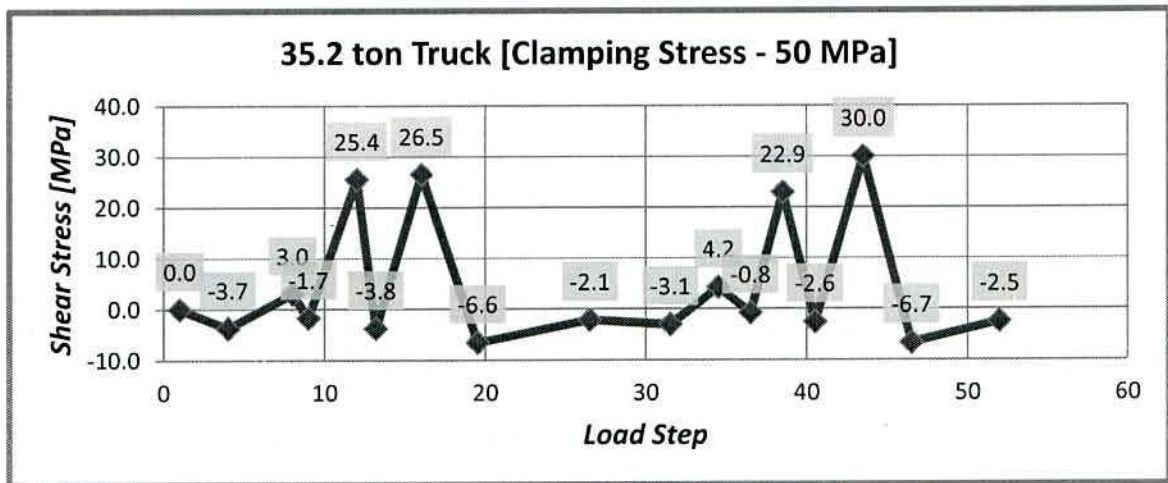


Figure 6.13 - Shear stress history for 150 MPa clamping stress under 35.2 ton truck loading

6.3.4 44 TON TRUCK LOADING

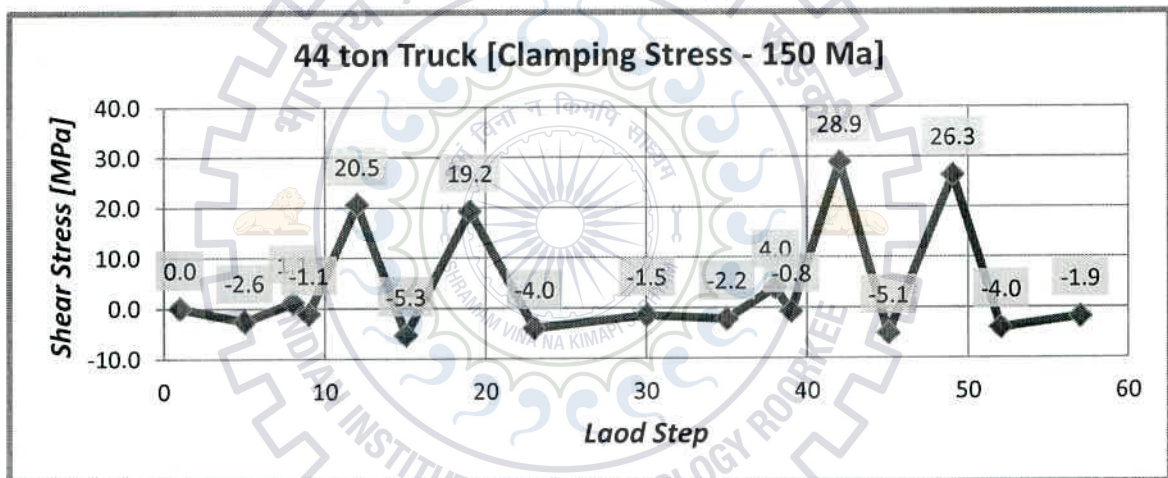


Figure 6.14 - Shear stress history for 150 MPa clamping stress under 44 ton truck loading

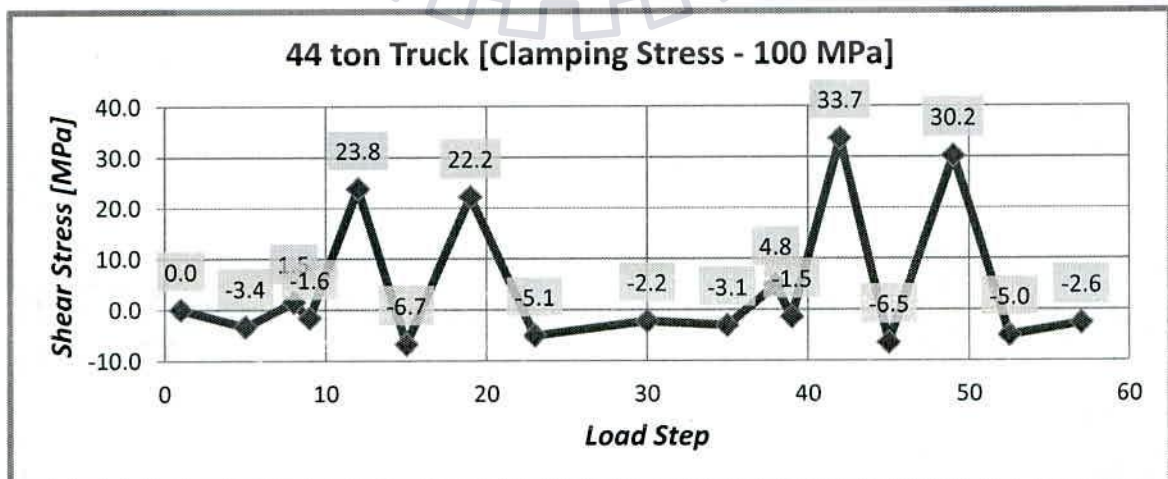


Figure 6.15 - Shear stress history for 100 MPa clamping stress under 44 ton truck loading

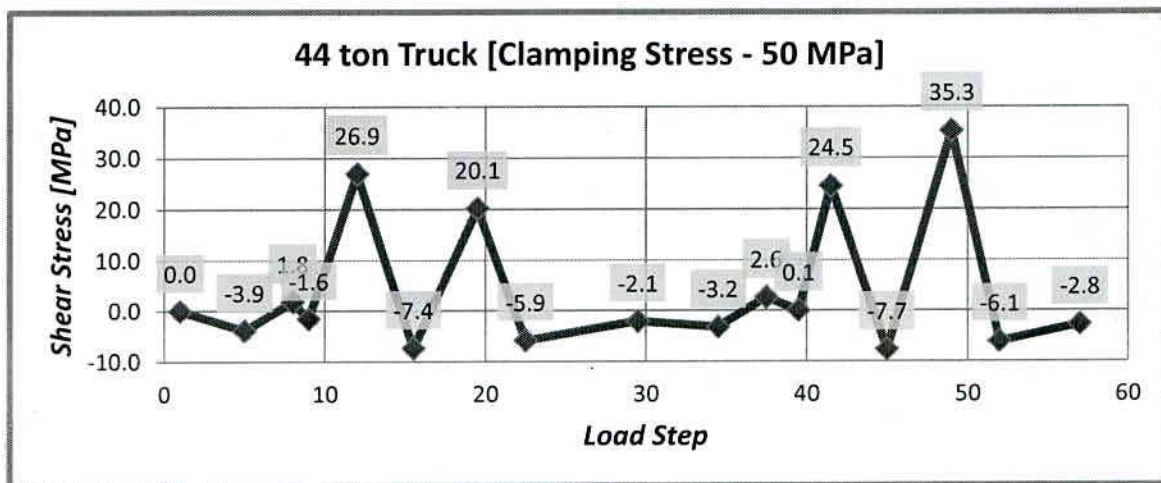


Figure 6.16 - Shear stress history for 50 MPa clamping stress under 44 ton truck loading

6.4 STRESS RANGE HISTOGRAM

As discussed earlier, the stress range histogram is plotted after processing the shear stress history using rain flow counting method. The stress range histograms for each type of vehicle with respect the three different clamping stresses in the following charts.

6.4.1 STANDARD TRUCK LOADING

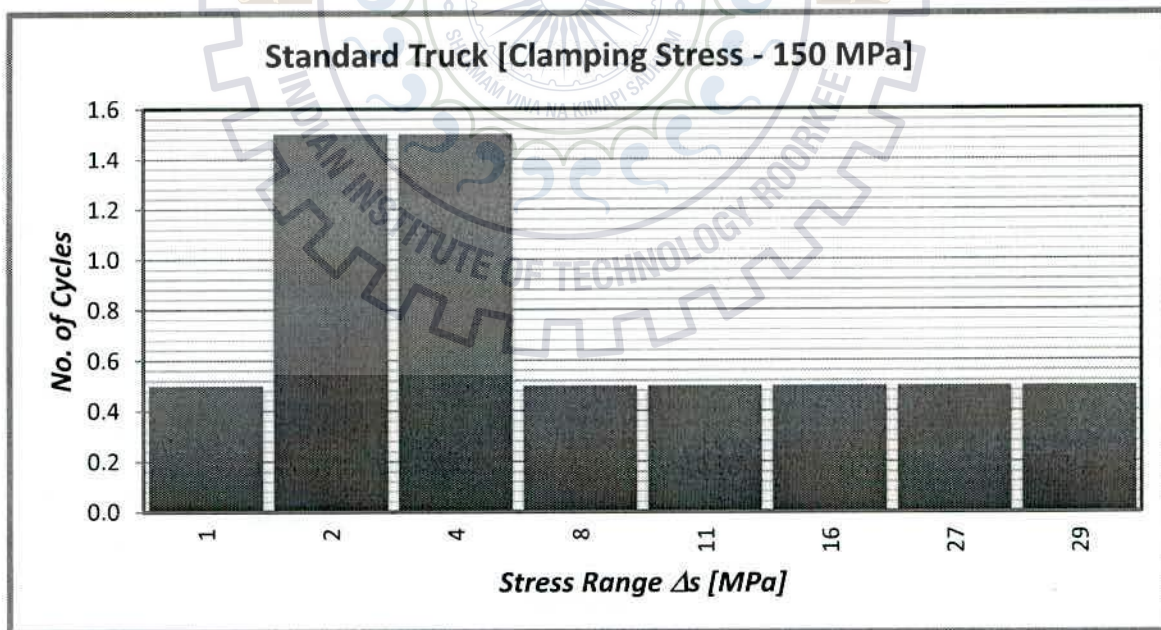


Figure 6.17 – Stress range histogram for 150 MPa clamping stress under standard truck loading

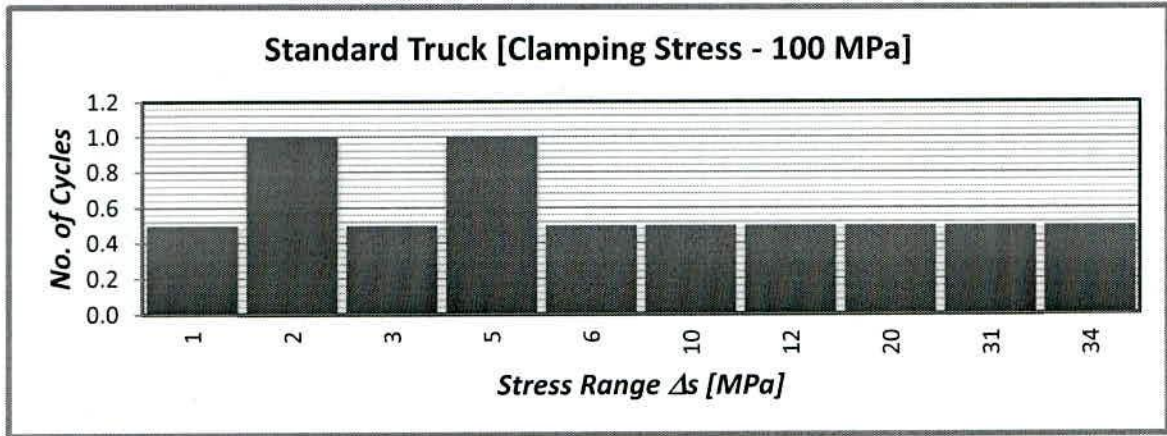


Figure 6.18 – Stress range histogram for 100 MPa clamping stress under standard truck loading



Figure 6.19 – Stress range histogram for 50 MPa clamping stress under standard truck loading

6.4.2 HEAVY TRUCK LOADING

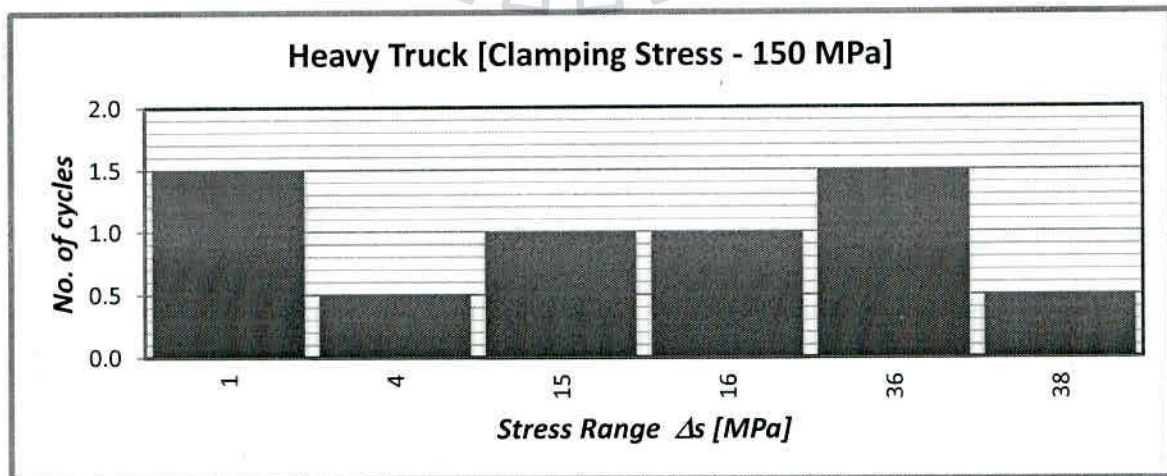


Figure 6.20 – Stress range histogram for 150 MPa clamping stress under heavy truck loading

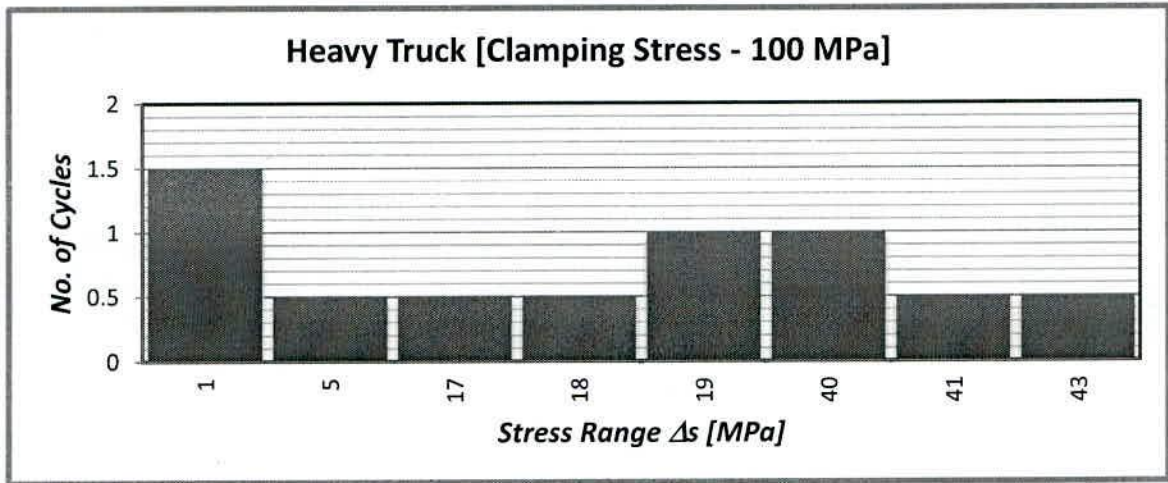


Figure 6.21 – Stress range histogram for 100 MPa clamping stress under heavy truck loading

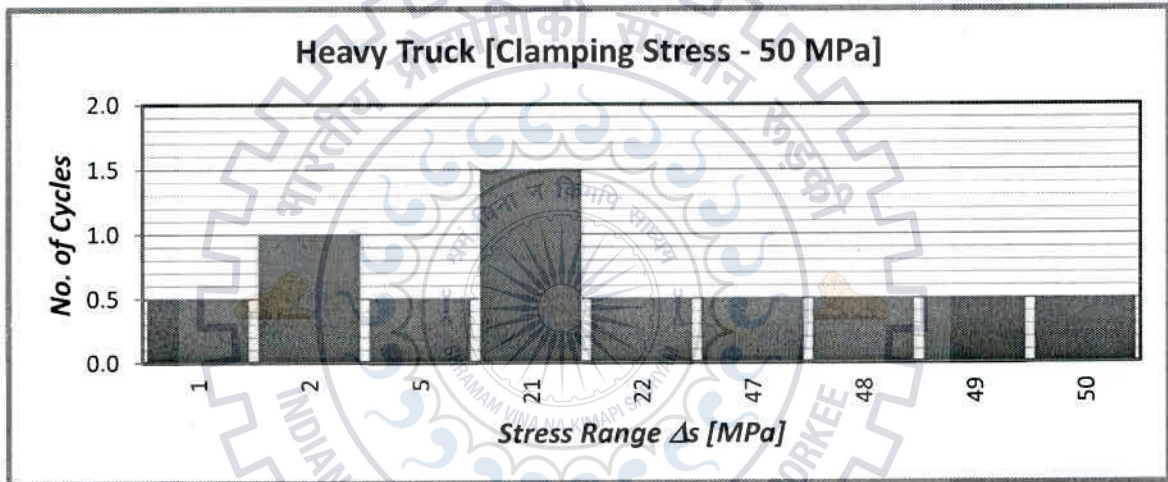


Figure 6.22 – Stress range histogram for 50 MPa clamping stress under heavy truck loading

6.4.3 35.2 TON TRUCK LOADING

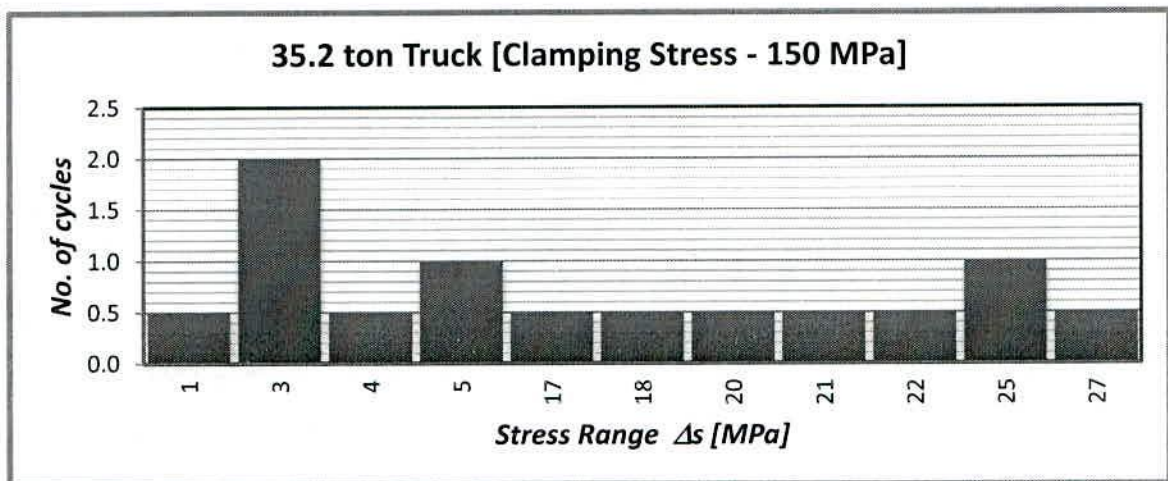


Figure 6.23 – Stress range histogram for 150 MPa clamping stress under 35.2 ton truck loading

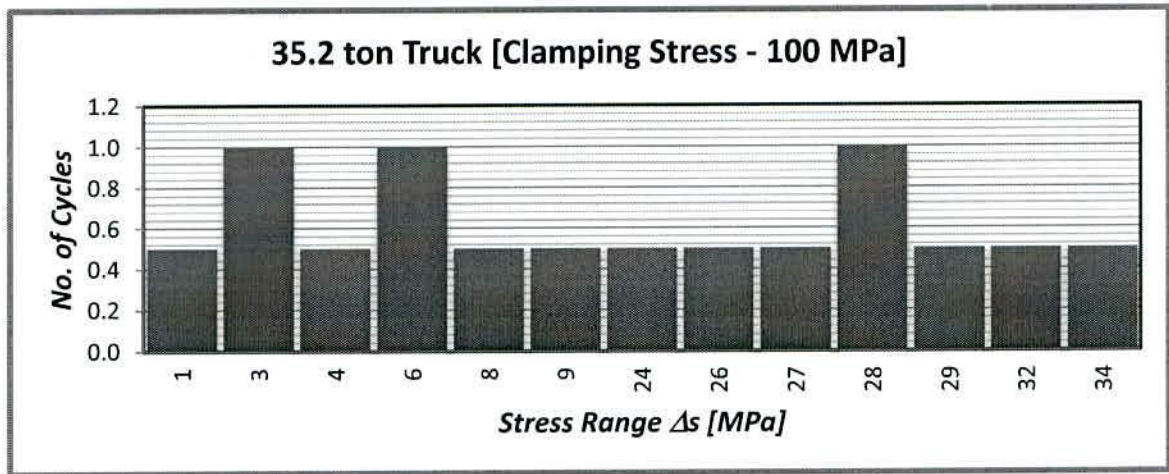


Figure 6.24 – Stress range histogram for 100 MPa clamping stress under 35.2 ton truck loading

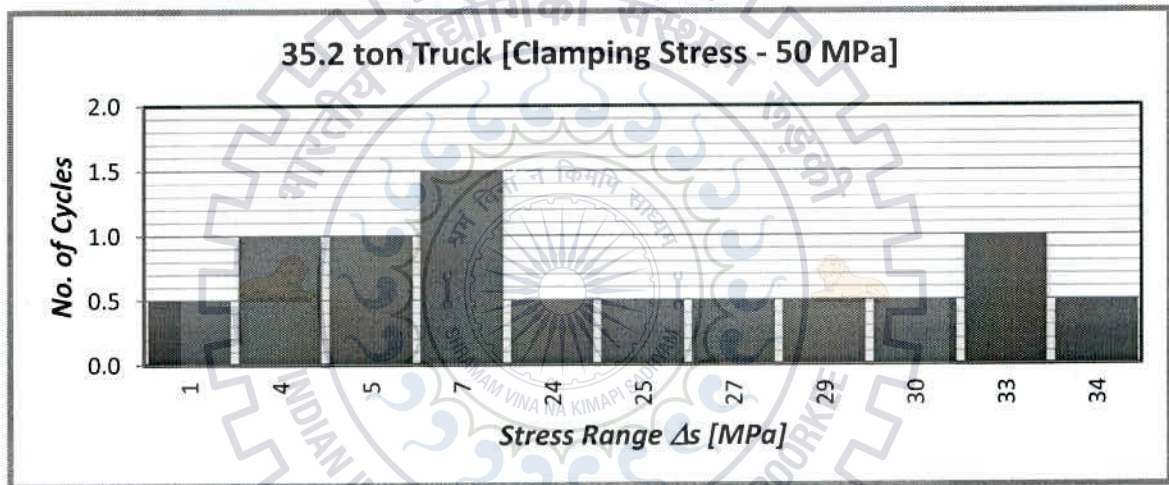


Figure 6.25 – Stress range histogram for 50 MPa clamping stress under 35.2 ton truck loading

6.4.4 44 TON TRUCK LOADING

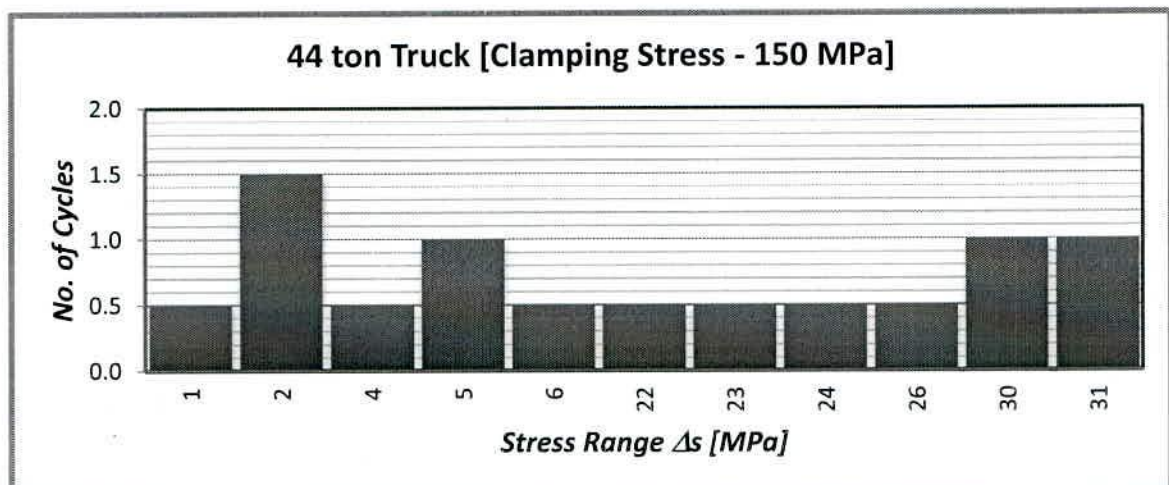


Figure 6.26 – Stress range histogram for 150 MPa clamping stress under 44 ton truck loading

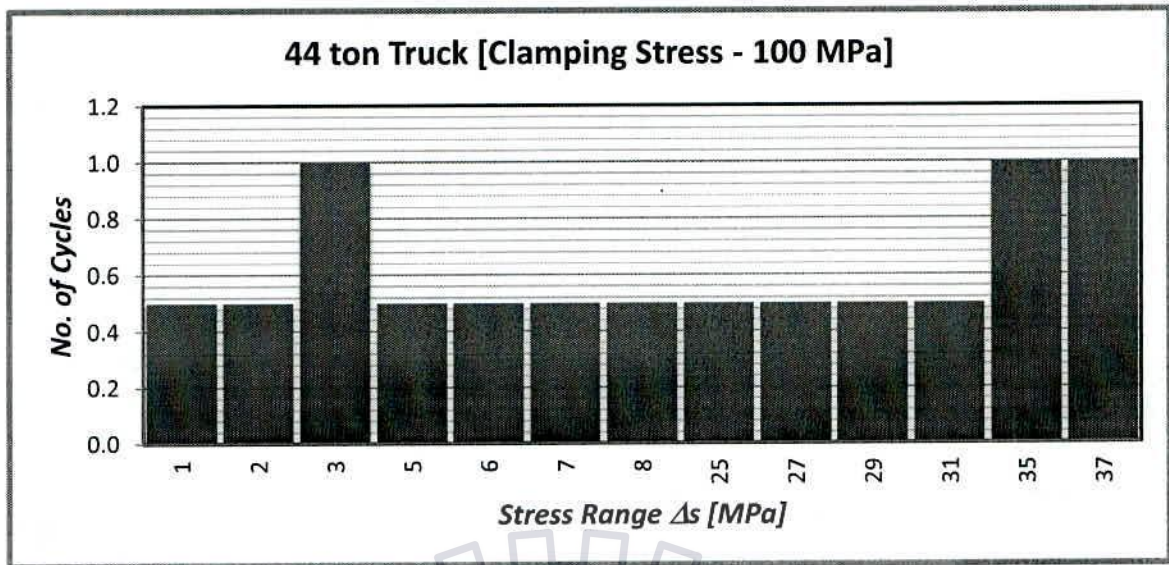


Figure 6.27 – Stress range histogram for 100 MPa clamping stress under 44 ton truck loading

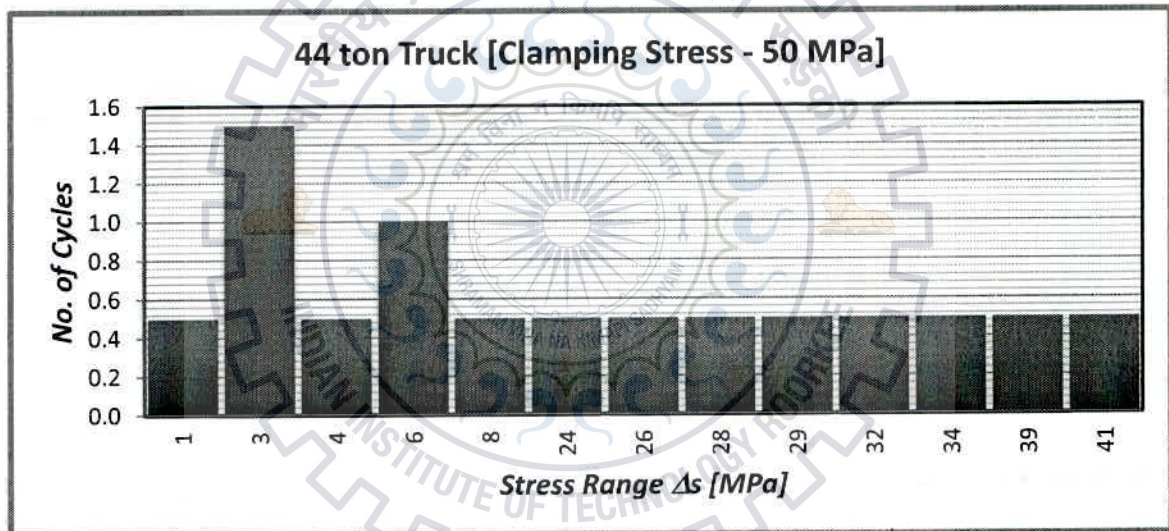


Figure 6.28 – Stress range histogram for 150 MPa clamping stress under 44 ton truck loading

6.5 FATIGUE DAMAGE IN RIVET

The fatigue damage caused in the rivet due to single passage of two back to back vehicles is computed by using ‘Palmgren-Miner damage rule’ which can be stated as “The damage at a certain stress range is proportional to the number of cycles”. In simple words, the ratio of number of cycles (n_i) at a certain stress range (Δ_s) and maximum allowable number of cycles (N_i) for that particular stress range gives the damage caused to that particular stress range (Δ_s).

Damage for a particular stress range (Δ_{s_i}) = $\frac{n_i}{N_i}$ Equation 6-a

Where,

n_i is the number of cycles occurring at stress range magnitude, Δ_{s_i} of a stress spectrum

N_i is the number of cycles corresponding to particular fatigue strength at stress range magnitude, Δ_{s_i}

The value of N_i can be determined by Wöhler’s curves for the corresponding value of Δ_s . For a particular material, the Wöhler’s curve shall be developed by performing fatigue experiments on the material samples obtained from the structure. This will ensure that the fatigue analysis carried out is accurate and that it gauges the current condition of the structure. However if the material sample of the bridge are not available, one can use the Wöhler’s curve available in the relevant standard codes of that region or any other data available in relevant literature, for material similar to the material of the bridge under study. For the current study, the Wöhler’s cure was obtained using the following expression.

$Log_{10}N = Log_{10}[1.53 \times 10^{12}] - 3Log_{10}S$ Equation 6-b

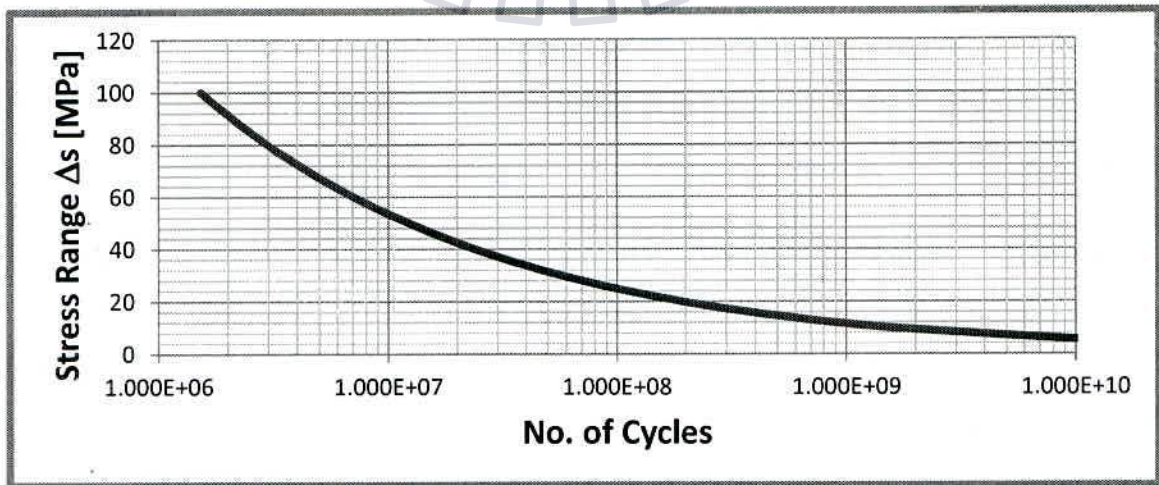


Figure 6.29 – Wöhler’s curve or S-N Curve

6.5.1 DAMAGE IN RIVET FOR CLAMPING STRESS 150 MPa

Table 6.2 – Damage – 150 MPa - Single passage of two standard trucks

Stress Range MPa	Cycle per vehicle n	Max no. of cycles N	Damage = n/N
1	0.5	9.305E+12	5.374E-14
2	1.5	2.320E+11	6.465E-12
4	1.5	2.919E+10	5.138E-11
8	0.5	2.603E+09	1.921E-10
11	0.5	1.238E+09	4.038E-10
16	0.5	3.478E+08	1.437E-09
27	0.5	7.777E+07	6.429E-09
29	0.5	6.172E+07	8.101E-09
Total Damage =			1.662E-08

Table 6.3 – Damage – 150 MPa – Single passage of two heavy trucks

Stress Range MPa	Cycle per vehicle n	Max no. of cycles N	Damage = n/N
1	1.5	1.530E+12	9.804E-13
4	0.5	1.932E+10	2.588E-11
15	1.0	4.795E+08	2.086E-09
16	1.0	3.686E+08	2.713E-09
36	1.5	3.387E+07	4.428E-08
38	0.5	2.862E+07	1.747E-08
Total Damage =			6.658E-08

Table 6.4 – Damage – 150 MPa – Single passage of two 35.2 ton trucks

Stress Range MPa	Cycle per vehicle n	Max no. of cycles N	Damage = n/N
1	0.5	8.396E+12	5.955E-14
3	2.0	7.284E+10	2.746E-11
4	0.5	1.821E+10	2.745E-11
5	1.0	1.668E+10	5.996E-11
17	0.5	3.081E+08	1.623E-09
18	0.5	2.422E+08	2.065E-09
20	0.5	1.850E+08	2.702E-09
21	0.5	1.762E+08	2.838E-09
22	0.5	1.420E+08	3.522E-09
25	1.0	1.005E+08	9.946E-09
27	0.5	7.441E+07	6.719E-09
Total Damage =			2.953E-08

Table 6.5 – Damage – 150 MPa – Single passage of two 44 ton trucks

Stress Range MPa	Cycle per vehicle n	Max no. of cycles N	Damage = n/N
0.8	0.5	3.616E+12	1.383E-13
2.3	1.5	1.330E+11	1.128E-11
3.7	0.5	2.984E+10	1.675E-11
5.0	1.0	1.224E+10	8.170E-11
6.2	0.5	6.417E+09	7.792E-11
21.7	0.5	1.502E+08	3.328E-09
23.2	0.5	1.226E+08	4.078E-09
24.3	0.5	1.060E+08	4.716E-09
25.9	0.5	8.828E+07	5.664E-09
30.0	1.0	5.667E+07	1.765E-08
31.4	1.0	4.931E+07	2.028E-08
Total Damage =			5.590E-08

6.5.2 **DAMAGE IN RIVET FOR CLAMPING STRESS 100 MPa**

Table 6.6 – Damage - 100 MPa – Single passage of two standard trucks

Stress Range MPa	Cycle per vehicle n	Max no. of cycles N	Damage = n/N
1	0.5	6.045E+12	8.271E-14
2	1.0	1.597E+11	6.261E-12
3	0.5	6.270E+10	7.975E-12
5	1.0	1.521E+10	6.573E-11
6	0.5	8.693E+09	5.752E-11
10	0.5	1.395E+09	3.585E-10
12	0.5	8.201E+08	6.097E-10
20	0.5	2.062E+08	2.425E-09
31	0.5	5.057E+07	9.886E-09
34	0.5	3.940E+07	1.269E-08
Total Damage =			2.611E-08

Table 6.7 – Damage – 100 MPa – Single passage of two heavy trucks

Stress Range MPa	Cycle per vehicle n	Max no. of cycles N	Damage = n/N
1	1.5	7.181E+11	2.089E-12
5	0.5	1.040E+10	4.806E-11
17	0.5	2.891E+08	1.730E-09
18	0.5	2.674E+08	1.870E-09
19	1	2.220E+08	4.504E-09
40	1	2.311E+07	4.328E-08
41	0.5	2.148E+07	2.328E-08
43	0.5	1.950E+07	2.564E-08
Total Damage =			1.004E-07

Table 6.8 – Damage - 100 MPa – Single passage of two 35.2 ton trucks

Stress Range MPa	Cycle per vehicle n	Max no. of cycles N	Damage = n/N
1	0.5	5.120E+12	9.766E-14
3	1.0	4.197E+10	2.382E-11
4	0.5	2.005E+10	2.494E-11
6	1.0	8.089E+09	1.236E-10
8	0.5	3.089E+09	1.619E-10
9	0.5	2.032E+09	2.460E-10
24	0.5	1.076E+08	4.645E-09
26	0.5	8.863E+07	5.642E-09
27	0.5	7.986E+07	6.261E-09
28	1.0	6.658E+07	1.502E-08
29	0.5	6.279E+07	7.963E-09
32	0.5	4.624E+07	1.081E-08
34	0.5	4.040E+07	1.238E-08
Total Damage =			6.330E-08

Table 6.9 – Damage – 100 MPa – Single passage of two 44 ton trucks

Stress Range MPa	Cycle per vehicle n	Max no. of cycles N	Damage = n/N
0.9	0.5	2.363E+12	2.116E-13
2.4	0.5	1.121E+11	4.461E-12
2.8	1.0	6.733E+10	1.485E-11
4.8	0.5	1.362E+10	3.672E-11
6.2	0.5	6.272E+09	7.972E-11
6.7	0.5	5.032E+09	9.936E-11
7.9	0.5	3.121E+09	1.602E-10
25.5	0.5	9.281E+07	5.387E-09
27.3	0.5	7.550E+07	6.622E-09
28.7	0.5	6.486E+07	7.709E-09
30.5	0.5	5.372E+07	9.308E-09
35.1	1.0	3.535E+07	2.829E-08
36.7	1.0	3.106E+07	3.220E-08
Total Damage =			8.991E-08

6.5.3 **DAMAGE IN RIVET FOR CLAMPING STRESS 150 MPa**

Table 6.10 – Damage – 50 MPa – Single passage of two standard trucks

Stress Range MPa	Cycle per vehicle n	Max no. of cycles N	Damage = n/N
1	0.5	1.786E+12	2.800E-13
3	1.5	5.765E+10	2.602E-11
6	0.5	8.587E+09	5.822E-11
7	0.5	5.287E+09	9.457E-11
14	0.5	5.284E+08	9.462E-10
18	0.5	2.550E+08	1.961E-09
27	0.5	7.494E+07	6.672E-09
33	0.5	4.150E+07	1.205E-08
35	0.5	3.559E+07	1.405E-08
38	0.5	2.697E+07	1.854E-08
Total Damage =			5.439E-08

Table 6.11 – Damage - 50 MPa – Single passage of two heavy trucks

Stress Range MPa	Cycle per vehicle n	Max no. of cycles N	Damage = n/N
1	0.5	9.384E+11	5.328E-13
2	0.5	2.580E+11	1.938E-12
2	0.5	1.854E+11	2.696E-12
6	0.5	6.005E+09	8.327E-11
20	1.0	1.830E+08	5.465E-09
22	1.0	1.386E+08	7.215E-09
46	0.5	1.531E+07	3.265E-08
47	0.5	1.520E+07	3.289E-08
48	0.5	1.398E+07	3.577E-08
49	0.5	1.266E+07	3.950E-08
Total Damage =			1.536E-07

Table 6.12 – Damage – 50 MPa – Single passage of two 35.2 ton trucks

Stress Range MPa	Cycle per vehicle n	Max no. of cycles N	Damage = n/N
1	0.5	1.883E+12	2.655E-13
4	1.0	2.054E+10	4.867E-11
5	1.0	1.451E+10	6.894E-11
7	1.5	5.177E+09	2.898E-10
24	0.5	1.150E+08	4.347E-09
25	0.5	9.246E+07	5.408E-09
27	0.5	7.642E+07	6.543E-09
29	0.5	6.111E+07	8.182E-09
30	0.5	5.510E+07	9.075E-09
33	1.0	4.443E+07	2.251E-08
34	0.5	4.001E+07	1.250E-08
Total Damage =			6.897E-08

Table 6.13 – Damage – 50 MPa – Single passage of two 44 ton trucks

Stress Range MPa	Cycle per vehicle n	Max no. of cycles N	Damage = n/N
1.2	0.5	9.428E+11	5.304E-13
3.0	1.5	5.667E+10	2.647E-11
3.8	0.5	2.781E+10	1.798E-11
5.8	1.0	7.842E+09	1.275E-10
7.7	0.5	3.355E+09	1.490E-10
24.5	0.5	1.046E+08	4.780E-09
26.0	0.5	8.696E+07	5.750E-09
27.5	0.5	7.343E+07	6.809E-09
28.5	0.5	6.584E+07	7.594E-09
32.2	0.5	4.581E+07	1.091E-08
34.3	0.5	3.786E+07	1.321E-08
39.2	0.5	2.543E+07	1.966E-08
41.4	0.5	2.160E+07	2.315E-08
Total Damage =			9.219E-08

6.5.4 DAMAGE CALCUALTION PER DAY

The damage calculated for each type of vehicle in the above section was for the passing of two vehicles back to back. The bridge will experience a number of such repetitions again and again in a single day. This number will depend on the traffic density. Since the traffic data was not available during this study, the frequency of the vehicles tabulated in table 5.1 and discussed in the section 5.2.2. The damage thus calculated for the passing of one set of vehicles is multiplied with the number of repetitions and the total damage caused due to each vehicle per day is calculated. The total damage per day is then added together to obtain the total damage per day for all type of vehicles. The damage in the rivet for different rivet clamping stress is tabulated below.

Table 6.14 – Total damage per day for 150MPa rivet clamping stress.

Rivet Clamping Stress = 150 MPa			
Vehicle	Damage due to combination of two vehicles	No. of vehicle combination per day	Damage per day
Standard Truck	1.66218E-08	100	1.66218E-06
Heavy Truck	6.65772E-08	75	4.99329E-06
35.2 Ton Truck	2.95299E-08	50	1.47649E-06
44 Ton Truck	5.59012E-08	25	1.39753E-06
Total damage per day =			9.5295E-06

Table 6.15 – Total damage per day for 100MPa rivet clamping stress.

Rivet Clamping Stress = 100 MPa			
Vehicle	Damage due to combination of two vehicles	No. of vehicle combination per day	Damage per day
Standard Truck	2.61071E-08	100	2.61071E-06
Heavy Truck	1.00355E-07	75	7.52663E-06
35.2 Ton Truck	6.32996E-08	50	3.16498E-06
44 Ton Truck	8.99094E-08	25	2.24774E-06
Total damage per day =			1.55501E-05

Table 6.16 – Total damage per day for 50MPa rivet clamping stress.

Rivet Clamping Stress = 50 MPa			
Vehicle	Damage due to combination of two vehicles	No. of vehicle combination per day	Damage per day
Standard Truck	5.43914E-08	100	5.43914E-06
Heavy Truck	1.53593E-07	75	1.15194E-05
35.2 Ton Truck	6.89652E-08	50	3.44826E-06
44 Ton Truck	9.21891E-08	25	2.30473E-06
Total damage per day =			2.27116E-05

6.6 ESTIMATION OF FATIGUE LIFE

The residual fatigue life can be computed from the following equation

$$Residual\ fatigue\ life\ (in\ days) = \frac{D_f - D_a}{D_p} \dots \dots \dots Equation\ 6-c$$

Where,

D_f is the fatigue damage sum at failure

D_a is the fatigue damage produced by past traffic

D_p is the fatigue damage produced by traffic during 24 hours

D_a would be zero if the S-N curves are generated for undamaged component

In Palmgren-Miner Hypothesis D_f is taken as unity.

However, based on experience of many research holders and statistical study it has been indicated that if 50% probability S-N curves are used, then to assess safe working life D_f should be taken as 0.3 in place of 1. This modification gives 97.5% confidence level for assessment. If the curve is assumed to be prepared by testing totally undamaged sample of material same as that of used in actual bridge, D_a becomes equal to zero.

So, in actual practice damage factor is taken as 0.3 to calculate the residual life of members. Thus modified equation is

$$D_f = \sum \frac{n_i}{N_i} = 0.3 \dots \dots \dots Equation\ 6-d$$

Hence residual life of members in years is determined by following expression:

$$Residual\ life\ in\ years = \frac{D_f}{D_y} = \frac{0.3}{Time\ in\ Days \times 365} \dots\dots\dots Equation\ 6-e$$

The fatigue life of rivet obtained for different clamping force of rivet is tabulated below.

Table 6.17 – Fatigue life in years for different clamping stress

Rivet Clamping Stress	Total damage in one day TD	Total damage in one year TD _y	Fatigue life
150 MPa	9.5295E-06	3.4783E-03	86.2 Years
100 MPa	1.5550E-05	5.6758E-03	52.9 Years
50 MPa	2.2712E-05	8.2897E-03	36.2 Years

The results tabulated in table 6.17 clearly show that the fatigue life of a rivet is directly proportional to the clamping stress. As the clamping stress is reduced, the fatigue life also decreases.

6.7 SUMMARY

- Rain flow counting method was used to decipher the complex shear stress history of the rivet obtained from ABAQUS analysis and stress range histogram as well as the number of corresponding stress cycles was acquired.
- S-N curve and Palmgren-Miner linear elastic damage hypothesis was used to obtain the damage in the rivet.
- Accordingly the fatigue life of the rivet for three different clamping force was obtained.

Chapter 7

CONCLUSIONS

7.1 SUMMARY

- Stress range concept is a very simple and useful method to predict the residual life of steel bridges.
- Residual life assessment of steel bridges is done using conventional method of S-N curves.
- The global model of the truss bridge was analysed in SAP-2000 and the load history due to different vehicle combinations was obtained.
- A local model of the riveted connection was modelled in ABAQUS. Load history obtained from SAP-2000 was applied as an external load and analysis was performed for different clamping force in the rivets.
- The top most rivet of the stringer was found to be the most critical rivet.
- The effect on fatigue life of the rivet due to variation in clamping force was studied.
- The failure of first rivet in the connection was considered to be end of life of the connection because; failure of one rivet will lead to overloading on other rivets of the connection which will lead to total failure of the connection.

7.2 CONCLUSIONS

- It was observed that the fatigue life of the rivet decreases with decrease in the clamping force. It also leads to loss in fatigue life of the connection.
- This behaviour of the connection can be attributed to the fact that, under high clamping force, the friction between the plate's increases and the load is actually transferred through friction between the plates. If the clamping force is lost, the plates get loosened and there is partial loss of frictional contact. In this case the load is transferred through shear and friction due to which more damage in the rivet is caused.
- There is a drastic reduction in the fatigue life when the clamping stress reduces to 100 MPa from 150 MPa. It further reduces when the clamping stress is 50 MPa. This shows the importance of clamping force in riveted connections.
- Since roadway bridges are subjected to less stress cycles their fatigue life is generally more as compared to railway bridges. Hence railway bridges are more critical for fatigue failure.

7.3 LIMITATIONS

- No field testing has been carried out to get exact stresses in the members of the bridge. The mathematical model created is assumed to give results similar to field results.
- The proposed methodology is based on stress range concept and can be applied to all types of bridges, provided relevant S-N curves are plotted before. The S-N curve used for fatigue analysis was assumed from the existing literature. A more precise assessment could have been carried out if the actual material data and corresponding S-N curve are available.
- Assumption was made while considering the vehicular live load on the bridge. Density of traffic and type of vehicles may differ in actuality. A more precise calculation would have been possible with actual traffic data.
- The eccentricity of vehicles considered was for the worst case scenario. This will not be the case throughout the design life of the bridge. Hence the actual fatigue life will differ from the calculations.
- Clamping force in all the 16 rivets was considered to be same for all the three scenarios of clamping force analysed. This may not be the case in reality.
- The coefficient of friction between the faces of elements was considered to be 0.3 based on the previous studies. An existent value of coefficient of friction will produce more accurate results.
- The rivets were considered to be of perfect shape which may not be the case in reality.
- Material degradation has not been considered apart from the loss of clamping force in the rivets
- Assessment following seismic actions is not covered.

7.4 SCOPE FOR FUTURE RESEARCH

- Behaviour of connection after the failure of the first rivet can be studied.
- Effect of dissimilar clamping stress in each rivet of the connection needs to be evaluated.
- Experiments can be carried out on large scale riveted connections of an actual bridge to validate the findings of this study.
- Other rivet defect scenarios like loss of rivet head, reduction in size of rivet head due to corrosion, eccentricity in the rivet, gap between rivet head and rivet hole, etc. can be considered.

- The fatigue analysis of other components of the connection like connecting angles, stringers and cross-girders can be carried out.
- The possibility of crack initiating and propagating in the rivet, connecting angles, stringers or cross-girders using fracture mechanics can be studied.
- The fatigue critical points of the connection details of the connection like rivet hole, angle fillet etc. can be studied in detail.



REFERENCES

"Assessment of Residual life of Ganga Bridge No. 110 Dn. (Near Kanpur) Lucknow Division Northern Railway" Report no. - BS-70, December 2004, RDSO Lucknow.

ABAQUS Version 6.8 (2008), Dassault Systems Simulia Corp, United States.

Åkesson, B. "Fatigue life of riveted railway bridges", PhD Dissertation, 1994, Chalmers University of Technology, Sweden.

Al-Emrani, M. and Kliger, R. "FE analysis of stringer-to-floor-beam connections in riveted railway bridges" *Journal of Constructional Steel Research*, 2003, pp. 803-818.

Banerji, P. and Chikermane, S. "Structural health monitoring of a steel railway bridge for increased axle loads", *IABSE Structural Engineering International*, February 2011, pp. 201–216.

Chaminda, S.S., Ogha, M., Dissanayake, R. and Taniwaki, K. "Different approaches for remaining life estimation of critical members in railway bridges" *Steel Structures*, July 2007, pp. 263-276.

de Jesus, A.M.P, Pereira, R.M.G. "FEM analysis of riveted connections aiming fatigue and fracture assessments", *Iberian Conference on Fracture and Structural Integrity*, March 2010, Porto, Portugal.

Fisher, J.W., Struik, J.H.A., and Kulak, G.L. "Guide to design criteria for bolted and riveted joints" *John Wiley & Sons*, New York, NY, 1974.

Ghule, V.V. "Health and residual life assessment of steel bridges ", M.Tech Dissertation, 2012, Indian Institute of Technology, Roorkee, India.

Haghani, R., Al-Emrani, M. and Heshmati, M. "Fatigue-prone details in steel bridges" *Buildings*, 2, 2012, pp. 456-476.

Helmerich., R.; Kuhn., B.; Nussbaumerx., A. "Assessment of existing steel structures. A guideline for estimation of the remaining fatigue life" *Structure and Infrastructure Engineering*, Vol. 3, No. 3, September 2007, pp. 245 – 255.

Imam, B.M., Righiniotis, T.D. and Chryssanthopoulos, M.K. "Fatigue assessment of riveted railway bridges" *Steel Structures*, 5, 2005, pp. 486-494.

Imam, B.M., Righiniotis, T.D. and Chryssanthopoulos, M.K. "Fatigue reliability of riveted connections in railway bridges" 3rd International ASRANet Colloquium, July 2006, Glasgow, U.K.

Imam, B.M., Righiniotis, T.D. and Chryssanthopoulos, M.K. "Numerical modelling of riveted railway bridge connections for fatigue evaluation" *Engineering Structures*, 2007, pp. 3071–3081.

Imam, B.M. and Righiniotis, T.D. "Fatigue evaluation of riveted railway bridges through global and local analysis" *Journal of Constructional Steel Research*, 2010, pp. 1411–1421.

Imam, B.M., Righiniotis, T.D. and Chryssanthopoulos, M.K. "Performance of steel structures under fatigue cyclic loading" *Journal of Civil Engineering and Architecture*, Vol. 5, No. 8, March 2011, pp. 265-272

IRC:24-2001 "Standard specifications and code of practice for road bridges - Section: V – Steel road bridges" The Indian Road Congress, New Delhi, India.

IRC:6-2000 "Standard specifications and code of practice for road bridges - Section: II - Loads and stresses" The Indian Road Congress, New Delhi, India.

IRC:SP-37-1991 "Guidelines for evaluation of load carrying capacity of bridges" The Indian Road Congress, New Delhi, India.

Kuehn, B., Lukić, M., Nussbaumer, A., Guenther, H. P., Helmerich, R., Herion, S., Kolstein, M.H., Walbridge, S., Androic, B., Dijkstra, o., and Bucak, Ö. "Assessment of existing steel structures: recommendations for estimation of remaining fatigue life" JRC Scientific and Technical Reports, 2008.

Larsson, T. "Fatigue assessment of riveted bridges" PhD Dissertation, 2009, Luleå University of Technology, Sweden.

Oka, V.G, Hopwood, T. and Harik. I.E. "Fatigue analysis of steel bridges using a portable microcomputer based strain gage system" *Computers & Structures*, Vol. 31, No. 2, 1989, pp. 151-186.

Pipinato, A., Pallegriano, C. and Modena, C. "Fatigue assessment of highway steel bridges in presence of seismic loading" *Engineering Structures* 33 (2011) - pp. 202–209.

Pipinato, A., Pallegriano, C., Bursi, O.S. and Modena, C. "High-cycle fatigue behavior of riveted connections for railway metal bridges" *Journal of Constructional Steel Research*, 2009, pp. 2167-2175.

Rodrigues, M.P.G., de Jesus, A.M.P. and Silva, A.L.L. "Comparison between alternative fe modelling strategies for riveted connections concerning fatigue assessments" *Revista da Associação Portuguesa de Análise Experimental de Tensões*, Vol. 19, 2011, pp. 19-31

Vermes, W.J. "Design and Performance of Riveted Bridge Connections" International Bridge Conference, June 2009, Pittsburgh, USA.